

Novel mechanisms of carboplatin resistance in epithelial ovarian cancer and their  
therapeutic potential

by

Samir Hamouda Barghout

A thesis submitted in partial fulfillment of the requirements for the degree of  
Master of Science

Medical Sciences - Obstetrics and Gynecology  
University of Alberta

©Samir Hamouda Barghout, 2015

## **Abstract**

Ovarian cancer is the fifth leading cause of cancer-related mortality in women. Epithelial ovarian cancer (EOC) constitutes approximately 90% of all ovarian malignancies. Platinum-based compounds have been used to treat EOC, with carboplatin currently being used as a first-line therapeutic agent in combination with paclitaxel. Despite the initial positive response to carboplatin, relapse occurs in most advanced EOC patients and resistance eventually develops, with a 5-year survival rate of only 30%. Accordingly, there is an urgent need to identify the molecular mechanisms underlying chemoresistance in EOC in order to develop more effective therapeutic strategies. To address this objective, the gene expression profiles of the EOC cell line A2780s (cisplatin-sensitive) and its derivative A2780cp (cisplatin-resistant) were compared by conducting DNA microarray and ingenuity pathway analysis (IPA). A number of genes were found to be differentially expressed between these two cell lines including RUNX3 and genes encoding several components of the Wnt/ $\beta$ -catenin signaling pathway. These genes were selected for further analysis as they have not been previously studied in the context of chemoresistance in EOC.

RUNX3 is a member of the RUNX family of transcription factors that act as developmental regulators and have an oncogenic role in EOC. Consistent with DNA microarray data, subsequent validation by Western blotting showed that RUNX3 expression was higher in A2780cp cells compared to A2780s cells. Further gain- and loss-of-function studies in A2780 cells confirmed the role of RUNX3 in EOC resistance to carboplatin-induced cytotoxicity. Interestingly, the

results demonstrate that RUNX3 upregulates the expression of cellular inhibitor of apoptosis 2 (cIAP2), suggesting a potential mechanism by which RUNX3 confers resistance to carboplatin.

In addition, DNA microarray analysis and subsequent validation by qRT-PCR suggested that the Wnt/ $\beta$ -catenin signaling pathway is more active in A2780cp cells compared to A2780s cells. Consistent with this finding, further analysis showed increased nuclear localization of  $\beta$ -catenin and higher  $\beta$ -catenin transcriptional activity in A2780cp cells compared to A2780s cells. Interestingly, chemical inhibition of Wnt/ $\beta$ -catenin signaling by CCT036477 sensitized A2780cp cells to carboplatin, especially at high concentrations. Further investigation of the effect of other Wnt/ $\beta$ -catenin signaling inhibitors is warranted. Two Wnt negative regulators, dickkopf-related protein 1 (DKK1) and secreted frizzled-related protein 1 (SFRP1), were among the down-regulated proteins in A2780cp cells. Gain- and loss-of-function approaches are planned to investigate their specific roles in chemoresistance in EOC.

In conclusion, our data suggest that RUNX3 contributes to carboplatin resistance of EOC cells and therefore it could be a potential therapeutic target. In addition, the Wnt/ $\beta$ -catenin signaling pathway is more active in resistant EOC cells, suggesting its potential contribution to chemoresistance in EOC.

## **Dedication**

*To*

*Mom, Dad, Yasmin, Salma and Maha*

## Acknowledgements

I would like express my gratitude to my supervisor **Dr YangXin Fu** for his academic guidance and support during my master research. His distinguished mentorship of my first graduate degree will be unforgettable throughout my career.

I am also thankful to my supervisory committee members **Dr Michael Weinfeld** and **Dr Lynne-Marie Postovit** for their insightful suggestions and fruitful discussions that helped considerably produce this work. I would like to thank other defense committee members **Dr Roseline Godbout** and **Dr Denise Hemmings** for taking the time to read and critically discuss my thesis with me.

I would like to thank my lab members, particularly **Nubia Zepeda** for active collaboration to produce this work, **Abul Kalam Azad** for guiding me through several laboratory techniques, and **Zhihua Xu** for distinguished technical assistance with laboratory techniques. I really appreciate **Dr Postovit's lab members** for their insightful discussions throughout ovarian cancer research team weekly meetings. In particular, I would like to thank **Krista Vincent** for bioinformatic analysis of publicly available data on ovarian cancer.

I would like to thank the **Gynecologic Oncology group** at the University of Alberta for assistance in collection of normal OSE and primary EOC cells; **Dr. Benjamin Tsang** (Ottawa Hospital Research Institute) for providing A2780s and A2780cp cells; and **Dr Yoshiaki Ito** (Cancer Science Institute of Singapore) for providing pcDNA-FLAG-RUNX3 (1-187). I also thank the staff of the **Flow Cytometry Facility at Cross Cancer Institute** for cell sorting and **Microscope**

**Unit at the Department of Obstetrics & Gynecology** for helping with imaging of immunocytochemistry. This research was generously supported by a start-up fund from the **Women and Children's Health Research Institute (WCHRI)** with funding donated by the **Royal Alexandra Hospital Foundation (RAHF)** to Dr. Fu.

I would like to acknowledge financial support by **MatCH Program, Faculty of Medicine and Dentistry/Alberta Health Services graduate studentship, and the Medical Science Graduate Program scholarship**. I was also supported by travel awards provided by **Department of Obstetrics & Gynecology, WCHRI and Faculty of Graduate Studies and Research (FGSR)** at The University of Alberta to present my data in two conferences in Toronto, Canada.

I would like to thank MatCH Program coordinators **Drs YangXin Fu, Sujata Persad, Sarah Hughes and Denise Hemmings** for their academic support, and Drs. **Persad and Shairaz Baksh** for rotation in their labs.

Finally, I would like to thank administrative staff in the **Departments of Obstetrics & Gynecology and Oncology, MatCH graduate program, Medical Sciences Graduate Program, FGSR, and WCHRI** for administrative support throughout my master study.

## Table of Contents

<i>Chapter/Section</i>	<i>Page</i>
<b>Chapter 1 Introduction</b>	<b>1</b>
1.1 Ovarian cancer	<b>2</b>
1.1.1 Epidemiology and risk factors	2
1.1.2 Types and histotypes of ovarian tumors	3
1.1.3 Staging of ovarian cancer	7
1.1.4 Grades of epithelial ovarian cancer (EOC)	7
1.1.5 Clinical presentation and diagnosis of EOC	8
1.1.6 Origin of EOC	9
1.1.7 Molecular pathogenesis of EOC	15
1.1.8 Management of EOC	17
1.1.9 Recurrence of EOC	20
1.1.10 Platinum-resistant EOC	20
1.1.11 Novel therapeutics of EOC	21
1.1.12 Experimental models of EOC	22
1.2 Platinum-based Cancer Therapeutics	<b>24</b>
1.2.1 Discovery of platinum-based compounds	24
1.2.2 Cellular handling and mechanism of action of cisplatin and carboplatin	27
1.2.3 Resistance to cisplatin and carboplatin	34
1.2.4 Safety of cisplatin and carboplatin	37
1.3 RUNX family of transcription factors	<b>39</b>

1.3.1	Overview of RUNX transcription factors	39
1.3.2	Structure of RUNX family members	39
1.3.3	Transcriptional activity RUNX transcription factors	41
1.3.4	Functions of RUNX transcription factors	41
1.3.5	RUNX proteins in cancer	42
1.3.6	RUNX proteins in EOC	43
1.4	Wnt/ $\beta$ -catenin signaling	<b>46</b>
1.4.1	Overview of Wnt signaling	46
1.4.2	Cascade and components of Wnt/ $\beta$ -catenin signaling	46
1.4.3	Functions of Wnt/ $\beta$ -catenin signaling	47
1.4.4	Aberrant Wnt/ $\beta$ -catenin signaling in cancer	50
1.4.5	Aberrant Wnt/ $\beta$ -catenin signaling in EOC	50
1.5	Preliminary data and hypotheses	<b>52</b>
<b>Chapter 2 Materials and Methods</b>		<b>53</b>
2.1	Reagents	54
2.2	Cell culture	54
2.3	Generating overexpression cells	55
2.4	Generating knockdown cells	56
2.5	Cytotoxicity assays	57
2.6	Preparation of whole cell lysates	58
2.7	Western blotting	59



2.8	RNA isolation and quantitative reverse transcription polymerase chain reaction (qRT-PCR) analysis	59
2.9	Immunocytochemistry (ICC)	60
2.10	Luciferase reporter assay	63
2.11	Data analysis	63
<b>Chapter 3 Results</b>		<b>65</b>
3.1	The role of RUNX proteins in EOC resistance to carboplatin	<b>66</b>
3.1.1	RUNX3 expression is elevated in A2780cp cells compared to A2780s cells	66
3.1.2	Cisplatin-resistant A2780cp cells are also carboplatin-resistant	70
3.1.3	RUNX3 overexpression in A2780s cells confers resistance to carboplatin	72
3.1.4	Knockdown of RUNX3 modestly increases the sensitivity of A2780cp cells to carboplatin	74
3.1.5	Overexpression of dnRUNX3 increases the sensitivity of A2780cp cells to carboplatin	77
3.1.6	dnRUNX3 decreases the expression of cellular inhibitor of apoptosis protein-2 (cIAP2) in A2780cp cells	82
3.2	The role of Wnt/ $\beta$ -catenin signaling in EOC resistance to carboplatin	<b>87</b>
3.2.1	$\beta$ -catenin localization is nuclear in A2780cp and membranous in A2780s cells	87
3.2.2	LEF/TCF-driven transcriptional activity of $\beta$ -catenin in A2780cp is higher than that in A2780s cells	90

3.2.3	Wnt extracellular modulators that negatively regulate Wnt/ $\beta$ -catenin signaling are down regulated in A2780cp cells	90
3.2.4	Chemical inhibition of Wnt/ $\beta$ -catenin signaling sensitizes A2780cp cells to carboplatin in a synergistic manner	93
<b>Chapter 4 Discussion</b>		<b>96</b>
4.1	The role of RUNX family members in EOC resistance to carboplatin	97
4.2	The role of Wnt/ $\beta$ -catenin signaling in EOC resistance to carboplatin	101
4.3	Potential crosstalk between RUNX transcription factors and Wnt/ $\beta$ -catenin signaling	104
4.4	Conclusions and future directions	105
<b>References</b>		<b>107</b>

## **List of Tables**

<b><i>Table number and title</i></b>	<b><i>Page</i></b>
Table 1.1 List of epithelial ovarian cancer (EOC) histotypes and their characteristics	5
Table 1.2 List of symptoms and physical findings of ovarian cancer	11
Table 1.3 Primary adjuvant chemotherapy for EOC	19
Table 1.4 Selected mechanisms of EOC resistance to cisplatin and carboplatin	38
Table 1.5 Signaling components and members of Wnt/ $\beta$ -catenin signaling	49
Table 2.1 Sequence of primers used in qRT-PCR experiments	62
Table 3.1 Summary of IC <sub>50</sub> values measured for different experiments by two cytotoxicity assays	86
Table 3.2 Combination index (CI) values for different combinations of CCT036477 and carboplatin	95

## List of Figures

<i>Figure number and title</i>	<i>Page</i>
Figure 1.1 Representative images of the four major histotypes of EOC	6
Figure 1.2 Representative images of the appearance of EOC	12
Figure 1.3 Proposed origin of EOC	14
Figure 1.4 Chemical structures of selected agents of platinum-based chemotherapeutics	26
Figure 1.5 Cellular handling of extracellular and cytosolic platinum	30
Figure 1.6 Diagrammatic representation of the structures of RUNX proteins	40
Figure 1.7 Schematic illustration of the Wnt/ $\beta$ -catenin signaling pathway	48
Figure 3.1 Expression of RUNX family members and CBF $\beta$ at the RNA level in EOC cells	68
Figure 3.2 Expression of RUNX family members and CBF $\beta$ at the protein level in EOC cells	69
Figure 3.3 A2780cp cells are more resistant to carboplatin than A2780s cells	71
Figure 3.4 Overexpression of RUNX3 renders EOC cells more resistant to carboplatin	73
Figure 3.5 Knockdown of RUNX3 moderately sensitizes A2780cp cells to carboplatin	75
Figure 3.6 Knockdown of RUNX3 potentiates carboplatin-induced apoptosis	76
Figure 3.7 Confirmation of dnRUNX3 overexpression in A2780cp cells by Western blotting	79

Figure 3.8 dnRUNX3 increases the sensitivity of A2780cp cells to carboplatin	80
Figure 3.9 dnRUNX3 potentiates carboplatin-induced apoptosis in A2780cp cells	81
Figure 3.10 Cellular inhibitor of apoptosis protein-2 (cIAP2) expression in A2780s and A2780cp cells	83
Figure 3.11 Changes in <i>RUNX3</i> expression are associated with changes in <i>cIAP2</i> expression in A2780s and A2780cp cells	84
Figure 3.12 dnRUNX3 overexpression is associated with decreased cIAP2 expression in A2780cp cells and potentiates carboplatin-induced cytotoxicity	85
Figure 3.13 IPA analysis of microarray data of A2780s-A2780cp paired cell line model suggests Wnt/ $\beta$ -catenin signaling is more active in A2780cp cells	88
Figure 3.14 $\beta$ -catenin intracellular localization in A2780s and A2780cp cells	89
Figure 3.15 $\beta$ -catenin transcriptional activity in A2780s and A2780cp cells	91
Figure 3.16 Expression of selected Wnt signalling components in A2780s and A2780cp cells	92
Figure 3.17 Combination of carboplatin with the $\beta$ -catenin inhibitor CCT036477 in A2780cp cells	94



### **List of Abbreviations**

<b><i>Abbreviation</i></b>	<b><i>Full Name</i></b>
<b>3D</b>	Three-dimensional
<b>A</b>	Adenine
<b>ABCB/C</b>	ATP-binding-cassette subfamily B/C
<b>AD</b>	Activation domain
<b>ALDH1</b>	Aldehyde dehydrogenase 1
<b>ALL</b>	Acute lymphoblastic leukemia
<b>AML</b>	Acute myeloid leukemia
<b>APC</b>	Adenomatosis Polyposis Coli
<b>ATM</b>	Ataxia telangiectasia mutated
<b>ATP7A/B</b>	Copper-transporting P-type ATPase A/B
<b>ATR</b>	Ataxia telangiectasia and Rad3 related
<b>AUC</b>	Area under the curve
<b>BCC</b>	Basal cell carcinoma
<b>Bcl-2</b>	B-cell lymphoma 2
<b>BMP</b>	Bone morphogenetic protein
<b>C/EBP</b>	CCAAT/enhancer-binding protein
<b>CA-125</b>	Cancer antigen 125 (also known as mucin 16 or MUC16)
<b>CBF<math>\alpha/\beta</math></b>	Core-binding factor $\alpha/\beta$
<b>CD44/117/133</b>	Cluster of Differentiation 44/117/133
<b>CDK</b>	Cyclin-dependent kinase inhibitor
<b>CI</b>	Combination index
<b>cIAP1/2</b>	Cellular inhibitor of apoptosis protein 1/2

<b>CIC</b>	Cortical inclusion cysts
<b>cis-DDP</b>	Cisplatin; <i>cis</i> -diamminedichloroplatinum
<b>CK-1</b>	Casein kinase-1
<b>CML</b>	Chronic myeloid leukemia
<b>CT</b>	Computed tomography
<b>CTNNB1</b>	Catenin (cadherin-associated protein), beta 1
<b>DAPI</b>	4',6-diamidino-2-phenylindole
<b>DKK</b>	Dickkopf
<b>DLEC1</b>	Deleted in lung and esophageal cancer 1
<b>DMEM</b>	Dulbecco's Modified Eagle Medium
<b>dnRUNX3</b>	Dominant-negative RUNX3
<b>DOC</b>	Sodium deoxycholate
<b>DVL</b>	Dishevelled
<b>EGFR</b>	Epidermal growth factor receptor
<b>EMT</b>	Epithelial-mesenchymal transition
<b>EOC</b>	Epithelial ovarian cancer
<b>ERK</b>	Extracellular signal-regulated kinase
<b>FACS</b>	Fluorescence-activated cell sorting
<b>FAP</b>	Familial adenomatous polyposis
<b>FBS</b>	Fetal bovine serum
<b>FDA</b>	US Food and Drug Administration
<b>FIGO</b>	International Federation of Gynecology and Obstetrics
<b>FZD</b>	Frizzled
<b>G</b>	Guanine
<b>GADD45<math>\alpha</math></b>	Growth arrest and DNA-damage-inducible protein 45 $\alpha$



<b>GAPDH</b>	Glyceraldehyde 3-phosphate dehydrogenase
<b>GEO</b>	Gene Expression Omnibus
<b>GFP</b>	Green fluorescent protein
<b>GM-CSF</b>	Granulocyte-macrophage colony-stimulating factor
<b>GSK-3<math>\beta</math></b>	Glycogen synthase kinase-3 $\beta$
<b>GST</b>	Glutathione S-transferase
<b>h</b>	Hour
<b>HBS</b>	HEPES-buffered saline
<b>HCC</b>	Hepatocellular carcinoma
<b>HDAC</b>	Histone deacetylase
<b>HEK 293T</b>	Human Embryonic Kidney 293T cells
<b>HER-2</b>	Human epidermal growth factor receptor 2
<b>HGSEOC</b>	High-grade serous EOC
<b>HMG</b>	High-mobility group
<b>HNPCC</b>	Hereditary non-polyposis colorectal cancer
<b>HNSCC</b>	Head and neck squamous cell carcinoma
<b>IAP</b>	Inhibitor of apoptosis protein
<b>IC<sub>50</sub></b>	Median inhibitory concentration
<b>ICC</b>	Immunocytochemistry
<b>ID</b>	Inhibitory domain
<b>IHC</b>	Immunohistochemistry
<b>IP</b>	Intraperitoneal
<b>IPA</b>	Ingenuity Pathway Analysis
<b>IV</b>	Intravenous
<b>JNK</b>	c-Jun N-terminal kinase

<b>LEF</b>	Lymphoid enhancer factor
<b>LGR5</b>	Leucine-rich repeat-containing G-protein coupled receptor 5
<b>LMP</b>	Low malignant potential
<b>LRP</b>	Lung resistance related protein
<b>LRP5/6</b>	Low-density lipoprotein receptor related proteins 5 and 6
<b>MAPK</b>	Mitogen-activated protein kinase
<b>MEK</b>	MAPK kinase; MAPKK
<b>MIS</b>	Müllerian inhibition substance
<b>MMP</b>	Matrix metalloproteinase
<b>MMR</b>	Mismatch repair
<b>MMTV</b>	Mouse mammary tumor virus
<b>MPO</b>	Myeloperoxidase
<b>MRP</b>	Multidrug resistance protein
<b>MYD88</b>	Myeloid differentiation primary response gene 88
<b>nCoR</b>	Nuclear receptor corepressor
<b>NER</b>	Nucleotide excision repair
<b>NOS</b>	Adenocarcinomas not otherwise specified
<b>OCT</b>	Organic cation transporter
<b>OPCML</b>	Opioid binding protein/cell adhesion molecule-like
<b>OS</b>	Overall survival
<b>OSE</b>	Ovarian surface epithelium
<b>PARP</b>	Poly(ADP-ribose)polymerase
<b>PBS</b>	Phosphate buffered saline
<b>PCP</b>	Planar cell polarity
<b>PDGF</b>	Platelet-derived growth factor

<b>PEBP2<math>\alpha/\beta</math></b>	Polyoma enhancer-binding protein 2 $\alpha/\beta$
<b>PEG3</b>	Paternally expressed 3
<b>PFS</b>	Progression-free survival
<b>PIC</b>	Protease inhibitor cocktail
<b>PIK3CA</b>	Phosphoinositide 3-kinase catalytic subunit- $\alpha$
<b>PKC<math>\iota</math></b>	Protein kinase C, iota
<b>PLAGL1</b>	Pleiomorphic adenoma gene-like 1
<b>PPAR</b>	Peroxisome proliferator-activated receptor
<b>PRKCI</b>	Protein kinase C iota type
<b>PTEN</b>	Phosphatase and tensin homolog
<b>qRT-PCR</b>	Quantitative reverse transcription polymerase chain reaction
<b>RASSF1</b>	Ras association domain-containing protein 1
<b>RASSF1</b>	Ras association domain family member 1
<b>RHD</b>	Runt-homology domain
<b>RIPA</b>	radioimmunoprecipitation assay
<b>RIPK4</b>	Receptor-interacting serine/threonine-protein kinase 4
<b>RT</b>	Room temperature
<b>RUNX</b>	Runt-related transcription factor
<b>SCC</b>	Squamous cell carcinoma
<b>SDS</b>	Sodium dodecyl sulfate
<b>SEM</b>	Standard error of the mean
<b>sFRP</b>	secreted Frizzled related protein
<b>SLC</b>	Solute carrier
<b>STIC</b>	Serous tubal intraepithelial carcinoma
<b>TBP</b>	TATA binding protein

<b>TCF</b>	T-cell factor
<b>TCR</b>	T cell receptor
<b>TGF<math>\beta</math></b>	Transforming growth factor- $\beta$
<b>TIC</b>	Tumor-initiating capacity
<b>TLE</b>	Transducin-like enhancer of split
<b>UBF</b>	Upstream binding factor
<b>VEGF</b>	Vascular endothelial growth factor
<b>wg</b>	Wingless
<b>WHO</b>	World Health Organization
<b>WIF</b>	Wnt-inhibitory factor
<b>XIAP</b>	X-linked inhibitor of apoptosis protein
<b><math>\alpha</math>FR</b>	$\alpha$ -folate receptor

# **Chapter 1**

## **Introduction**

## **1. Introduction**

### **1.1 Ovarian cancer**

#### **1.1.1 Epidemiology and risk factors**

According to the Canadian cancer statistics 2014<sup>1</sup>, ovarian cancer represents 2.9% of the estimated new cases of cancer, ranking 8<sup>th</sup> in terms of cancer incidence in the female population of Canada. In addition, it has been estimated that the percent lifetime probability of developing ovarian cancer in this population is 1.4%. In terms of the mortality rate, ovarian cancer ranks 5<sup>th</sup> with a percentage of 4.7%. In this respect, ovarian cancer constitutes the leading cause of death due to gynecologic malignancies<sup>2</sup>. The 5-year observed survival proportion\* for ovarian cancer patients is approximately 42%, ranking 8<sup>th</sup> in terms of low survival. In 2009, approximately 10,695 cases were diagnosed since 1999, putting ovarian cancer 13<sup>th</sup> among other cancers in terms of 10-year prevalence. Similar percentages of incidence, mortality and prevalence have been reported in the developed world including the United States<sup>3</sup> and the United Kingdom<sup>2</sup>. In the developing world, ovarian cancer ranked 8<sup>th</sup> in terms of both incidence and mortality rates. Globally, it ranked 7<sup>th</sup> and 8<sup>th</sup> in terms of incidence and mortality rates, respectively. In this regard, 2012 global cancer statistics estimated a total of 238,700 new ovarian cancer cases and 151,900 deaths from ovarian cancer<sup>4</sup>.

Based on epidemiological studies, ovarian cancer risk is positively correlated with the ovulation status. In this respect, it was found that pregnancy and the use of oral contraception may decrease the risk of ovarian cancer because they are

---

\*The 5-year observed survival proportion is an epidemiological measure that estimates the proportion of cancer patients who remain alive after five years from diagnosis.

associated with decreased ovulation. Similarly, lactation, tubal ligation, and hysterectomy are associated with decreased risk of ovarian cancer<sup>5-8</sup>. Conversely, nulliparity<sup>†</sup>, early menarche, late menopause, increasing age, perineal talc use, endometriosis, Lynch syndrome, BRCA1/2 mutation and positive family history of ovarian or breast cancer together with infertility therapeutics that stimulate ovulation may increase the risk of ovarian cancer<sup>2,5,8-12</sup>.

### **1.1.2 Types and histotypes of ovarian tumors**

Ovarian tumors are a group of different diseases with distinct origin, molecular and histological properties, which have common anatomical location—the ovary<sup>13</sup>. In this sense, they have been classified based on their origin into three major types: surface epithelial-stromal tumors, sex cord-stromal tumors and germ cell tumors<sup>14</sup>.

Surface epithelial-stromal tumors were believed to originate from the ovarian surface epithelium (OSE), although this is currently controversial as detailed later. On the other hand, the sex cord-stromal and germ cell tumors arise from the granulosa-theca cells and ovarian germ cells, respectively<sup>14</sup>. Each of these three types has a number of subtypes with distinct histological and molecular features, as detailed in the World Health Organization (WHO)-approved classification<sup>15</sup>.

Based on histology, surface epithelial-stromal tumors are further subdivided into histotypes. The four major histotypes are serous, mucinous, endometrioid, and clear cell ovarian tumors<sup>13</sup>. Other less common histotypes include the transitional cell (Brenner type), squamous, mixed, and undifferentiated

---

<sup>†</sup> Nulliparity refers to women's status of never giving birth to children

histotypes<sup>5,16</sup>. Surface epithelial-stromal tumors that are not assigned a specific histotype are termed adenocarcinomas not otherwise specified (NOS)<sup>14</sup>.

Some extraovarian malignancies, which exist in the pelvic and abdominal cavities concomitantly with ovarian tumors, have identical histological and clinical properties to those of ovarian tumors. However, it cannot be determined whether the ovarian tumor is the origin of these extraovarian tumors or whether they simply have common features due to their shared embryonic precursor —the coelomic mesothelium. In such cases, these malignancies are classified as extraovarian peritoneal carcinoma<sup>5,14</sup>.

As mentioned above, the histotypes of ovarian cancer have distinctive origin, histological features, risk factors, genetic aberrations, tumor marker profiles, and therapeutic response<sup>16</sup>. In addition, each of these histotypes is further divided into benign, borderline and malignant categories<sup>14,17</sup>. Borderline tumors demonstrate low malignant potential (LMP), with epithelial proliferation in a fashion similar to malignant tumors, but without invasion of the adjacent stroma. However, they may also metastasize in 10% of cases<sup>18</sup>. **Table 1.1** summarizes the features of the major four histotypes of surface epithelial-stromal tumors and **Figure 1.1** shows representative images of these subtypes.

Malignant surface epithelial-stromal tumors are simply termed epithelial ovarian cancer (EOC), which will be the focus of the thesis and therefore will be reviewed in detail below.



**Table 1.1 List of epithelial ovarian cancer (EOC) histotypes and their characteristics** (compiled from text in Ref. 14)

<b>A. Serous EOC</b>
<ul style="list-style-type: none"> <li>▪ Composed of cells resembling those lining the fallopian tube</li> <li>▪ Malignant serous EOC is the most common EOC subtype, and constitutes 50% of all ovarian malignancies</li> </ul>
<b>B. Mucinous EOC</b>
<ul style="list-style-type: none"> <li>▪ Composed of cells resembling those of the endocervical epithelium (endocervical/müllerian type) or those of the intestinal epithelium (intestinal type)</li> <li>▪ Borderline intestinal-type or malignant mucinous EOC may be associated with <i>pseudomyxoma peritonei</i> (abdominal and pelvic accumulation of large amounts of mucoid material with few tumor cells independent of primary tumor dissemination)</li> <li>▪ Malignant mucinous EOC constitute 5–10% of all malignant ovarian malignancies</li> </ul>
<b>C. Endometrioid EOC</b>
<ul style="list-style-type: none"> <li>▪ Composed of cells resembling those lining the uterus (endometrial cells)</li> <li>▪ May be linked with endometriosis or endometrial cancer</li> <li>▪ Malignant endometrioid EOC is the second most common EOC subtype, and constitutes 10–25% of all ovarian malignancies.</li> <li>▪ It has a better prognosis than either mucinous or serous subtypes</li> </ul>
<b>D. Clear cell EOC</b>
<ul style="list-style-type: none"> <li>▪ Composed of clear, peg-like or hobnail-like cells</li> <li>▪ Mostly malignant; benign and borderline tumors are scarce</li> <li>▪ Clear cell EOC constitutes 4–5% of all ovarian malignancies</li> <li>▪ It has the worst prognosis among all other EOC subtypes</li> </ul>

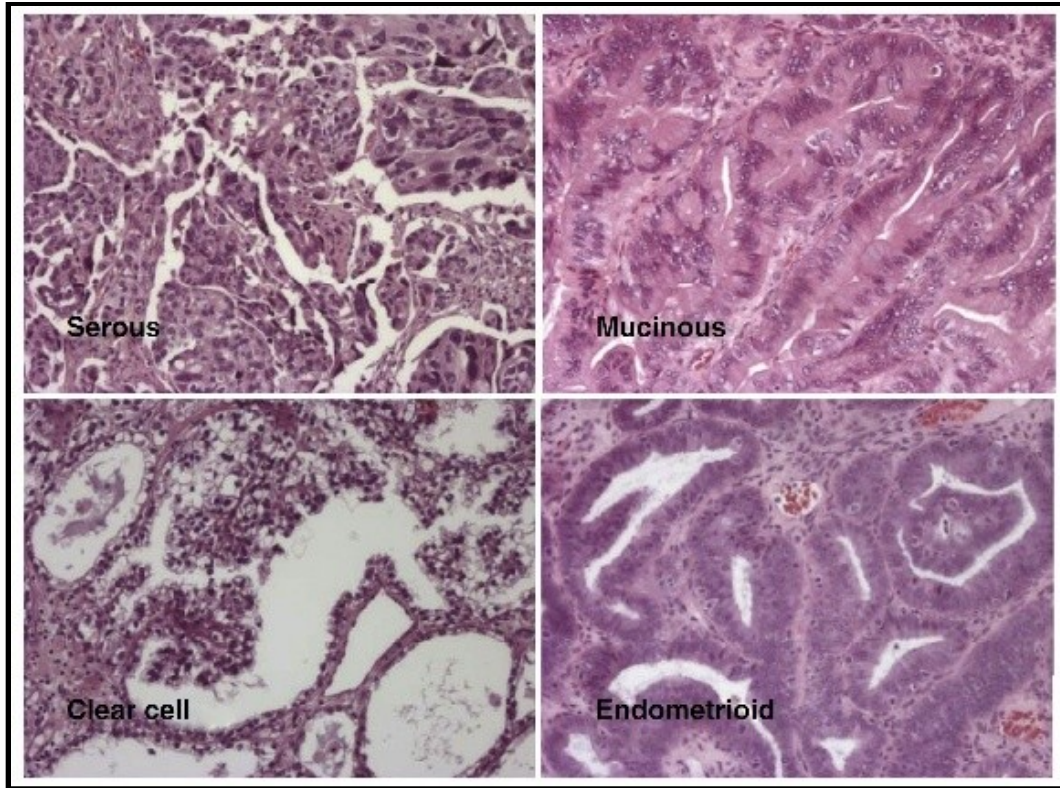


**Figure 1.1 Representative images of the four major histotypes of EOC.** The major histotypes of EOC are serous, mucinous, clear cell, and endometrioid histotypes. Other less common histotypes include the transitional cell (Brenner type), squamous, mixed, and undifferentiated histotypes (*not* shown). Reproduced with permission from Bast *et al.*, 2014<sup>16</sup>.

### **1.1.3 Staging of ovarian cancer**

A staging system for ovarian cancer has been developed by the International Federation of Gynecology and Obstetrics (FIGO), with the purpose of standardizing disease terminology worldwide and stratifying patients into prognostic groups with specific treatment options<sup>19</sup>. Based on this staging system, ovarian cancer is classified into four stages (I through IV) dependent on ovarian, pelvic, or peritoneal involvement, and the presence of distant metastases<sup>2</sup>. Stage I is limited to the ovaries, while stage II involves pelvic extension or primary peritoneal cancer. In stage III, the disease involves spread to the peritoneum and/or metastasis to the retroperitoneal lymph nodes. Stage IV involves distant metastasis excluding peritoneal metastases<sup>20</sup>. Early-stage ovarian cancer includes stages I and II, while advanced-stage ovarian cancer includes stages III and IV<sup>5</sup>.

### **1.1.4 Grades of epithelial ovarian cancer (EOC)**

EOC is the most common type of ovarian cancer representing approximately 90% of all ovarian malignancies. EOC is classified into type I (low-grade) and type II (high-grade) based on the growth rate, expression profile, prognosis, and response to therapy<sup>21</sup>. This classification is usually combined with the histotype-based classification, so that a specific histotype may be described as low- or high-grade. Low-grade EOC includes low-grade and borderline serous cancers, low-grade endometrioid cancers, together with mucinous and clear-cell cancers. High-grade EOC represents the majority of EOCs, and includes high-grade serous cancers, and high-grade endometrioid cancers<sup>18,22-24</sup>. The two types differ in terms of their underlying genetic and epigenetic aberrations. Low-grade EOC is

diagnosed in early stages (I or II), demonstrates slow growth properties, is resistant to conventional chemotherapy, and frequently estrogen receptor-positive and therefore may respond to hormonal therapy<sup>18,22-24</sup>.

On the other hand, high-grade EOC is more common, diagnosed in later stages (III or IV), grows rapidly, responds better to chemotherapy, but shows less response to hormonal therapy<sup>18,22-24</sup>.

### **1.1.5 Clinical presentation and diagnosis of EOC**

Ovarian cancer typically presents as a cystic mass in the pelvic region. It has been named the “silent killer” because a large percentage of early-stage ovarian cancer patients are asymptomatic<sup>18,25</sup>. Conflicting with this is another study that reports 95% of patients had symptoms before diagnosis<sup>19</sup>. The symptoms are, however, nonspecific and resemble those of other gastrointestinal, genitourinary and gynecological conditions. Therefore, symptom-based early diagnosis of ovarian cancers is still elusive. **Table 1.2** enlists the reported symptoms and physical findings of ovarian cancer.

Generally, ovarian cancer should be suspected in women with enlarged or palpable ovary. In this respect, transvaginal ultrasonography is preferred to computed tomography (CT) scanning in the assessment of pelvic masses<sup>25</sup>. A transvaginal ultrasonogram demonstrating complex ovarian cysts composed of both solid and cystic components provides preliminary diagnosis of ovarian cancer, which needs to be confirmed surgically rather than by percutaneous biopsy to avoid tumor spillage<sup>25</sup>. Elevated postmenopausal CA-125 (MUC16) serum levels together with the presence of an abdominal or pelvic mass is highly

suggestive, but not diagnostic, of ovarian cancer. CA-125 serum levels are more important in the screening and early detection of ovarian cancer<sup>18,25</sup>, the assessment of response to chemotherapy<sup>4,5,26,27</sup> and the early detection of recurrent disease<sup>17</sup>. **Figure 1.1** shows an intraoperative appearance and a transvaginal ultrasonogram of EOC.

#### **1.1.6 Origin of EOC**

There was a prevailing theory that EOC originates either directly from OSE or from cortical inclusion cysts (CICs) that are derived from OSE<sup>28-30</sup>. This theory proved recently to be very controversial<sup>11</sup>. The reason for this controversy is the inability of pathologists to find *in situ* ovarian lesion. In this respect, high-grade serous EOC is the only epithelial cancer lacking an established precancerous lesion<sup>31</sup>. In addition, EOC histotypes resemble epithelia of extraovarian sites in terms of histologic features. Serous EOC exhibits tissue architecture similar to that of the surface epithelium of the fallopian tube, endometrioid and clear-cell EOC resemble endometrioid carcinomas of the uterus, and mucinous EOC resembles endocervical glands or gastrointestinal epithelium<sup>31</sup>. This led scientists to postulate that EOC represents metastases from extraovarian cancer lesions<sup>13,32-34</sup>. An additional dimension to this controversy is the embryonic origin of the ovary as compared to other extraovarian sites. Whereas the ovary and its OSE are of coelomic origin, EOC is histologically similar to normal fallopian tubes, endocervical glands and endometrium. These structures arise from the müllerian duct, which has a mesodermal origin. The mechanism by which ovarian tumorigenesis elicits transformation into müllerian-like histology is not well

understood<sup>31</sup>. In 2005, it was demonstrated that *HOX* genes play an important role in this transformation<sup>23,24</sup>.

**Table 1.2 List of symptoms and physical findings of ovarian cancer** (compiled from texts in Refs. 5,25)

<b>A. Symptoms</b>
<ul style="list-style-type: none"> <li>▪ Abdominal fullness</li> <li>▪ Pain (abdominal, pelvic, side of trunk, flank, back, rectal)</li> <li>▪ Bloating (due to increased abdominal pressure from ascites or involvement of the omentum)</li> <li>▪ Dyspepsia, food intolerance, intestinal gas</li> <li>▪ Diarrhoea</li> <li>▪ Vomiting</li> <li>▪ Early satiety, anorexia</li> <li>▪ Fatigue, low energy, general weakness</li> <li>▪ Headache</li> <li>▪ Shortness of breath</li> <li>▪ Unintentional weight loss</li> <li>▪ Urinary burning, dysuria</li> </ul>
<b>B. Physical findings</b>
<ul style="list-style-type: none"> <li>▪ Palpable ovarian mass</li> <li>▪ Ascites</li> <li>▪ Pleural effusions</li> <li>▪ Sister Mary Joseph's nodule (an umbilical mass non-specific to ovarian cancer that can be linked to gastric, pancreatic, gallbladder, colon, and appendiceal cancers)</li> <li>▪ Extraabdominal involvement of the pleural space and occasionally pulmonary parenchyma</li> <li>▪ Paraneoplastic syndromes such as hypercalcemia and subacute cerebellar degeneration associated with anti-Purkinje-cell antibodies</li> <li>▪ Leser-Trélat sign (sudden appearance of seborrheic keratoses) occasionally foretells ovarian cancer</li> <li>▪ Trousseau's syndrome (migratory superficial thrombophlebitis): palmar fasciitis, dermatomyositis, and polyarthrititis</li> </ul>

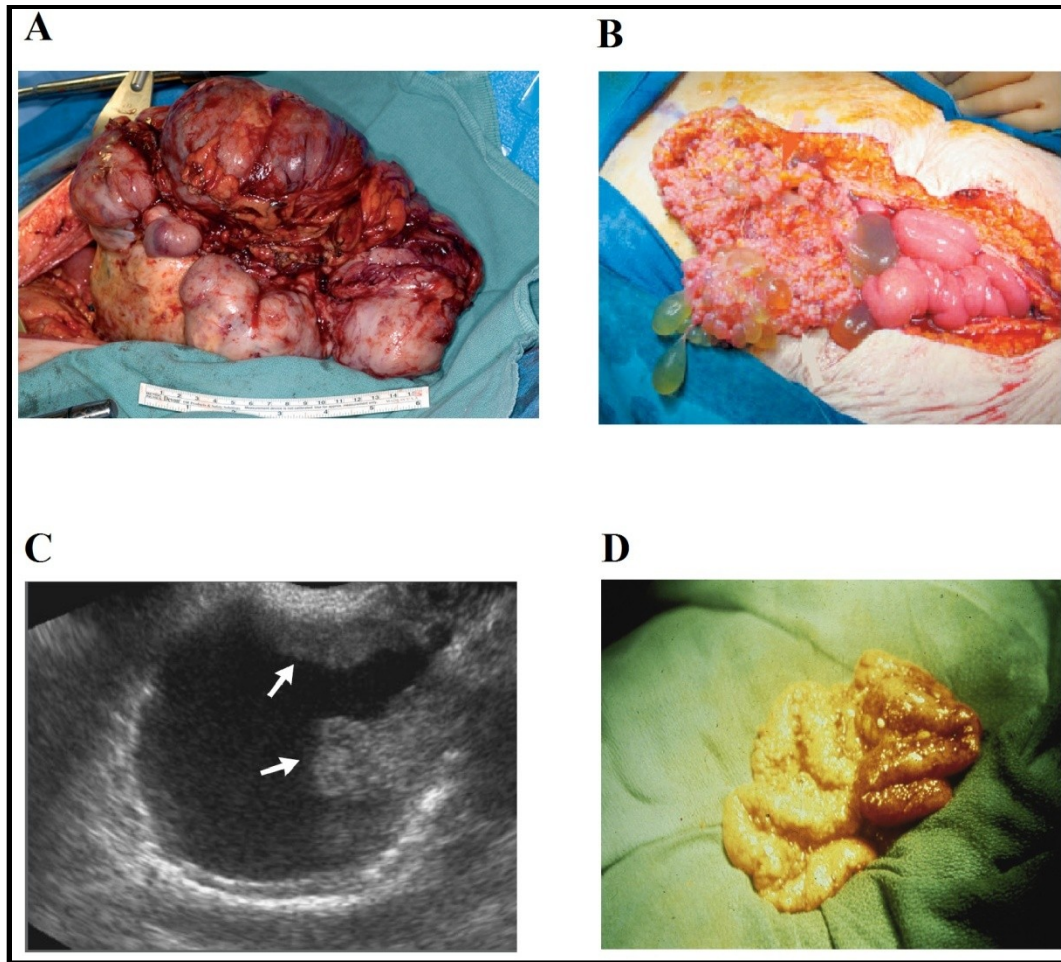


**Figure 1.2 Representative images of the appearance of EOC.** A and B, Typical intraoperative appearance of advanced EOC with omental involvement. C, Typical appearance of a complex cyst on a transvaginal ultrasonogram; arrows indicate solid components within the fluid-filled cyst D, Intraperitoneal metastases from EOC on the peritoneal surface. Figures were reproduced with permission from the following references: Figure A from Hennessy *et al.*, 2009<sup>5</sup>, Figures B and C from Cannistra, 2004<sup>25</sup> (copyright Massachusetts Medical Society), and Figure D from Bast *et al.*, 2014<sup>16</sup>.



To resolve the controversy regarding EOC origin, it was hypothesized that EOC arises from extraovarian sites such as the fallopian tube epithelium and the mesothelium covering the surface of the peritoneal cavity<sup>31</sup>. This hypothesis has been extensively reviewed<sup>22,30,35-40</sup> and was experimentally tested in mouse models<sup>41,42</sup>.

Briefly, it was previously proposed that EOC originates from OSE because of ‘incessant ovulation’ associated with continuous destruction and repair of OSE together with the formation of CICs and surges of hormones and cytokines in the ovarian microenvironment. These events lead to an inflammatory environment that is conducive to ovarian tumorigenesis<sup>28</sup>. This theory proved to be partially correct as evidenced by subsequent epidemiologic and experimental studies that support the role of inflammation and incessant ovulation in EOC tumorigenesis<sup>5,22,29</sup>.

Recently, it has been proposed that a large proportion of the major ovarian malignancy— high-grade serous EOC, arises from carcinoma of the fallopian tube called serous tubal intraepithelial carcinoma (STIC) which spreads to the ovary. A small proportion, however, is believed to arise from CICs formed after implantation of tubal (müllerian) tissue rather than metaplastic OSE (mesothelial coloemic) tissue<sup>22</sup>. In this sense, the origin of high-grade serous EOC is assumed to be tubal rather than ovarian. The ovarian microenvironment was found to be more supportive of tumor progression than the tubal microenvironment. **Figure 1.2** summarizes the proposed theories regarding the origin of EOC.

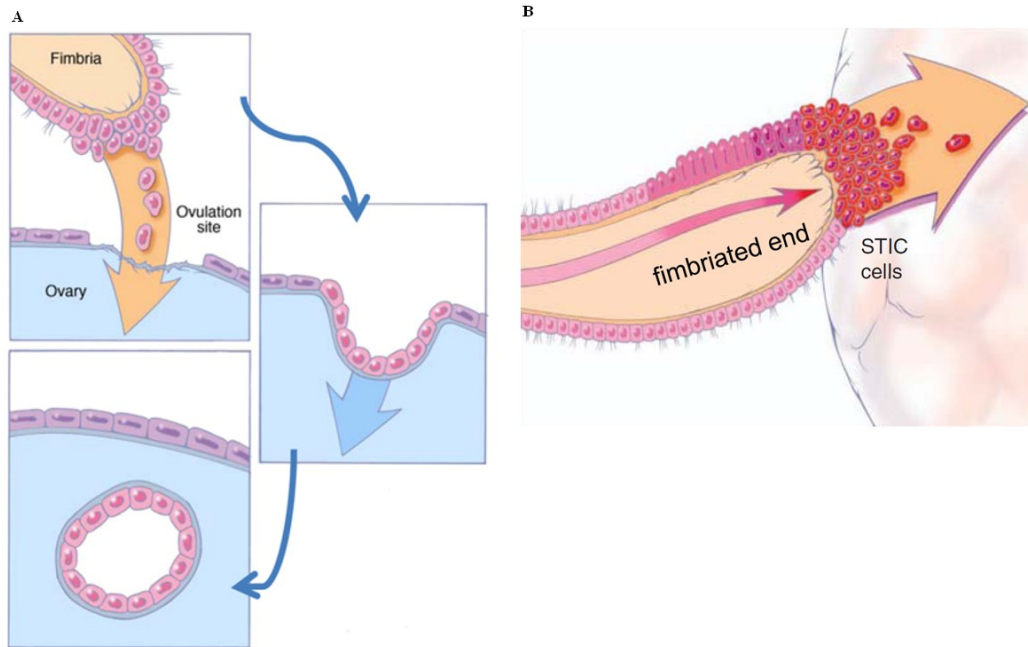


**Figure 1.3 Proposed origin of EOC.** A, Fallopian tubes fimbria shed normal cells on the ovary, which undergo invagination and formation of CICs. CICs, in the proinflammatory ovarian microenvironment, undergo malignant transformation and develop EOC. B, STIC cells directly disseminate or exfoliate onto the ovarian surface and start tumor progression to form a new tumor seemingly arising in the ovary. Figures and text adapted with permission from Kurman and Shih, 2010<sup>39</sup>.

### 1.1.7 Molecular pathogenesis of EOC

EOC is a heterogeneous disease with a multitude of genetic and epigenetic defects<sup>13,16,18</sup>. Both inactivating (deletion, loss of heterozygosity, mutation, promoter methylation) and activating (amplification, mutation and hypomethylation) genetic and epigenetic aberrations have been documented<sup>16</sup>. Histone modifications and miRNAs have been also implicated in EOC. The extent of genomic instability has been found to positively correlate with the high tumor grade and late stages<sup>18</sup>.

Germline mutations of *BRCA1*, *BRCA2* and hereditary non-polyposis colorectal cancer (HNPCC) mismatch repair genes are found in approximately 10–15% of ovarian cancers. These germline mutations contribute to genomic instability in hereditary cases of EOC, together with *TP53* which is mutated in 60–80% of both sporadic and familial cases<sup>18</sup>.

Other examples of aberrant tumor suppressor genes in EOC include *PTEN* (Phosphatase and tensin homolog), *ARHI* (*DIRAS3*), *PLAGL1* (pleiomorphic adenoma genelike 1), and *PEG3* (paternally expressed 3). *RASSF1* (Ras association domain family member 1), *DLEC1* (deleted in lung and esophageal cancer 1) and *OPCML* (opioid binding protein/cell adhesion molecule-like) were also reported to be epigenetically silenced in EOC<sup>16,18,43,44</sup>.

Along with tumor suppressor genes, a number of oncogenes have been implicated in the pathogenesis of EOC such as *KRAS*, *PIK3CA* (Phosphoinositide 3-kinase catalytic subunit- $\alpha$ ), *BRAF*, *RAB25*, *CTNNB1* ( $\beta$ -catenin), *PRKCI*, *MYC*, *EGFR*, and *NOTCH3*<sup>18,43</sup>.

As mentioned above, the genetic and epigenetic profiles of different EOC types are among the criteria used for the classification of EOC into two prognostic grades—low-grade (type I) and high-grade (type II) EOC. Low-grade EOCs exhibit more frequent *PTEN*, *PIK3CA*, *KRAS*, *BRAF* and *CTNNB1* mutations. *TP53* mutations occur in a small fraction of these cases; therefore, genomic instability is lower in low-grade EOC. Conversely, high-grade EOCs have *TP53* mutations in approximately 80% of cases which leads to marked genomic instability<sup>45</sup>.

Specifically, low-grade serous EOC is characterized by mutations in *KRAS* and/or *BRAF* ( $\geq 60\%$ ). Low-grade endometrioid EOC have mutations in *CTNNB1*, *PTEN* and *PIK3CA* with microsatellite instability. Mucinous EOC, a low-grade EOC, exhibits mutations in *KRAS*, and *TP53* mutation associated with transition from borderline tumor to carcinoma. Clear cell EOC has *PTEN* mutation or loss of heterozygosity together with *PIK3CA* mutation. On the other hand, high-grade serous EOC have *TP53* mutation (up to 80%) and aberrant *BRCAl*. In addition, high-grade endometrioid EOC resembles the serous phenotype together with having *PIK3CA* mutations<sup>18</sup>.

All these genetic aberrations are responsible for the aberrant signaling of EOC. In this respect, a number of signaling pathways are activated in EOC including PI3K (70%), Src ( $>50\%$ ), IL-6–IL-6R or JAK–STAT3 (70%), lysophosphatidic acid (LPA; 90%), MEKK3–IKK–NF- $\kappa$ B ( $>50\%$ ), PKC $\iota$  (78%), RAS–MEK–MAPK ( $<50\%$ ; mostly in low-grade EOC), Endothelin receptor, NOTCH, Wnt, Müllerian inhibition substance (MIS) and vascular endothelial

growth factor (VEGF) signaling pathways<sup>2,16,18,43</sup>. As a result, alterations in the biology of ovarian/tubal cells (survival, proliferation, epithelial-mesenchymal transition [EMT], stemness, DNA repair, metabolism, and angiogenesis) contribute to EOC development and progression.

#### **1.1.8 Management of EOC**

Upon preliminary diagnosis of EOC based on findings from physical examination and transvaginal ultrasonography, surgery is indicated for the purpose of histopathological definitive diagnosis, tumor debulking (primary cytoreduction), and assessment of the FIGO stage<sup>2,25,46</sup>. Surgery includes total hysterectomy, bilateral salpingo-oophorectomy, tumor debulking, and omentectomy<sup>47,48</sup>. The goal of cytoreduction is to achieve total macroscopic tumor clearance with minimal residual visible disease<sup>46</sup>. Cytoreductive surgery with minimal residual disease has been associated with high survival rates<sup>49</sup>. Neoadjuvant (preoperative) platinum-based chemotherapy is indicated in cases where complete cytoreduction is not possible<sup>2,46,50</sup>.

It has been recommended that patients with early-stage (I/IIa) EOC receive adjuvant platinum-based chemotherapy due to positive effects on patient survival<sup>51,52</sup>. There is no data regarding superiority of platinum-paclitaxel combination to platinum therapy alone in such settings<sup>25,46</sup>.

For advanced disease (stage III/IV), platinum-based chemotherapy has been the first-line chemotherapy for approximately 40 years<sup>2,13</sup>. Currently, the standard of care chemotherapy in advanced EOC is carboplatin (at least 6 cycles) in

combination with paclitaxel<sup>53,54</sup>. This chemotherapy regimen continues for approximately 4.5 months<sup>2</sup>.

Clinical trials have shown a clinical benefit of the high-dose intraperitoneal carboplatin as compared to the low-dose intravenous carboplatin<sup>55-57</sup>. Likewise, a dose-dense weekly regimen of paclitaxel was found to be superior to conventional regimens in terms of progression-free survival (PFS) and overall survival (OS)<sup>58,59</sup>. **Table 1.3** details the adjuvant chemotherapy regimen of EOC.

In addition, new developments in understanding EOC biology led to the incorporation of novel molecularly targeted therapeutics in therapeutic regimens. In this respect, bevacizumab (antibody that targets VEGF) and pazopanib (VEGF receptor tyrosine kinase inhibitor) were used as maintenance therapeutics<sup>2,60,61</sup>.

**Table 1.3 Primary adjuvant chemotherapy for EOC** (reproduced with permission from Ref. 8)

<b>Intravenous regimens</b>	1) Paclitaxel (175 mg/m <sup>2</sup> over 3 h IV) followed by carboplatin (AUC 5-7.5 IV over 1 h) on day 1, every 3 weeks for 6 cycles
	2) Docetaxel (60-75 mg/m <sup>2</sup> over 1 h IV) followed by carboplatin (AUC 5-6 IV over 1 h) on day 1, every 3 weeks for 6 cycles
	3) Dose-dense paclitaxel (80 mg/m <sup>2</sup> IV over 1 h) on days 1, 8, and 15 plus carboplatin (AUC 6 IV over 1 h) on day 1, every 3 weeks for 6 cycles
<b>Intraperitoneal regimen</b>	Paclitaxel (135 mg/m <sup>2</sup> IV infusion over 24 h) on day 1, cisplatin (75-100 mg/m <sup>2</sup> IP) on day 2, and paclitaxel (60 mg/m <sup>2</sup> IP) on day 8, every 3 weeks for 6 cycles

*AUC: area under the curve; IV: intravenous; h: hour; IP: intraperitoneal*

### **1.1.9 Recurrence of EOC**

Recurrence of EOC can be detected by monitoring serum CA-125 concentration. CA-125 level doubling constitutes an early indicator of recurrent disease. In such settings, second-line chemotherapy is indicated<sup>8</sup>. The choice of chemotherapeutic agents largely depends on the nature of the recurrent disease as to platinum sensitivity. In this regard, recurrent EOC developing in less than 6 months following platinum chemotherapy is considered platinum-resistant. Otherwise, platinum sensitivity is expected if recurrence occurs beyond 6 months in direct proportionality to the latency of the recurrence after platinum treatment<sup>8</sup>.

For platinum-sensitive recurrent EOC, carboplatin is used alone or in combination with either paclitaxel or gemcitabine. Carboplatin can be alternatively followed by a second agent with efficacy against EOC. This paradigm is termed sequential drug delivery<sup>62</sup>. On the other hand, platinum-resistant recurrent EOC is treated with other agents such as altretamine, bevacizumab, docetaxel, epirubicin, etoposide, gemcitabine, ifosfamide, irinotecan, liposomal doxorubicin, paclitaxel, tamoxifen, topotecan or vinorelbine<sup>62</sup>.

### **1.1.10 Platinum-resistant EOC**

Platinum resistance in the context of EOC was defined as “the absence of response to primary platinum therapy or the recurrence of the disease within 6 months of platinum treatment despite initial response”<sup>62-64</sup>. More recently, another classification divided EOC based on response to platinum therapy into 4 categories. The ‘platinum-refractory’ category includes patients with disease



progression during treatment or within 4 weeks following the last dose; ‘platinum-resistant’ category includes patients with progression within 6 months of platinum treatment; ‘partially platinum-sensitive’ category with disease progressing between 6 and 12 months; and ‘platinum-sensitive’ category with disease progressing after 12 months<sup>8,65,66</sup>.

Most patients with recurrent EOC will ultimately have platinum-refractory/resistant disease<sup>8,46</sup>. Patients in these categories were found to have poor prognosis with short OS (less than 12 months). As discussed above, a number of agents can be administered in such settings. Therefore, the priority, in drug selection, is given to those agents with favorable safety profiles to maintain or improve the patient’s quality of life<sup>8,46</sup>. In line with this strategy, sequential single agents rather than combination treatments are employed to minimize possible toxicities<sup>46</sup>.

At the molecular level, a number of mechanisms have been implicated in EOC resistance to platinum therapy<sup>67,68</sup>. These mechanisms will be covered later in **Section 1.2**.

#### **1.1.11 Novel therapeutics of EOC**

Recent advances in understanding the biology of EOC led to the emergence of a multitude of novel therapeutics with the aim of achieving better efficacy and tolerability along with overcoming resistance<sup>2,18,69</sup>.

As mentioned above, a proportion of EOC patients harbor *BRCA1/2* mutations. Since *BRCA1/2* are essential for double-stranded DNA damage repair via homologous recombination, such patients have greater dependency on the

poly(ADP-ribose) polymerase (PARP) single-strand repair pathway. Therefore, administration of PARP inhibitors to these patients leads to more effective and tumor-selective therapeutic outcomes<sup>70,71</sup>; this therapeutic approach is termed synthetic lethality<sup>72,73</sup>. In this respect, the PARP inhibitor—olaparib, has proven to be effective in clinical trials on BRCA1/2-mutated EOC patients<sup>74</sup>. As the first synthetic lethality-based clinical drug, olaparib received US Food and Drug Administration (FDA) approval in December 2014 for the “treatment of advanced ovarian cancer associated with defective BRCA genes”<sup>75</sup>.

A number of molecularly targeted therapeutics were investigated in the treatment of EOC including agents targeting angiogenesis, platelet-derived growth factor (PDGF), EGFR, ErbB receptor family, PI3K–AKT pathway, farnesyl transferase, endothelin receptor, NOTCH 3 pathway, Src kinase, mTOR, and  $\alpha$ -folate receptor ( $\alpha$ FR)<sup>8,69,76</sup>. Therapeutics targeting VEGF proved to be more promising candidates than other investigational molecularly targeted therapeutics<sup>8,69,76</sup>.

### **1.1.12 Experimental models of EOC**

EOC have been experimentally studied using a number of preclinical models with varying advantages and disadvantages. These models include cell lines developed from ascites or whole tumor tissue of EOC patients such as HEYA8, OVCAR-4, SKOV3 and CAOV-3 cells<sup>21,77</sup>. A recent report evaluated cell lines in terms of their representativeness of high-grade serous EOC (HGSEOC), and consequently classified these cell lines into *likely*, *possibly* and *unlikely* to be HGSEOC<sup>78</sup>. Based on this classification, OVCAR-4 and CAOV-3 are *likely* high-

grade serous, ES2 and OV90 are *possibly* high-grade serous, whereas HEYA8, SKOV3 and A2780 are *unlikely* high-grade serous.

Resistance can be modeled by exposing the parental cell line to the chemotherapeutic agent of interest to develop a laboratory-evolved paired resistance model such as A2780s (cisplatin-sensitive) and A2780cp (cisplatin-resistant) cells<sup>79</sup>. This model has been used in our study to explore novel molecular mechanisms of chemoresistance to carboplatin. Other models include three-dimensional (3D) culture models that mimic the tumor microenvironment effect, co-culture of mesothelial cells with EOC cells, and complex 3D organotypic models with epithelial and stromal components including the superficial layer of the peritoneum (mesothelium). Other models include spontaneous, xenograft, syngeneic and transgenic mouse models of EOC<sup>21,77</sup>.

## 1.2 Platinum-based cancer therapeutics

### 1.2.1 Discovery of platinum-based compounds

Cisplatin (*cis*-diamminedichloroplatinum [cis-DDP ];  $\text{PtII}(\text{NH}_3)_2\text{Cl}_2$ ) is the prototype of platinum-based antineoplastic agents<sup>48</sup>. Initially termed Peyrone's chloride or Peyrone's salt, it was chemically synthesized and characterized by Michele Peyrone in 1845<sup>80,81</sup>. More than a century later, it was accidentally rediscovered by Barnett Rosenberg in 1965<sup>82</sup>. Rosenberg was studying the effect of electric field on cell division of *Escherichia coli*. In his experiments, he observed that *E. coli* changed from short rods into long filaments upon the application of the electric field. Unexpectedly, the observed effect was found to be elicited by the electrolysis products of platinum electrodes included in the growth chamber, not due to the electric field itself<sup>83</sup>. Upon chemical analysis of these products, two platinum-based compounds were identified— cisplatin and its *trans* isomer; cisplatin was much more active<sup>82</sup>. Later on, Rosenberg experimentally investigated the anticancer effect of cisplatin on a murine tumor model. In these experiments, cisplatin was found to have potent antitumor activity<sup>84</sup>. Therefore, Peyrone was the first to chemically synthesize cisplatin and Rosenberg was the first to discover its biological effects<sup>81</sup>. After a number of preclinical and clinical studies, cisplatin received FDA approval in 1978 for the treatment of metastatic testicular and ovarian cancers<sup>83,85,86</sup>.

The discovery of cisplatin was followed by other attempts to find better platinum-based compounds that broaden their spectrum of utility in different malignancies and minimize the dose-limiting toxicity of cisplatin (nephrotoxicity,

neurotoxicity and ototoxicity) together with overcoming the emerging resistance against this drug. These attempts ultimately led to the development of carboplatin (*cis*-diammine(cyclobutane-1,1-dicarboxylato) platinum (II))<sup>85,87-91</sup>. Carboplatin received FDA approval in 1989 for the palliative management of ovarian cancer after previous chemotherapy. In 1991, it was approved as a frontline agent for the treatment of ovarian cancer<sup>83</sup>. Later on, a number of other platinum-based compounds were developed including oxaliplatin, satraplatin, picoplatin, eptaplatin, lobaplatin, and nedaplatin. These agents have specific efficacy and safety profiles, although they share closely similar mechanisms of action<sup>48,83,92-95</sup>. It is also noteworthy that satraplatin is the first orally available platinum-based chemotherapeutic agent<sup>96</sup>. The chemical structures of these compounds are illustrated in **Figure 1.3**.

As mentioned in **Section 1.1.8**, carboplatin is currently the first-line and the major antineoplastic agent in the management of EOC. In addition, carboplatin is the most closely related platinum compound to cisplatin compared to other agents in this therapeutic class<sup>97,98</sup>. Moreover, most efficacy and resistance studies were conducted on cisplatin, especially in the context of EOC as it was originally used in this disease before carboplatin. Therefore, the focus in the next sections will be mainly on these two agents.

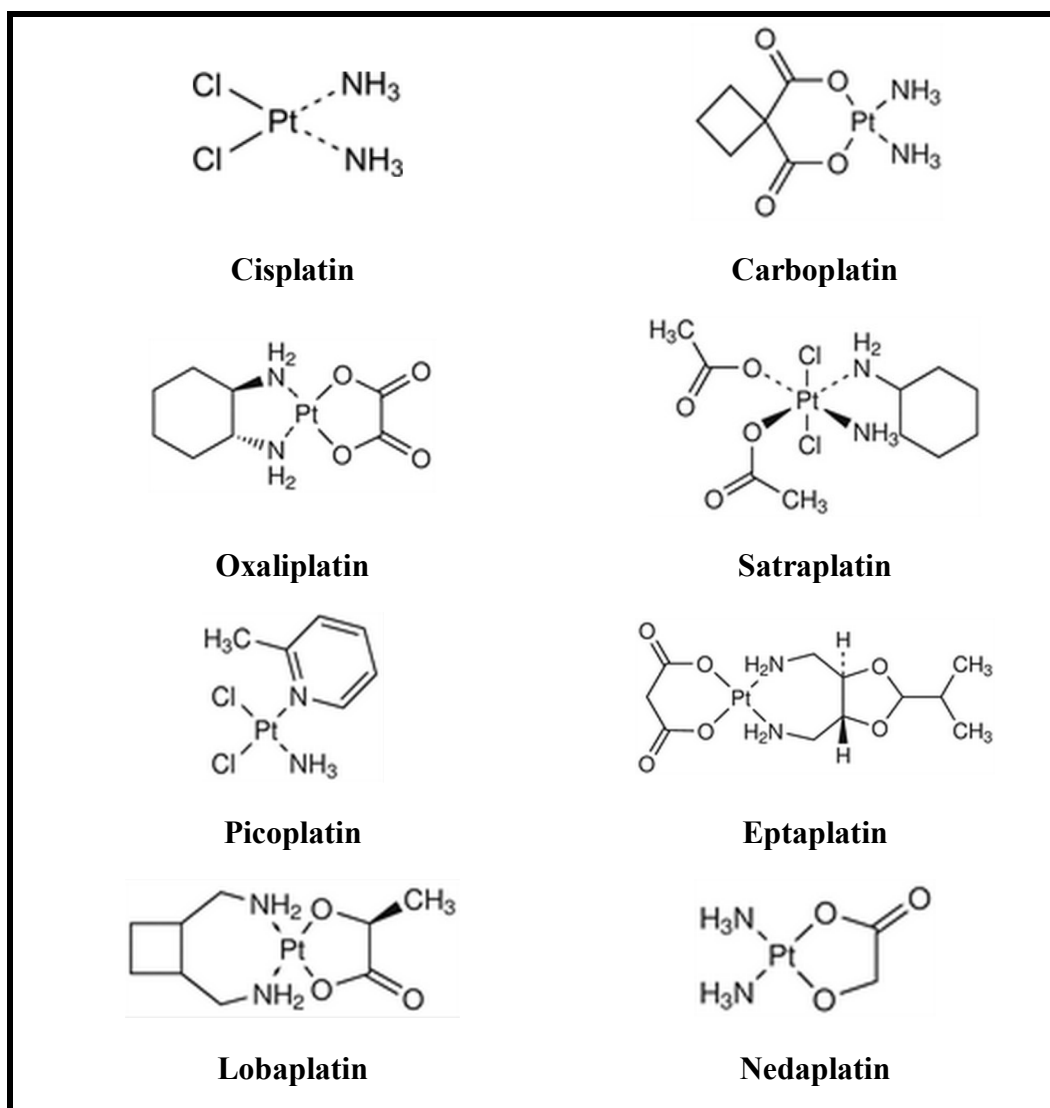


**Figure 1.4 Chemical structures of selected agents of platinum-based chemotherapeutics.** Platinating agents or platinum-based compounds represent an important class of chemotherapeutics. This class comprises many agents that share similar modes of action and specific efficacy, safety and biopharmaceutical profiles. Cisplatin and carboplatin are the only agents used in the context of EOC. These structures were retrieved from individual drug monographs in Brayfield, 2015<sup>48</sup>.

### 1.2.2 Cellular handling and mechanism of action of cisplatin and carboplatin

Although platinum-based compounds interact with several biological targets, DNA has long been considered as the primary target of these compounds. To exert their effects, it is mandatory for these drugs to pass through biological membranes to the cytosol and then to the nucleus in order to bind DNA and initiate a cascade of signaling events that mediate their cytotoxicity. This cascade will be detailed below as most resistance mechanisms are considered as alterations/adaptive responses to one or more steps of this cascade.

**i. Cellular uptake** Cisplatin and carboplatin are taken up into the cell by passive diffusion together with active transport mainly by the copper transporter CTR1 and to a lesser extent by the organic cation transporters (OCTs) OCT1, OCT2 and OCT3. Both transporter types belong to the solute carrier (SLC) family<sup>98-101</sup>. The extent of cellular accumulation of platinum-based compounds has been correlated to the chemosensitivity to these agents<sup>101</sup>. In addition, the mutual mechanisms of copper and platinum transport into the cell explain the potential of copper to competitively inhibit platinum uptake, and therefore induce resistance<sup>98</sup>. Moreover, organ-specific toxicity such as nephrotoxicity, which is a major dose-limiting side effect of cisplatin, has been associated with high renal expression of OCT2. Conversely, OCT transporters do not effectively transport carboplatin; therefore, it has lower nephrotoxicity<sup>99</sup>. Other putative uptake mechanisms include endocytosis,  $\text{Na}^+/\text{K}^+$  ATPase-gated channels and aquaporins<sup>98</sup>.

**ii. Intracellular trafficking and biotransformation** Platinum accumulates in a variety of vesicular structures most importantly lysosomes, which transport platinum into the nucleus. Accumulation in the lysosomes might occur by transport of cytosolic platinum via the intracellular copper adenosine triphosphate transporters ATP7A and ATP7B or by direct transport of extracellular platinum via the endocytotic route<sup>99</sup>. Cytosolic platinum may be also directly transported to the nucleus by passive diffusion<sup>101</sup>.

To exert its action, cytosolic platinum undergoes an essential aquation (speciation; hydrolysis) step in which one or more leaving groups (chloride groups in cisplatin) are replaced by water molecule<sup>83,98</sup>. Chemically, this aquation step converts cisplatin into a neutral molecule that can easily penetrate through the lipid bilayer of biological membranes<sup>101</sup>. Pharmacologically, this step converts cisplatin into a highly reactive metabolite that interacts readily with biomolecules such as DNA. In addition, this activation step depends on the intracellular chloride, sodium and potassium levels, pH and redox status of the cell<sup>83,98</sup>.

Since aquation is the rate-limiting step that governs interaction of platinum with DNA, the kinetics of this step is a major determinant of drug potency. In this respect, it was found that the aquation rate constant of carboplatin is approximately 100-fold lower than that of cisplatin<sup>102-104</sup>. Because of this slower activation, carboplatin is much less potent than cisplatin as it needs longer time to elicit the same extent of DNA crosslinks. To account for these differences, carboplatin has been given by continuous intravenous injection over 3–5 days in some therapeutic regimens. It is noteworthy, however, that once the same extent



of DNA damage is achieved by either drug, the efficacy is not expected to be different<sup>105</sup>.

Cytosolic platinum may be inactivated by conjugation with thiol-containing biomolecules such as metallothioneins or glutathione. The latter reaction is catalyzed by glutathione S-transferases (GSTs). These conjugation reactions interfere with the accumulation of effective concentrations of platinum in the nucleus<sup>83</sup>.

**iii. Cellular and nuclear efflux** Cytosolic platinum can be directly effluxed by ATP7A/B. Alternatively, the glutathione S-conjugates are effluxed by multidrug resistance protein-1 (MRP2; ABCC2), MDR1 (ABCB1), MRP1 (ABCC1), MRP3 (ABCC3) and MRP5 (ABCC5) pumps<sup>83</sup>. At the nuclear membrane level, a nuclear extrusion transporter termed lung resistance related protein (LRP) has been implicated in nuclear cisplatin efflux<sup>99,101</sup>. The expression of these transporters has been correlated with chemoresistance<sup>83</sup>. **Figure 1.4** summarizes the cellular handling of extracellular and cytosolic platinum.

**iv. Interaction with DNA** As mentioned above, the aquated platinum metabolite possesses high reactivity towards biomolecules including DNA. It covalently binds to DNA at the N7 position of the imidazole ring of purine bases mainly guanine (G) and to a lesser extent adenine (A). As a result, it forms either monofunctional/bifunctional crosslinks or adducts via replacement of one/two leaving groups, respectively. The two amine groups (carrier ligands) remain attached to platinum<sup>106</sup>.

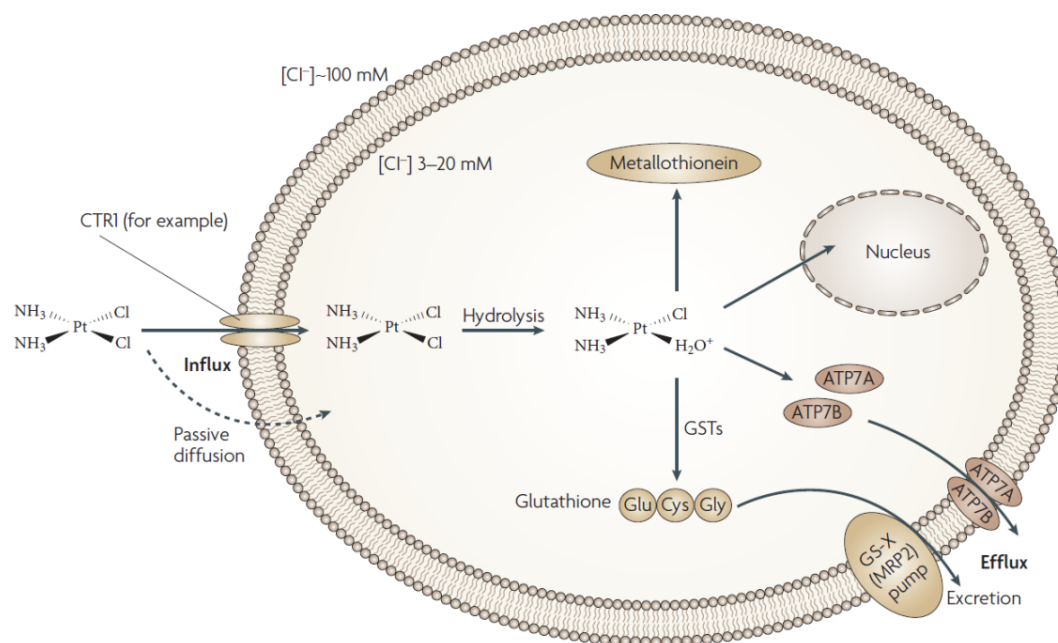


**Figure 1.5 Cellular handling of extracellular and cytosolic platinum.**

Extracellular platinum is taken up by the cell via passive diffusion or active transport mainly by CTR1. The intracellular platinum is then activated by an aquation step that depends on intracellular chloride levels. A fraction of aquated platinum is transported to the nucleus where it binds its primary target—DNA. Another fraction is either directly effluxed by ATP7A/B transporters or after conjugation with thiol-containing biomolecules such as metallothioneins or glutathione, then effluxed by the MRP2 pump. The expression level of these biomolecules is among the determinants of resistance to platinum. Cisplatin is shown here, and most of the mechanisms apply to carboplatin. Reproduced with permission from Kelland, 2007<sup>83</sup>.

The majority of the crosslinks involves bases on the same DNA strand, and are therefore termed intrastrand crosslinks. Approximately 80-90% of all adducts involve adjacent bases. The GpG 1,2-intrastrand crosslinks constitute 60–65% of all crosslinks as compared to the ApG 1,2-intrastrand crosslinks which constitute 20–25%<sup>83</sup>. In addition, non-adjacent bases may be involved as is the case with the GpXpG 1,3-intrastrand crosslink (X stands for an intervening base) which occur at a frequency of approximately 2%. Guanine monofunctional adducts rarely occur ( $\approx$  2%). On the other hand, guanine bases on opposite strands may be involved in the formation of G–G interstrand crosslinks. These occur rarely at a frequency of approximately 2% of all adducts<sup>83,107-109</sup>. Generally speaking, the extent of platinum cytotoxicity is directly proportional to the total level of platinum bound to DNA especially intrastrand DNA crosslinks<sup>110</sup>.

**v. Recognition of DNA damage** The formation of DNA adducts/crosslinks initiates a cascade of signaling events that start with DNA damage recognition. DNA distortion elicited by adduct formation widens the DNA minor groove surface available for binding by more than 20 proteins, including high-mobility group (HMG) proteins (HMG1 and HMG2), DNA repair proteins (hMSH2 or hMutS $\alpha$  proteins of the mismatch repair [MMR] complex), transcription factors (upstream binding factor [hUBF] and TATA binding protein [TBP]) and histone H1<sup>98,110,111</sup>. These proteins may exhibit more preferential binding to adducts formed by specific platinum compounds compared to others<sup>110</sup>. Moreover, each of them may initiate distinct downstream signaling events that contribute differently to platinum-induced cytotoxicity. These signaling events lead ultimately to a

number of outcomes including inhibition of replication and transcription, cell cycle arrest, DNA repair and cell death<sup>98</sup>.

In addition to their signal-transducing function, these recognition proteins may have a more direct role in inducing cytotoxicity. For example, HMG1 was found to shield platinum-DNA adducts from nucleotide excision repair (NER)<sup>110</sup>.

**vi. Transduction of DNA damage signals** A number of signaling pathways are activated in response to recognition of DNA-platinum adducts including PI3K/AKT, c-ABL, p53 and MAPK/JNK/ERK pathways. These in turn modulate cell cycle checkpoints, DNA repair and cell death pathways<sup>98</sup>.

Briefly, activation of cell cycle checkpoints leads to cell cycle arrest to permit DNA damage repair. NER is the major pathway implicated in the repair of platinum–DNA adducts. The activity of the NER pathway positively correlates with resistance to platinum compounds. Accordingly, specific testicular cancer types exhibit high sensitivity to platinum due to low constitutive NER capacity<sup>83,98,112</sup>. On the other hand, the MMR pathway is critical for induction of cytotoxicity. MMR induces cell death by either initiating futile cycles of repair indirectly leading to apoptosis or invoking direct apoptotic signaling through ATM/ATR. Therefore, defective MMR has been correlated with resistance to platinum compounds. For example, downregulation of MSH2 or MLH1 (components of MMR machinery) is associated with cisplatin resistance in human ovarian tumor cell lines<sup>98,113-115</sup>.

p53 plays a central role in platinum-induced cytotoxicity. DNA damage directly and indirectly activates p53, which modulates the expression of a

multitude of downstream target genes encoding proteins involved in DNA repair, cell cycle arrest and apoptosis. These include the cyclin-dependent kinase inhibitor (CDK) inhibitor p21<sup>Waf1/Cip1</sup>, GADD45 $\alpha$ , and the pro-apoptotic protein Bax. Therefore, p53 plays an important role in both cell survival and death following platinum exposure in a complex and highly coordinated process. Generally, if the DNA damage is overwhelmingly extensive, apoptosis is induced<sup>99</sup>.

It is noteworthy that platinum compounds induce cell death via either apoptosis or necrosis at low and high doses, respectively. Apoptosis starts with translocation of Bax to the mitochondria leading to a cascade of events, involving cytochrome c release. As a result, the intrinsic apoptotic (caspase 9–caspase 3) pathway is activated and apoptosis occurs. The extrinsic (Fas/FasL-activated caspase 8–caspase 3) apoptotic pathway has also been implicated in platinum-induced cytotoxicity<sup>110</sup>. The antiapoptotic Bcl-2 family members and inhibitors of apoptosis proteins (IAPs) have a role in the regulation of apoptosis, and might contribute to resistance to chemotherapeutics including platinum-based compounds<sup>116,117</sup>.

On the other hand, excessive DNA damage induces hyperactivation of poly(ADP-ribose)polymerase (PARP), which utilizes NAD<sup>+</sup>/ATP to perform its enzymatic functions. As a result of this hyperactivity, ATP depletion may be such that it induces necrotic death<sup>98</sup>.

**vii. Non-genotoxic mechanisms of platinum-induced cytotoxicity** DNA damage has been considered to be the major trigger of platinum cytotoxicity.

However, a substantial body of evidence exists that platinum exerts its effects by mechanisms other than induction of DNA damage. These mechanisms involve lysosomal toxicity, endoplasmic reticulum stress, cytosolic events and effects involving the plasma membrane and cytoskeleton (reviewed by Sancho-Martinez *et al.*<sup>99</sup>). Consistent with this, it was found that only 1% of the gross amount of cisplatin taken up by the cell is bound to the DNA, suggesting that platinum cytotoxicity is initiated in the cytoplasm and is markedly enhanced by nuclear effects<sup>118,119</sup>. Taken together, platinum-based compounds induce a number of widespread cellular events that lead ultimately to their cytotoxic action. Nonetheless, cancer cells may exhibit inherent insensitivity to platinum compounds (intrinsic resistance) or initial responsiveness followed by development of resistance (acquired resistance). Since the focus of the thesis is on the molecular mechanisms of acquired resistance of EOC to carboplatin, these mechanisms will be reviewed in detail in the following section.

### **1.2.3 Resistance to cisplatin and carboplatin**

Antineoplastic agents frequently suffer from therapeutic failure due to decreased efficacy within safe dosage ranges— a status defined as resistance. This problem applies to platinum-based compounds despite their widespread cytotoxic effects. Resistance generally is subdivided into intrinsic and acquired categories. Intrinsic resistance constitutes the inherent insensitivity of cancer cells to antineoplastic agents as is the case with resistance of colon and renal cancers to platinum-based compounds<sup>83,110,120</sup>. This intrinsic resistance may derive from increased expression of P-glycoprotein<sup>121</sup> or from intrinsic differences in DNA

repair mechanisms<sup>122</sup>. On the other hand, acquired resistance is developed by initially sensitive cancers after repeated exposure to antineoplastic agents, as is the case with the resistance of EOC to platinum compounds<sup>123</sup>.

The definition of chemotherapy resistance varies between laboratory and clinical settings. In laboratory settings, resistance to a specific anticancer agent is defined as the increase in the median inhibitory concentration (IC<sub>50</sub>) by at least 2-fold<sup>79</sup>. In clinical settings, resistance is defined as the progression of the disease within the clinically safe therapeutic dosage ranges of the drug<sup>68</sup>. In the context of EOC, a number of clinically drug-resistant categories have been defined as discussed above in **Section 1.1.10**.

Among platinum-based compounds, most of the resistance studies have been conducted with cisplatin. In addition, cisplatin and carboplatin have been considered, in most settings, as more closely related to one another than other members of this therapeutic class. In this regard, they share a similar mode of action and a broad range of cross-resistance<sup>98,124</sup>, which might not be evident in other platinum compounds such as oxaliplatin<sup>125</sup>. Therefore, resistance to these two agents has been discussed on the grounds of having common resistance mechanisms, and this hypothesis will be adopted in this thesis<sup>115</sup>. Resistance mechanisms to platinum compounds have been extensively reviewed<sup>67,68,110,120,122,123,126-129</sup>. Here, a general outline of these mechanisms is presented, with a focus on those mechanisms encountered in the context of EOC.

Generally, acquired resistance mechanisms to platinum compounds are classified into pharmacokinetic (systemic changes that interfere with drug

accumulation in the tumor in therapeutically effective concentrations) and pharmacodynamic (localized changes that interfere with drug action; these include cancer cell- and tumor microenvironment-specific mechanisms)<sup>68</sup>.

Examples of the molecular mechanisms affecting resistance include decreased drug uptake, increased efflux, increased detoxification by conjugation, increased DNA repair (mainly NER machinery), increased tolerance to DNA damage (defective MMR machinery), and dysfunctional apoptosis<sup>110</sup>. Other mechanisms involve altered mitochondria, altered proliferative signaling (e.g. HER-2/neu and the PI3K pathways), epigenetic changes, induction of both EMT and stemness and changes in microRNAs<sup>123,126</sup>.

In EOC, a multitude of resistance mechanisms have been reported (**Table 1.4**). Nonetheless, resistance still represents a major cause of therapeutic failure in the management of EOC, resulting in a 5-year survival rate of only 30% in advanced EOC<sup>68</sup>. Therefore, it is crucial to identify novel mechanisms in order to effectively manage the platinum-resistant disease.

It is noteworthy that resistance to carboplatin is multifactorial in nature, and it is common to find multiple resistance mechanisms operative in the same patient and even in the same tumor because of inter- and intra-tumor heterogeneity, respectively. Accordingly, combination therapy is an important therapeutic strategy to overcome resistance. Another factor to consider is the clinical relevance of resistance mechanisms identified preclinically (either in cell lines or animal models), which is the case with most currently identified mechanisms<sup>110</sup>.



#### **1.2.4 Safety of cisplatin and carboplatin**

EOC was initially treated with cisplatin. As a result of its high toxicity profile (nephrotoxicity, peripheral neurotoxicity and ototoxicity), cisplatin has been replaced with carboplatin which lacks these side effects. The major dose-limiting toxicity of carboplatin is myelosuppression (thrombocytopenia and neutropenia)<sup>128</sup>. At conventional carboplatin doses, thrombocytopenia has been reported in 20–40% of patients and severe neutropenia in less than 20%. At high doses, myelosuppression has been reported in more than 90% of patients. In such settings, granulocyte-macrophage colony stimulating factor (GM-CSF) is administered to avoid life-threatening complications<sup>128</sup>.

**Table 1.4 Selected mechanisms of EOC resistance to cisplatin and carboplatin**

<i>Altered components in resistance</i>	<i>References</i>
Transporters	130-132
Detoxification machinery (GSH and metallothioneins)	133,134
DNA damage response	135-137
Apoptosis	138-140
Tumor microenvironment	141-143
Proliferative signaling	144,145
miRNAs	146-154
Transcription factors and coactivators	155-159
EMT and stemness	160-162
Other alterations	163-167

### 1.3 RUNX family of transcription factors

#### 1.3.1 Overview of RUNX transcription factors

RUNX (Runt-related transcription factor) family of genes are also termed acute myeloid leukemia (AML), core-binding factor- $\alpha$  (CBF $\alpha$ ) or polyoma enhancer-binding protein-2 $\alpha$  (PEBP2 $\alpha$ ) family<sup>168</sup>. They represent an evolutionarily conserved group of genes in both simple and complex metazoans, which is suggestive of their biological importance<sup>169</sup>. They have multiple roles in both development and homeostasis. In mammals, three RUNX genes have been identified, namely: *RUNX1*, *RUNX2* and *RUNX3*<sup>170</sup>.

#### 1.3.2 Structure of RUNX family members

The three RUNX proteins share a number of evolutionarily conserved domains. Most important, they share a 128-amino-acid Runt domain (Runt-homology domain; RHD) which is responsible for DNA binding and dimerization with a common cofactor named CBF $\beta$  (core-binding factor  $\beta$ ) or PEBP2 $\beta$  (polyomavirus enhancer binding protein 2 $\beta$ )<sup>168,171</sup>. CBF $\beta$  does not interact with DNA itself, but enhances DNA binding and stability of RUNX proteins<sup>172,173</sup>. The structural basis of CBF $\beta$  interaction with RUNX1 protein and subsequent DNA binding has been solved<sup>174,175</sup>. Other conserved domains include the activation domain (AD), the inhibitory domain (ID), and the VWRPY motif at the C-terminus. This last motif is responsible for the interaction with transcription corepressors<sup>176</sup>. RUNX2 protein possesses a unique domain termed QA domain that consists of tandem repeats of glutamine and alanine amino acids<sup>169</sup> (**Figure 1.5**).

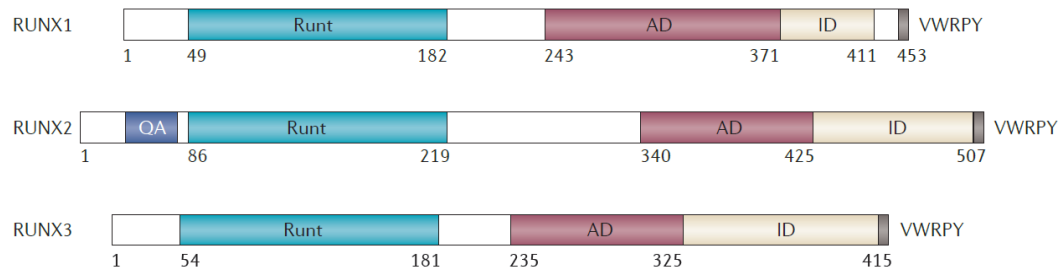


**Figure 1.6 Schematic illustration of the structures of RUNX proteins.** The RUNX family of transcription factors comprises three members RUNX1, 2 and 3. They share Runt, AD and ID domains together with C-terminus VWRPY motif. QA domain is unique to RUNX2. Adapted with permission from Ito *et al.*, 2015<sup>169</sup>.

### **1.3.3 Transcriptional activity of RUNX family of transcription factors**

RUNX proteins bind to DNA at a consensus target sequence (AACCGCA), which is facilitated by CBF $\beta$ . As a result, transcription of many target genes is activated or repressed<sup>177</sup>. The specific outcome is governed by the proximity of binding sites to either co-activators (p300, CCAAT/enhancer-binding protein [C/EBP], ETS, MYB and SMADs) or co-repressors (Groucho–transducin-like enhancer of split [Groucho–TLE], histone deacetylases [HDACs], mSin3A and nuclear receptor corepressor [nCoR]), and the availability of these co-activators/co-repressors in the nucleus. In addition, a number of post-translational modifications regulate the transcriptional activity of RUNX proteins, including phosphorylation, acetylation and ubiquitination<sup>168,178</sup>. These modifications affect the subcellular localization and stability of RUNX proteins<sup>169</sup>.

### **1.3.4 Functions of RUNX family of transcription factors**

RUNX proteins serve as transcription factors that regulate various developmental, homeostatic and pathological processes. In this respect, they modulate cell lineage specification, proliferation, differentiation, apoptosis, cell cycle progression, stress (hypoxia and DNA damage) responses, oncogene-induced senescence, ribosomal biogenesis, inflammatory responses, EMT and stemness<sup>169,176</sup>. The roles of RUNX proteins in these processes constitute the outcome of crosstalk with a plethora of signaling pathways such as transforming growth factor- $\beta$  (TGF $\beta$ ), bone morphogenetic protein (BMP), PI3K, Wnt, NOTCH, estrogen, Hippo/MST2, and Hedgehog signaling pathways<sup>179-182</sup>.

The biological functions of RUNX proteins are mediated via modulation of a number of target genes that encode components involved in apoptosis (p14/p19<sup>ARF</sup>; p21<sup>WAF1</sup>), TGF $\beta$  signaling (TGF $\beta$ R1), hematopoietic differentiation (TCR $\alpha$ , - $\beta$ , - $\gamma$ , - $\delta$ , CD3 $\epsilon$ , CD4, GM-CSF, IL-3, IgA1, IgC $\alpha$ , M-CSFR, myeloperoxidase [MPO], C/EBP $\delta$ ), cell cycle regulation (cyclin D3) and bone development (bone sialoprotein, osteopontin, collagenase-3, VEGF)<sup>168</sup>. It is noteworthy that RUNX family members might exert redundant or antagonistic functions, which are mostly context-dependent (cell- or tissue-specific)<sup>169</sup>.

Knockout studies in mice confirmed the fundamental role of each of the RUNX members in different biological processes. Specifically, RUNX1 is important for hematopoiesis, immune responses, hair follicle development, and nociceptive sensory neuronal regulation. RUNX2 is implicated in skeletal development, skin and hair follicle development and specification of alveolar cell maturation in mammary glands during pregnancy. RUNX3 is involved in differentiation of gastric epithelial cells, neuronal cell fate specification, macrophage and T cell differentiation, and dendritic cell maturation<sup>169</sup>. Therefore, aberrations in RUNX genes lead to a number of diseases, most prominently cancer.

### **1.3.5 RUNX proteins in cancer**

RUNX proteins play fundamental roles in cancer-related processes such as proliferation, differentiation, apoptosis, stress (hypoxia and DNA damage) response, and oncogene-induced senescence. Therefore, aberrant expression or mutations of *RUNX* genes contribute to a broad spectrum of malignancies. In this

respect, RUNX1 has been implicated in acute myeloid leukemia (AML), acute lymphoblastic leukemia (ALL), chronic myeloid leukemia (CML), invasive endometrioid carcinoma, breast cancer, and squamous cell carcinoma (SCC)<sup>183,184</sup>. RUNX2 is involved in osteosarcoma, breast cancer and prostate carcinomas<sup>169,185</sup>. RUNX3 has been implicated in a broad spectrum of cancers. These include neuroblastoma, glioma, basal cell carcinoma (BCC), AML, hepatocellular carcinoma (HCC), EOC, head and neck squamous cell carcinoma (HNSCC), chondrosarcoma, thyroid, skin, esophageal, breast, prostate, lung, gastric, bladder, and colon cancers<sup>169,186-191</sup>. RUNX members may exert either oncogenic or tumor-suppressive effects based on cellular context and spatiotemporal regulation<sup>169,192,193</sup>. Tumor suppressive effects derive from the capacity to induce differentiation, growth arrest and senescence. On the other hand, oncogenic effects derive from the ability of specific members to induce transformation, differentiation block, EMT and stemness<sup>168</sup>. Since EOC is the focus of the thesis, the role of RUNX proteins in EOC will be discussed below.

### **1.3.6 RUNX proteins in EOC**

RUNX1 and RUNX2 were found to be overexpressed in EOC including LMP tumors, high-grade primary tumors and metastatic disease. Methylation status of *RUNX1* and *RUNX2* genes in primary EOC tumors was *not* significantly different from that in EOC omental metastases, suggesting that metastatic behavior of EOC was *not* dependent on methylation-based epigenetic modulation of these two genes<sup>194,195</sup>. Conversely, they were found to be hypomethylated and overexpressed in primary cell cultures developed from post-chemotherapy tumors

from serous EOC patients, as compared to cultures derived from matched primary pre-chemotherapy tumors<sup>196</sup>, suggesting RUNX1 and RUNX2 might have a role in chemoresistance. In line with their potential oncogenic role in EOC, knockdown of either RUNX1 or RUNX2 led to the inhibition of proliferation, migration and invasion of EOC cells, and was associated with a gene expression profile characterized by downregulation of a number of oncogenic pathways and induction of tumor suppressive pathways<sup>194,195</sup>. These reports suggest that RUNX1 and RUNX2 might be potential therapeutic targets in EOC.

In another study, RUNX2 was found to be overexpressed in EOC patient tissues (n=116) as compared to normal ovarian tissues, and its expression level in high clinical stages (III and IV) correlated with shorter OS and PFS. This suggests that RUNX2 could serve as a potential prognostic marker for EOC<sup>197</sup>.

RUNX3 expression was found to be higher in malignant and borderline serous EOC patient specimens compared to normal ovarian epithelium specimens, as assessed by both immunohistochemistry (IHC) and quantitative reverse transcription polymerase chain reaction (qRT-PCR). Subsequent gain- and loss-of-function studies in the EOC cell lines SKOV3 and OVCAR429, respectively suggested a role for RUNX3 in promoting EOC progression<sup>197</sup>. This oncogenic role of RUNX3 was consolidated by another study in 2011<sup>190</sup>. Conversely, RUNX3 was reported to be inactivated in other cancers including endometrial carcinoma<sup>198</sup>.

As mentioned above, CBF $\beta$  is essential for adequate transcriptional activity of RUNX proteins. In line with the oncogenic role of RUNX proteins in EOC,



knockdown of CBF $\beta$  in SKOV3 cells led to a significant suppression of their anchorage-independent growth. Whether this oncogenic activity is dependent on RUNX proteins has yet to be elucidated<sup>199</sup>.

## 1.4 Wnt/ $\beta$ -catenin signaling

### 1.4.1 Overview of Wnt signaling

Wnt designation is derived from the fly *Wingless* (*wg*) gene and *Int-1* (now named *Wnt1*) proto-oncogene. The *wg* gene of *Drosophila melanogaster* was identified in 1980 as a gene implicated in segment polarity during larval development<sup>200</sup>, and *Int-1* gene was discovered in 1982 as a gene activated by *integration* of mouse mammary tumor virus (MMTV) proviral DNA in virally induced breast tumors<sup>201</sup>. In 1987, *wg* gene was found to be a homolog of *Int-1*, and they constitute a part of a large conserved family of genes; therefore, the contracted name Wnt has been proposed<sup>202-205</sup>.

Wnt signaling has been subdivided into canonical (Wnt/ $\beta$ -catenin;  $\beta$ -catenin-dependent) and non-canonical ( $\beta$ -catenin-independent) Wnt signaling pathways based on the involvement of  $\beta$ -catenin as an effector<sup>206</sup>. Non-canonical signaling includes the Wnt/ $\text{Ca}^{+2}$  and planar cell polarity (PCP) signaling pathways. The focus in this thesis will be on Wnt/ $\beta$ -catenin signaling.

### 1.4.2 Cascade and components of Wnt/ $\beta$ -catenin signaling

Wnt/ $\beta$ -catenin signaling has been extensively reviewed in the biomedical literature<sup>207-219</sup>. Briefly, Wnt/ $\beta$ -catenin signaling starts with the binding of secreted extracellular Wnt ligands to their receptors belonging to Frizzled (FZD) family—an interaction that requires co-receptors called low-density lipoprotein receptor related proteins 5 and 6 (LRP5/6). The activated FZD receptor initiates a cascade of intracellular signaling events by activating the Dishevelled proteins (DVL) to inactivate a destruction (degradation) complex that phosphorylates and

therefore directs  $\beta$ -catenin to proteasomal degradation. The destruction complex consists of Adenomatosis Polyposis Coli (APC), Axin, glycogen synthase kinase-3 $\beta$  (GSK-3 $\beta$ ) and casein kinase-1 (CK-1). The stabilized  $\beta$ -catenin accumulates in the cytosol and then translocates into the nucleus.  $\beta$ -catenin, the effector of canonical Wnt signaling, serves as a transcriptional co-activator that associates in the nucleus with the T-cell factor/lymphoid enhancer factor (TCF/LEF) family of transcription factors and modulate the transcription of a large set of target genes. Wnt/ $\beta$ -catenin signaling is regulated by extracellular modulators that belong to three families, namely: secreted Frizzled related proteins (sFRPs), Wnt-inhibitory factor (WIF-1), and Dickkopfs (DKKs)<sup>220</sup>. The signaling cascade and components of Wnt/ $\beta$ -catenin signaling are summarized in **Figure 1.6** and **Table 1.5**, respectively.

### **1.4.3 Functions of Wnt/ $\beta$ -catenin signaling**

Activation of Wnt/ $\beta$ -catenin signaling leads to the transcriptional modulation of a large set of target genes involved in cell proliferation, differentiation, survival, migration, genetic stability, cell fate specification, polarity, adhesion, hematopoiesis and self-renewal in stem cells<sup>205,206,221-224</sup>. Therefore, Wnt/ $\beta$ -catenin signaling is fundamental for many developmental and homeostatic processes, as evidenced by knockout studies in mice<sup>204</sup>. Accordingly, aberrant Wnt/ $\beta$ -catenin signaling leads to multiple diseases including cancer, osteoarthritis, renal disease, cardiovascular diseases, fibrosis and neurodegenerative diseases<sup>225-</sup>

<sup>227</sup>.

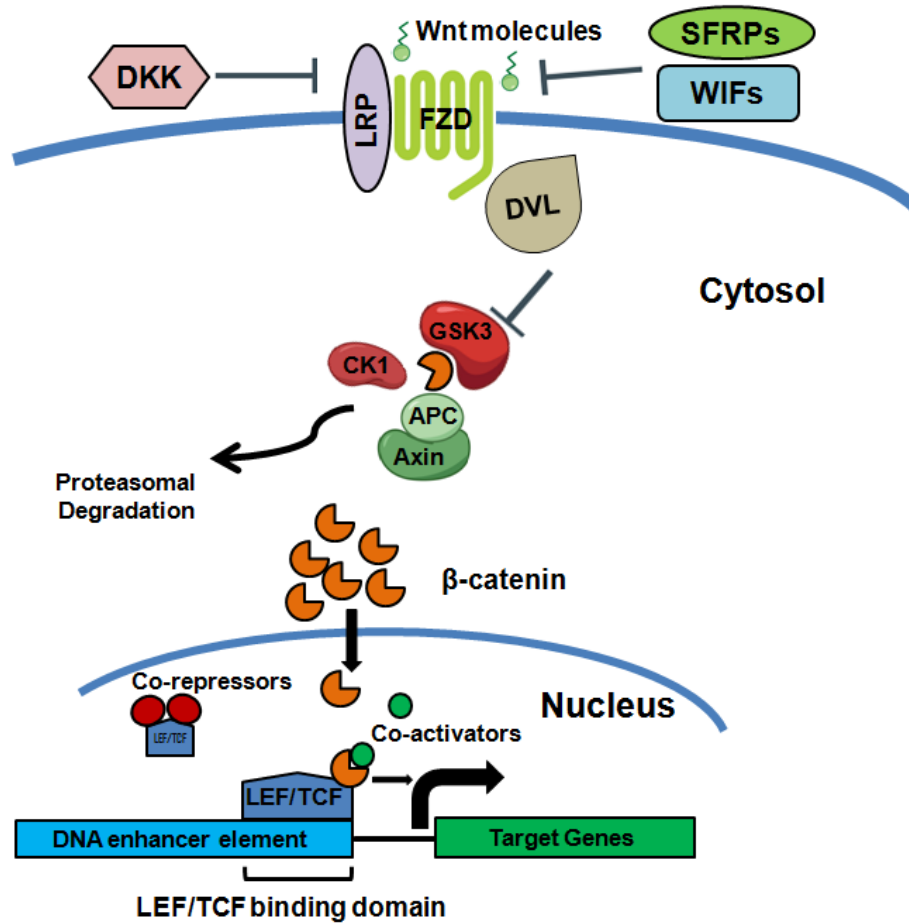


**Figure 1.7 Schematic illustration of the Wnt/β-catenin signaling pathway.**

The Wnt ligand binds FZD receptors and this binding is facilitated by LRP5/6 coreceptors. This interaction activates DVL that inhibits the destruction complex composed of GSK-3, CK1, APC, and Axin. As a result, β-catenin is stabilized and accumulates in the nucleus and binds LEF/TCF to exert its transcriptional effects. Adapted from Clevers and Nusse, 2012 and Cadigan and Waterman, 2012<sup>203,209</sup>.

**Table 1.5 Signaling components and members of Wnt/ $\beta$ -catenin signaling**  
(Reproduced with permission from Ref. 220)

<i><b>Component</b></i>	<i><b>Members</b></i>
Wnt ligands	Wnt-1(Wg), Wnt-2, Wnt-2B, Wnt-3, Wnt-3A, Wnt-4, Wnt-5A, Wnt-5B, Wnt-6, Wnt-7A, Wnt-7B, Wnt-8A, Wnt-8B, Wnt-9A, Wnt -9B, Wnt-10A, Wnt-10B, Wnt -11, Wnt -16
Extracellular modulators	sFRP1-5; DKK1-4; WIF-1
FZD receptors	FZD1-10
LRP receptors	LRP5/6
Dishevelleds	DVL1-3
$\beta$ -Catenin destruction complex	Axin, APC, GSK-3, CK-1, protein phosphatases (PP1 and PP2A)
Effector	$\beta$ -catenin (Armadillo)
Transcription factors	TCF-1, TCF-3, TCF-4; LEF-1

#### 1.4.4 Aberrant Wnt/ $\beta$ -catenin signaling in cancer

As a result of its central role in multiple biological processes particularly in stem cell biology, aberrant Wnt/ $\beta$ -catenin signaling has been implicated in a variety of cancers<sup>203</sup>. Mutations in the *APC* gene were found in patients with familial adenomatous polyposis (FAP) and in sporadic colorectal cancers<sup>228-231</sup>. In addition, stabilizing  $\beta$ -catenin mutations were identified in melanoma and colon cancer cell lines<sup>232-234</sup>. *AXIN1* and *AXIN2* mutations were associated with colon cancer<sup>235,236</sup>. SFRPs silencing and Wnt or FZD overexpression were associated with colorectal and mammary carcinogenesis<sup>237,238</sup>. DVLs have been found to be overexpressed in NSCLC and mesothelioma<sup>239,240</sup>. Moreover, WIF1 is downregulated in prostate, breast, lung, and bladder cancer<sup>241</sup>. Activating *LRP5* mutations were associated with thyroid tumours<sup>242</sup>. *LEF1* mutations were associated with sebaceous gland tumors in humans, but in these tumors, Wnt- $\beta$ -catenin signaling is inactivated<sup>243</sup>. Other cancers with Wnt- $\beta$ -catenin signaling implication include glioma and urological cancers<sup>244,245</sup>. Given the broad spectrum of malignancies driven by this central pathway either directly or indirectly, and its role in stemness and EMT, several Wnt- $\beta$ -catenin-targeted therapeutics have been developed and tested in various cancers<sup>206,225,246-253</sup>.

#### 1.4.5 Aberrant Wnt/ $\beta$ -catenin signaling in EOC

As mentioned in **Section 1.1.7**, a number of signaling pathways are deregulated in EOC and foster tumor progression. Among these pathways, Wnt/ $\beta$ -catenin signaling is of special interest as  $\beta$ -catenin, is the 7<sup>th</sup> gene in terms of mutation frequency (6%) in EOC<sup>254</sup>. Other studies reported  $\beta$ -catenin mutation

frequencies of 14% in mucinous EOC and up to 54% in endometrioid EOC<sup>255-259</sup>. Wnt/ $\beta$ -catenin signaling may be hyperactivated via indirect stabilization of  $\beta$ -catenin by other pathways such as PI3K, which phosphorylates GSK3 $\beta$ , leading to inhibition of its activity and therefore enhancing  $\beta$ -catenin stability<sup>260</sup>. Likewise, the receptor-interacting serine/threonine-protein kinase 4 (RIPK4) promotes progression of ovarian adenocarcinoma by activating Wnt/ $\beta$ -catenin signaling via phosphorylation of DVL2<sup>261</sup>.

Other components of Wnt/ $\beta$ -catenin signaling are deregulated in EOC. With respect to Wnt ligands, Wnt7a was found to drive EOC progression in a murine model<sup>262</sup>; other non-canonical Wnt ligands such as Wnt5a were reported to have conflicting effects on EOC progression<sup>263-268</sup>. For extracellular modulators of Wnt/ $\beta$ -catenin signaling, *DKK2* and *SFRP5* were reported to be epigenetically silenced in EOC cell lines and patient samples<sup>160,269</sup>. *DKK1* was found to be negatively correlated to invasiveness of EOC cells *in vitro*<sup>270</sup>. Conflicting with this study is a report of *DKK1* overexpression in serous EOC and its implication in invasiveness<sup>271</sup>. In addition, re-expression of *SFRP4* suppressed EMT and cell migration in serous EOC cell lines<sup>272</sup>, and its expression was positively correlated with lower tumor grade of mucinous EOC<sup>273</sup>. Among Wnt receptors, the expression of *FZD5* was associated with worse prognosis in EOC<sup>260</sup>.

## **1.5 Preliminary data and hypotheses**

The gene expression profiles of the two paired cell lines A2780s and A2780cp were determined using a cDNA gene expression microarray followed by data analysis using Ingenuity Pathway Analysis (IPA) software and literature reviewing<sup>274</sup>. Thousands of genes were found to be differentially expressed between the two cell lines. Based on data analysis, RUNX proteins and Wnt/ $\beta$ -catenin signaling were selected for further assessment of their role in chemoresistance of EOC to carboplatin. Two hypotheses have been addressed in the thesis:

1. RUNX proteins contribute to carboplatin resistance in EOC cells
2. Wnt/ $\beta$ -catenin signaling is upregulated in resistant EOC cells and might contribute to the development of carboplatin resistance.



## **Chapter 2**

# **Materials and Methods**

## 2. Materials and Methods

### 2.1 Reagents

Carboplatin, puromycin, neutral red dye, and polybrene were purchased from Sigma-Aldrich. The protease inhibitor cocktail (PIC) was purchased from Roche. G418 was purchased from Invitrogen. Anti-RUNX3 antibody (ab40278; R3-5G4), anti-tubulin antibody (ab59680) and anti-DKK1 antibody (ab109416; EPR4759) were purchased from Abcam. Anti-RUNX2 antibody (#8486; D1H7), anti-RUNX1 antibody (#4334), anti-SFRP1 antibody (#3534; D5A7), anti- $\beta$ -catenin antibody (#8480; D10A8), anti-cIAP2 antibody (#9770), anti-PARP and anti-cleaved PARP antibodies (#9915) were purchased from Cell Signaling Technology. Anti- $\beta$ -actin antibody (A5441; AC-15) and anti-FLAG antibody (F1804; M2) were purchased from Sigma-Aldrich. Anti-CBF- $\beta$  antibody (sc-56751; 141,4,1) was purchased from Santa Cruz Biotechnology.

### 2.2 Cell culture

Human ovarian cancer cell lines A2780s and A2780cp were cultured in DMEM/F12 medium. HEK 293T and Phoenix-Ampho cells were cultured in DMEM medium. All the culture media were supplemented with 10% fetal bovine serum (FBS), 100 U/ml penicillin, and 100  $\mu$ g/ml streptomycin.

The paired A2780s and A2780cp cells were provided by Dr. Benjamin Tsang (Ottawa Hospital Research Institute). A2780 cells were established from the tissues of untreated ovarian cancer patient<sup>275</sup>. They have *ARID1A*, *BRAF*, *PIK3CA* and *PTEN* mutations, but lack *TP53* mutations<sup>78</sup>. In this respect, they do not belong to the most common EOC histotypes— high-grade serous EOC<sup>78</sup>. The

cisplatin-resistant A2780cp cells were derived from cisplatin-sensitive A2780s cells by chronic exposure of the parental cells to stepwise-increasing concentrations of cisplatin<sup>275</sup>. The starting dose of cisplatin was 3 nM. A2780 cells were exposed to the drug in the form of 3-day cycles. Each concentration was employed for 3 cycles, with recovery periods in between, taking a total period of 3-6 weeks for each concentration. The concentration was then escalated in a doubling fashion until A2780cp cell line was generated<sup>275</sup>. The IC<sub>50</sub> for A2780cp was approximately 10-fold that for A2780s cells as assessed by cytotoxicity assays (see **Chapter 3**).

### **2.3 Generating overexpression cells**

MSCVpac vectors were obtained from BC Cancer Research Institute. Phoenix-Ampho cells were used for overexpression experiments. The calcium phosphate method was used to transfect Phoenix-Ampho cells with the empty retroviral vector (MSCVpac) or a retroviral vector containing the appropriate human cDNA according to the experiment. The appropriate volume of the expression plasmid (e.g., 10 µg of plasmid DNA) was added to molecular-grade H<sub>2</sub>O to a final volume of 450 µL, followed by vortexing and spinning. CaCl<sub>2</sub> (50 µL of 2.5 M solution) was then added to each tube dropwise. Then the solution was transferred to a tube containing 500 µL of 2X HEPES-buffered saline (HBS), followed by mixing and incubation for 5 minutes at room temperature (RT). The solution was then added dropwise to the Phoenix-Ampho cells, and cells were incubated overnight at 37°C. After 24 h, the media were replaced with fresh medium. The next day, the medium from the Phoenix-Ampho cells was filtered

(through Millex<sup>®</sup> syringe-driven Filter Unit 0.33 µm) and added to target cells (A2780s or A2780cp cells). Polybrene (8 mg/mL) was added to the target cells to a final concentration of 8 µg/mL (1/1000 dilution). Positively infected cells were selected by treatment with 1-2.5 µg/ml of puromycin to generate A2780s/Vector and A2780s/RUNX3.

For overexpression of dominant-negative RUNX3 (dnRUNX3) cells, A2780cp cells were stably transfected with pcDNA3.1 vector or pcDNA-FLAG-RUNX3 (1-187) (kindly provided by Dr. Yoshiaki Ito, Cancer Science Institute of Singapore) using GeneJuice<sup>®</sup> Transfection Reagent (Novagen) and selected by treatment with 500 µg/ml of G418. pcDNA-FLAG-RUNX3 (1-187) expresses a truncated form of RUNX3 that contains the runt domain but lacks the transactivation domain at the carboxyl terminus. dnRUNX3 (1-187) functions as a dominant negative form of RUNX3<sup>177,187,276</sup>.

## **2.4 Generating knockdown cells**

293T cells were transfected with a lentivirus vector (pLentiLox) containing an shRNA targeted against a random sequence (shRandom: 5'-GTT GCT TGC CAC GTC CTA GAT-3') or an shRNA targeted against the RUNX3 gene (shRUNX3D: 5'-GGA CCC TAA CAA CCT TCA AGA-3' or shRUNX3E: 5'-GCC GTC TCA TCC CAT ACT TCT-3') and packaging plasmids by the calcium phosphate method as described in **Section 2.3** with few modifications. RRE, REV and VSVG plasmids (5 µg each) were included with the expression plasmids in the first reaction mixture to serve as packaging plasmids. A2780cp cells were infected with lentivirus containing shRandom, shRUNX3D or shRUNX3E. Since

pLentiLox vector expresses green fluorescent protein (GFP), positively infected cells were purified by fluorescence-activated cell sorting (FACS) for GFP positive cells to generate A2780cp/shRandom, A2780cp/shRUNX3D and A2780cp/shRUNX3E cells.

## 2.5 Cytotoxicity assays

Cytotoxicity of carboplatin was determined by two cytotoxicity assays: neutral red uptake assay and clonogenic assay. Neutral red uptake assay was adapted from Repetto *et al.*<sup>277</sup> and the clonogenic assay from protocols described by Munshi *et al.* and Franken *et al.*<sup>278,279</sup>.

The principle of neutral red uptake assay is based on the ability of viable cells, not dead cells, to take up neutral red dye into the lysosomes. This capacity distinguishes viable and dead cells, and the extent of dye uptake is directly proportional to the number of viable cells. In this protocol, cells were seeded in 96-well plate at a plating density of 2,000-3,000 cells per well. The next day, cells were treated with increasing concentrations of carboplatin for 72 h. After that, media were aspirated and new media containing neutral red dye (33 µg/ml) were added. Cells were then incubated for at least 3 h at 37°C. The cells were then washed once with phosphate buffered saline (PBS) and lysed with destaining solution (50% ethanol and 1% acetic acid in H<sub>2</sub>O) to extract the dye. Plates were gently shaken until the color became homogenously distributed in the wells. Absorbance was then measured at 540 nm using the FLUOstar Omega microplate reader.

The principle of the clonogenic assay depends on the ability of cells to undergo division to produce colonies (composed of at least 50 cells). In this assay, cells were seeded in 6-well plates at a plating density (per well) starting from 50 cells for control wells (untreated) up to 3200 cells for wells treated with the highest concentration of carboplatin (200  $\mu$ M). Six hours after seeding, cells were treated with increasing concentrations of carboplatin for 24 hours. The medium with carboplatin was then replaced with fresh medium and cells were allowed to grow for 9-11 days. The colonies formed were then gently washed with phosphate-buffered saline (PBS), fixed with methanol/acetic acid (3:1) solution and stained with crystal violet (0.5 % in methanol). Colonies of  $\geq 50$  cells were counted and the viability was calculated using these equations: plating efficiency (PE) = count of colonies formed in control wells/number of cells seeded in control wells; percent viability = (count of colonies formed in treated wells/number of cells seeded in these wells x PE) x 100. Cell viability was expressed as a percentage relative to the respective untreated controls.

## **2.6 Preparation of whole cell lysates**

Cells were washed twice with PBS, and then treated with modified radio-immunoprecipitation assay (RIPA) lysis buffer to prepare whole cell lysates as previously described<sup>280</sup>. The modified RIPA buffer used was composed of 50 mM Tris pH 7.4, 150 mM NaCl, 1 mM EDTA, 0.1% sodium dodecyl sulfate (SDS), 1% sodium deoxycholate (DOC), 1 % Triton X-100, 10 mM sodium pyrophosphate ( $\text{NaP}_2\text{O}_7$ ), 10 mM sodium fluoride (NaF), 1 mM sodium orthovanadate ( $\text{Na}_3\text{VO}_4$ ), 1X PIC. Cell lysates were collected, followed by brief

sonication and centrifugation at 13,000 rpm for 15 minutes at 4°C. Supernatant containing the whole cell lysate was collected. Protein concentration was quantified using the DC protein assay (Bio-Rad™).

## **2.7 Western blotting**

Equal amount of proteins were loaded into each lane of an SDS polyacrylamide gel and transferred to a nitrocellulose membrane. Immunoblotting was performed using anti-RUNX1 (1:1000), anti-RUNX2 (1:1000), anti-RUNX3 (1:1000), anti- $\beta$ -actin (1:1000), anti-tubulin (1:1000), anti-PARP (1:1000), anti-cleaved PARP (1:1000), anti-cIAP2 (1:1000) antibodies. IRDye® 800CW secondary antibodies were used (LI-COR Biosciences). Membranes were scanned and analyzed using an Odyssey® IR scanner and Odyssey® imaging software 3.0.

## **2.8 RNA isolation and quantitative reverse transcription polymerase chain reaction (qRT-PCR) analysis**

Cells were washed twice with PBS and were then homogenized with TRIzol® Reagent (Life Technologies). Chloroform was then added (0.2 mL of chloroform per 1 mL of TRIzol) followed by incubation for 2–3 minutes at RT. After that, tubes were centrifuged at 12,000  $\times g$  for 15 minutes at 4°C. The homogenate separated into a clear upper aqueous layer (containing RNA), an interphase, and a red lower organic layer (containing the DNA and proteins). The aqueous layer was separated and RNA precipitated with 100% isopropanol (0.5 mL of isopropanol per 1 mL of TRIzol). This was followed by incubation at RT for 10 minutes and centrifugation at 12,000  $\times g$  for 10 minutes at 4°C. The supernatant was then removed leaving the precipitated RNA pellet. The pellet was

subsequently washed with 75% ethanol (1 mL per 1 mL of TRIzol) followed by brief vortexing and centrifugation at  $7,500 \times g$  for 5 minutes at 4°C. After washing, the pellet was left to dry for 5–10 minutes. RNA pellet was then resuspended in RNase-free water. RNA concentration was measured using a DU 730<sup>®</sup> spectrophotometer (Beckman Coulter).

cDNA was prepared using SuperScript<sup>®</sup> II Reverse Transcriptase (Invitrogen) in the presence of RNaseOUT Recombinant Ribonuclease Inhibitor (Invitrogen), random primers, 25mM dNTP using a Veriti<sup>®</sup> 96 well thermal cycler (Life Technologies) as per the manufacturer's instructions. The qRT-PCR reaction mixture was composed of 10  $\mu$ l of SYBR<sup>®</sup> Select Master Mix (Applied Biosystems), 1  $\mu$ l of 10  $\mu$ M primers (forward/reverse), 1  $\mu$ l of 50 ng/ $\mu$ l cDNA and 8.5  $\mu$ l of dH<sub>2</sub>O. qRT-PCR was conducted using the Mastercycler<sup>®</sup> ep Realplex real-time PCR system (Eppendorf). Fold changes were calculated based on the  $\Delta\Delta C_T$  method<sup>281</sup>. Experimental samples were first normalized to GAPDH and then to the control samples. Primer sequences are listed in **Table 2.1**.

## **2.9 Immunocytochemistry (ICC)**

The cells were seeded in an 8-well chamber at a plating density of 10,000 cells/chamber. After reaching approximately 50% confluency, cells were washed with PBS, and then fixed by adding 4% paraformaldehyde (diluted in PBS) for 10 minutes at RT. The cells were then permeabilized by adding permeabilization buffer (PBS with 4% FBS and 0.15% Triton X-100) for 10 minutes at RT. The cells were then incubated with appropriate primary antibodies for 1 hour at RT with gentle shaking. Anti- $\beta$ -catenin (1:100 in permeabilization buffer) and anti- $\beta$ -



RUNX3 (1:100) antibodies were used. Secondary antibodies were then added (1:300 dilutions were employed) for 30 minutes at RT with gentle shaking in the dark. Cells were then washed with permeabilization buffer followed by PBS at RT. After that, 4',6-diamidino-2-phenylindole (DAPI; 1  $\mu$ g/mL in PBS) was added for 5 minutes at RT with gentle shaking, followed by washing twice with PBS. DAPI serves as a nuclear stain. Images were taken using a fluorescence microscope (ZEISS™).

**Table 2.1 Primer sequences for qRT-PCR experiments**

<b><i>Gene</i></b>	<b><i>Forward primer</i></b>	<b><i>Reverse primer</i></b>
<b><i>RUNX1</i></b>	5'-ACT ATC CAG GCG CCT TCA CCT ACT-3'	5'-TAG TAC AGG TGG TAG GAG GGC GAG-3'
<b><i>RUNX2</i></b>	5'-ACG AAT GCA CTA TCC AGC CAC CTT-3'	5'-ATA TGG AGT GCT GCT GGT CTG GAA-3'
<b><i>RUNX3</i></b>	5'-TGG CAG GCA ATG ACG AGA ACT ACT-3'	5'-TGA ACA CAG TGA TGG TCA GGG TGA-3'
<b><i>CBFB</i></b>	5'-CAC AGG AAC CAA TCT GTC TCT C-3'	5'-CCT TGC CTG CTT CTC TTT CT -3'
<b><i>cIAP2</i> <b>(<i>BIRC3</i>)</b></b>	5'-CAA GCC AGT TAC CCT CAT CTA C-3'	5'-CTG AAT GGT CTT CTC CAG GTT C-3'
<b><i>GAPDH</i></b>	5'-GGA CCT GAC CTG CCG TCT AGA A-3'	5'-GGT GTC GCT GTT GAA GTC AGA G-3'

## 2.10 Luciferase reporter assay

Cells were seeded in 24-well plates at a plating density of  $5 \times 10^4$  cells/well. After 24 h, cells were transfected with either TOPFlash or FOPFlash plasmids (Addgene).

TOPFlash plasmid is a firefly luciferase reporter of  $\beta$ -catenin-mediated transcriptional activation. It contains seven *functional* TCF/LEF binding sites. Conversely, FOPFlash contains *mutant* TCF/LEF binding sites, and serves as a control to account for background luminescence. Each of these plasmids was co-transfected with a Renilla luciferase reporter driven by the CMV promoter, to serve as a transfection control. After 48 hrs, transcriptional activity was assessed using the Dual-Luciferase<sup>®</sup> Reporter Assay kit (Promega) as per the manufacturer's instructions. Briefly, cells were washed with PBS, followed by lysis with passive lysis buffer and lysates were transferred to new tubes. Aliquots of 20  $\mu$ l were pipetted into a 96-well plate. Luminescence was measured using Luciferase Assay Substrate in Luciferase Assay Buffer II (LARII) and Stop & Glo<sup>®</sup> Reagent by a FLUOstar Omega microplate reader. Readings for Firefly luciferase were normalized to their respective Renilla luciferase value, and then TOPFlash to their respective FOPFlash readings in each cell line. The relative  $\beta$ -catenin transcriptional activity of A2780s was expressed as 1.

## 2.11 Data analysis

Data are shown as mean  $\pm$  SEM of three to five independent experiments. Statistical analysis and IC<sub>50</sub> calculation were performed using GraphPad Prism 5. Drug-drug interaction analysis to assess potential synergism was conducted using

COMPUSYN™ software according to the Chou-Talalay method<sup>282</sup>. Statistical significance between each two independent groups was determined by the unpaired t-test and defined as  $P < 0.05$ .

## **Chapter 3**

# **Results**

### 3. Results

Genome expression profiles of A2780s and A2780cp were compared by cDNA microarray followed by IPA analysis. The analysis revealed thousands of differentially expressed genes between these two cell lines. Based on a review of the literature, RUNX3 and the Wnt/ $\beta$ -catenin signaling pathway were selected for further analysis.

#### 3.1 The role of RUNX proteins in EOC resistance to carboplatin

##### 3.1.1 RUNX3 expression is elevated in A2780cp cells compared to A2780s cells

From the microarray data generated in our laboratory, *RUNX3* gene expression was found to be approximately 22-fold greater in A2780cp cells compared to A2780s cells<sup>274</sup>. In addition, RUNX3 was reported to be overexpressed in EOC in two previous studies<sup>190,283</sup>. These findings were confirmed in our laboratory in EOC tissue samples using normal OSE cell cultures as non-cancerous controls<sup>274</sup>, and by the analysis of the microarray data from the Gene Expression Omnibus (GEO) database<sup>284</sup>.

To validate the microarray data and determine whether RUNX proteins are involved in chemoresistance of EOC, their expression was tested in cisplatin-sensitive A2780s cells and the cisplatin-resistant counterpart A2780cp cells. qRT-PCR showed that RUNX1, RUNX3 and CBF $\beta$  RNA levels were higher in A2780cp cells by 7.3, 20.2 and 2.2 fold, respectively, than that in A2780s. RUNX2 RNA levels were similar in A2780s and A2780cp cells (**Figure 3.1**).

Western blotting was subsequently conducted to confirm these data at the protein level. It showed that RUNX3 expression was markedly elevated and RUNX1 expression was slightly higher in A2780cp cells compared to A2780s cells (**Figure 3.2**). We detected two RUNX3 bands in EOC cells, which is consistent with previous studies in EOC<sup>190</sup>, human basal cell carcinomas<sup>285</sup> and human endothelial cells<sup>286</sup>. These two bands could represent two isoforms of RUNX3 or are generated by phosphorylation modification or proteolytic cleavage<sup>285</sup>. No changes in protein level were observed for CBF $\beta$ . RUNX2 was undetectable at the protein level. Anti-RUNX2 antibody was validated using RUNX2-expressing granulosa cell tumor cells as a positive control (not shown). Taken together, these data suggest that RUNX3 expression is elevated in the chemoresistant EOC cells and tissues, and its elevation is detectable at both the RNA and protein levels. Therefore, RUNX3 was selected for further analysis.

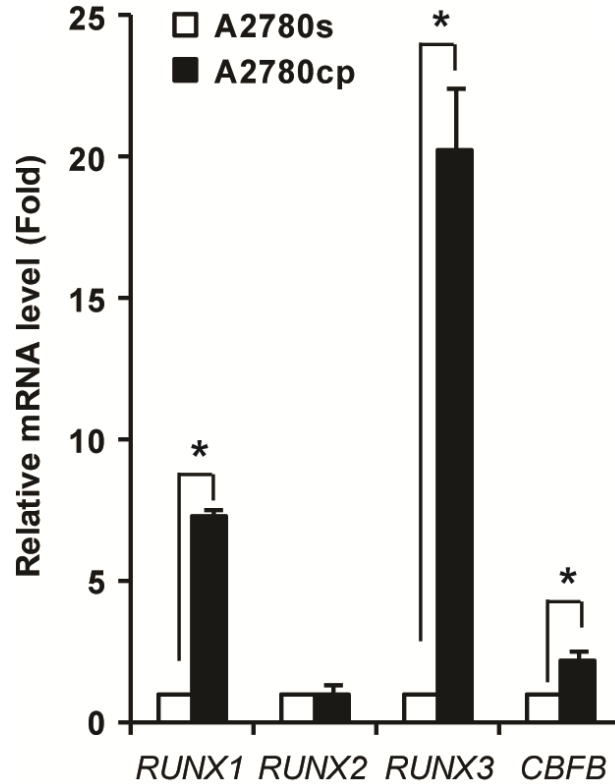


**Figure 3.1 Expression of RUNX family members and CBF $\beta$  at the mRNA level in EOC cells.** Expression of RUNX1, RUNX2, RUNX3, and CBF $\beta$  in A2780s and A2780cp cells was examined by qRT-PCR. Data are shown as mean  $\pm$  SEM of three independent experiments. \*Significantly different ( $P < 0.05$ ). RUNX1, RUNX2 and RUNX3 data were previously reported in our laboratory<sup>274</sup>, and were included here in the same graph with CBF $\beta$  data for the purpose of comparison.



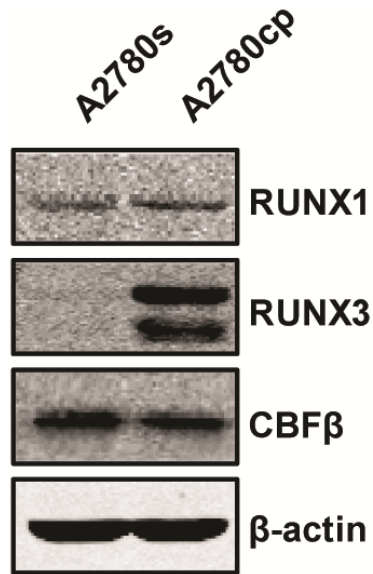


**Figure 3.2 Expression of RUNX family members and CBFβ at the protein level in EOC cells.** Expression of RUNX1, RUNX3, and CBFβ in A2780s and A2780cp cells was examined by Western blotting. β-actin was used as a loading control. RUNX3 data were previously reported in our laboratory<sup>274</sup>, and were included here in the same graph with RUNX1 and CBFβ data for the purpose of comparison.

### 3.1.2 Cisplatin-resistant A2780cp cells are also carboplatin-resistant

The cisplatin-resistant A2780cp cells were derived from cisplatin-sensitive A2780s cells by exposing A2780s cells to stepwise-increasing concentrations of cisplatin<sup>275</sup>. Carboplatin and cisplatin share similar modes of action and a broad range of cross-resistance<sup>83,124</sup>. Because carboplatin is currently more often used than cisplatin as the first-line therapeutic agent in the treatment of ovarian cancer due to its low toxicity profile when compared to cisplatin<sup>53,287,288</sup>, carboplatin was used for this study. To validate the use of this paired cell model for carboplatin study, relative viability after exposure to increasing concentrations of carboplatin was assessed using the clonogenic assay. As expected, cisplatin-resistant A2780cp cells were also resistant to carboplatin (**Figure 3.3**). The IC<sub>50</sub> values for carboplatin were 35.5  $\mu$ M and 3.7  $\mu$ M in A2780cp and A2780s cells, respectively (see **Table 3.1** for summary of IC<sub>50</sub> values from different experiments).

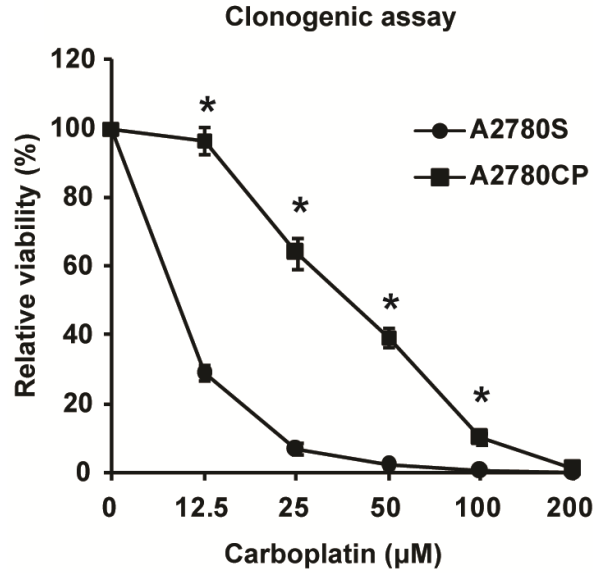


**Figure 3.3 A2780cp cells are more resistant to carboplatin than A2780s cells.**

A2780s and A2780cp cells were treated with increasing concentrations of carboplatin and cell viability was measured by the clonogenic assay. Cell viability was expressed as a percentage relative to the respective untreated controls (0 μM carboplatin). Data are shown as mean ± SEM of three independent experiments.

\*Significantly different from the A2780s cells treated with the same concentration of carboplatin ( $P < 0.05$ ).

### **3.1.3 RUNX3 overexpression in A2780s cells confers resistance to carboplatin**

To determine whether elevated expression of RUNX3 is associated with carboplatin resistance, RUNX3 was stably overexpressed in A2780s cells to generate A2780s/Vector and A2780s/RUNX3 cells (**Figure 3.4A**) followed by clonogenic assay. The clonogenic assay showed that A2780s/RUNX3 cells were significantly more resistant to carboplatin-induced cytotoxicity than A2780s/Vector cells (**Figure 3.4B**). The IC<sub>50</sub> values for carboplatin were 7.9  $\mu$ M and 3.6  $\mu$ M in A2780s/RUNX3 and A2780s/Vector cells, respectively. Taken together, these results indicate that elevated expression of RUNX3 renders EOC cells more resistant to carboplatin.

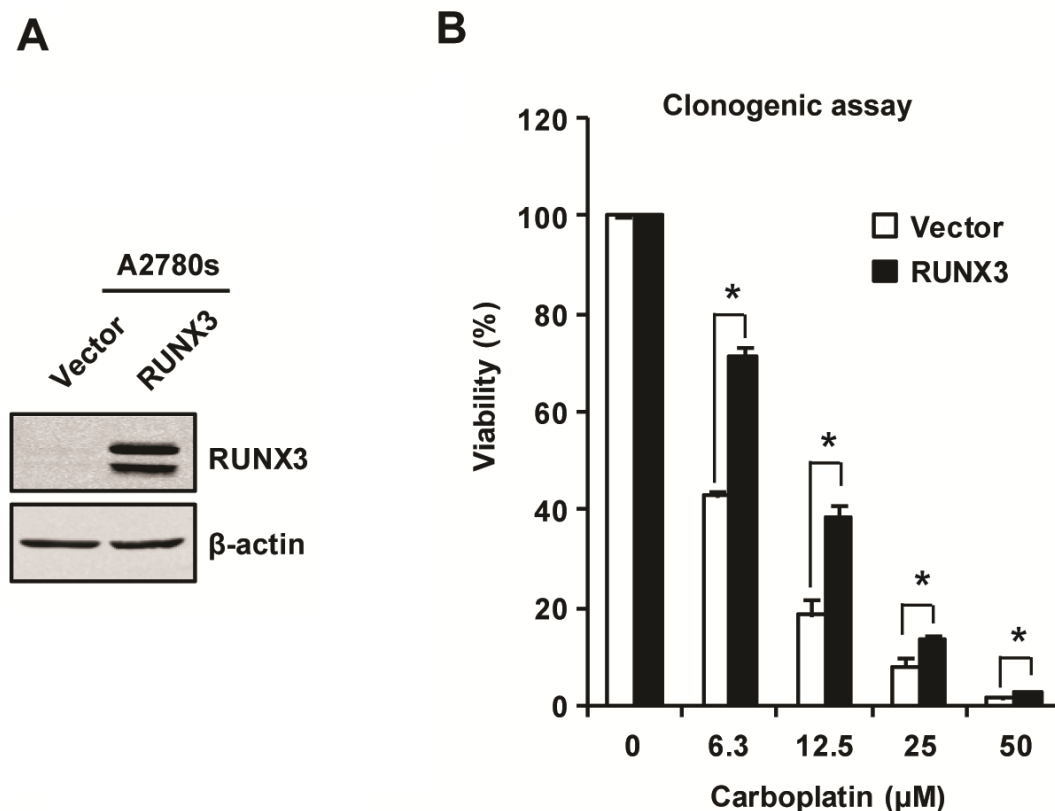


**Figure 3.4 Overexpression of RUNX3 renders EOC cells more resistant to carboplatin.** (A) Overexpression of RUNX3 in A2780s/RUNX3 cells was confirmed by Western blotting.  $\beta$ -actin was used as the loading control. (B) A2780s/Vector and A2780s/RUNX3 cells were treated with increasing concentrations of carboplatin and cell viability was determined by the clonogenic assay and expressed as a percentage relative to the respective untreated controls. Data are shown as mean  $\pm$  SEM of three independent experiments. \*Significantly different ( $P < 0.05$ ).

#### **3.1.4 Knockdown of RUNX3 modestly increases the sensitivity of A2780cp cells to carboplatin**

Next, we tested whether RUNX3 inactivation could sensitize A2780cp cells to carboplatin. To do so, RUNX3 was stably knocked down in A2780cp cells using two lentivirus-delivered shRNA constructs (shRUNX3D and shRUNX3E) targeting two distinct sequences of human *RUNX3* (**Figure 3.5A**)<sup>286</sup>. RUNX3 knockdown and control A2780cp cells were treated with increasing concentrations of carboplatin for 72 h. Neutral red uptake assay showed that knockdown of RUNX3 increased the sensitivity of A2780cp cells to 200  $\mu$ M carboplatin, but not the lower doses of carboplatin (**Figure 3.5B**). The IC<sub>50</sub> values for carboplatin in A2780cp/shRandom, A2780cp/shRUNX3D and A2780cp/shRUNX3E were 123.4, 92.8 and 103.9  $\mu$ M, respectively.

To determine whether RUNX3 knockdown renders A2780cp cells more sensitive to apoptosis induced by carboplatin, A2780cp/shRandom, A2780cp/shRUNX3D and A2780cp/shRUNX3E cells were treated with 200  $\mu$ M carboplatin for 72 h and carboplatin-induced cleavage of PARP was detected as a marker of apoptosis by Western blotting. Carboplatin-induced cleavage of PARP was more pronounced in RUNX3 knockdown cells compared to the control cells, suggesting that RUNX3 knockdown potentiates carboplatin-induced apoptosis in A2780cp cells (**Figure 3.6A**). Quantification showed that shRUNX3D and shRUNX3E increased carboplatin-induced production of cleaved PARP by 2.2 and 1.9 fold, respectively, compared to shRandom (**Figure 3.6B**).

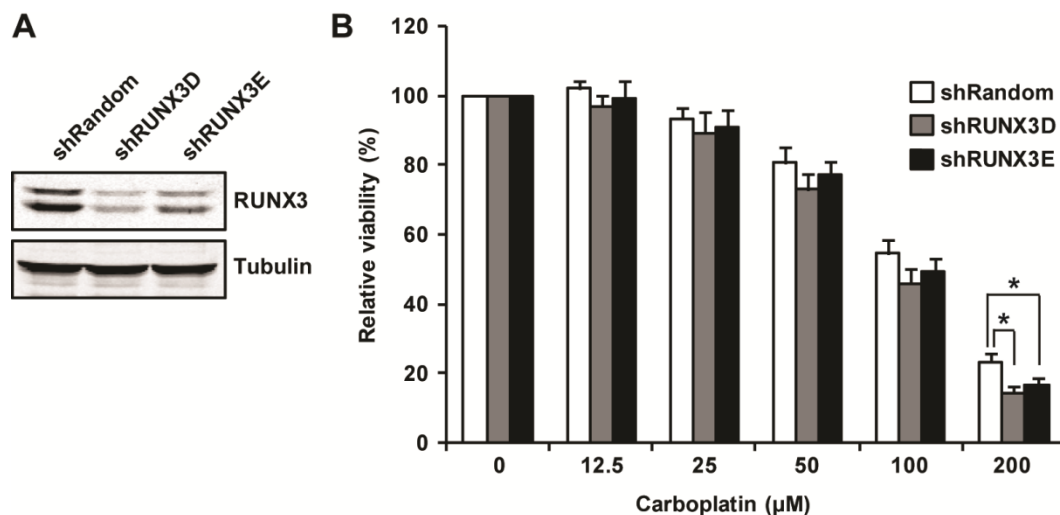


**Figure 3.5 Knockdown of RUNX3 moderately sensitizes A2780cp cells to carboplatin.** (A) Stable knockdown of RUNX3 by two different shRNA constructs (shRUNX3D and shRUNX3E) in A2780cp cells was confirmed by Western blotting. Tubulin or  $\beta$ -actin was used as the loading control. (B) These cells were treated with increasing concentrations of carboplatin. Cell viability was determined by the neutral red uptake assay and expressed as a percentage relative to the respective untreated controls. Data are shown as mean  $\pm$  SEM of three independent experiments. \*Significantly different ( $P < 0.05$ ).

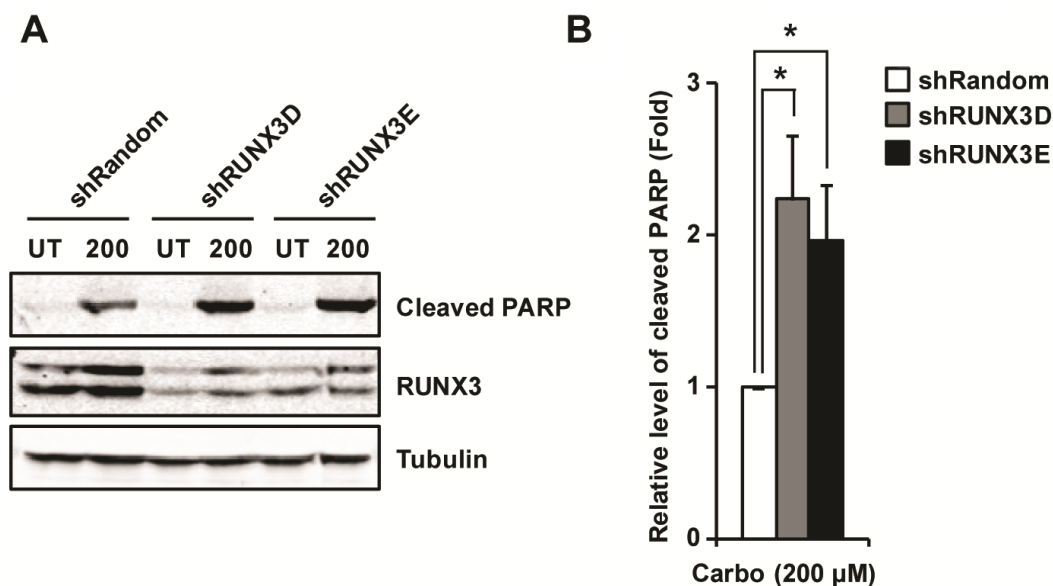


**Figure 3.6 Knockdown of RUNX3 potentiates carboplatin-induced apoptosis.**

(A) A2780cp/shRandom, A2780cp/shRUNX3D and A2780cp/shRUNX3E cells were left untreated or treated with 200 μM carboplatin for 72 h. Carboplatin-induced PARP cleavage was measured by Western blotting using antibody against the cleaved PARP. Tubulin was used as the loading control. (B) The Western blotting results of carboplatin-induced PARP cleavage were quantified using Odyssey imaging software. The density of the cleaved PARP bands was normalized to that of tubulin. The density of the bands in the carboplatin-treated A2780cp/shRandom cells was designated as 1. The relative level (fold change) of cleaved PARP was shown as mean ± SEM of four independent experiments.

\*Significantly different ( $P < 0.05$ ).



### **3.1.5 Overexpression of dnRUNX3 increases the sensitivity of A2780cp cells to carboplatin**

RUNX proteins (RUNX1-3) have been shown to have overlapping and distinct biological functions depending on cell context<sup>289</sup>. A truncated form of RUNX3 (RUNX3 1-187; dnRUNX3) containing the intact Runt domain but lacking the activation domain at the carboxyl-terminus functions in a dominant negative manner<sup>187,276</sup>, and has been shown to inhibit the functions of other RUNX proteins<sup>187,276,290</sup>.

To determine whether dnRUNX3 is more potent in sensitizing A2780cp cells to carboplatin than RUNX3 knockdown, either the empty vector pcDNA3.1 or pcDNA-FLAG-RUNX3 (1-187) were stably overexpressed in A2780cp cells. The resultant cells were referred to as A2780cp/Vector and A2780cp/dnRUNX3 cells, respectively. Overexpression of dnRUNX3 did not affect the expression of the endogenous RUNX1, RUNX3 and CBF $\beta$  in A2780cp cells (**Figure 3.7**).

Neutral red uptake assay and clonogenic assay showed that A2780cp/dnRUNX3 cells were more sensitive to carboplatin than A2780cp/Vector cells (**Figure 3.8**). Overexpression of dnRUNX3 decreased IC<sub>50</sub> for carboplatin by 0.27-fold (from 110  $\mu$ M to 79.8  $\mu$ M) as determined by the neutral red uptake assay and by 0.52-fold (from 36.9  $\mu$ M to 17.6  $\mu$ M) as determined by the clonogenic assay in A2780cp cells.

To determine whether dnRUNX3 renders A2780cp cells more sensitive to carboplatin-induced apoptosis, A2780cp/Vector and A2780cp/dnRUNX3 cells were treated with 200  $\mu$ M carboplatin for 48 or 72 h and carboplatin-induced

cleavage of PARP was assessed. As shown in **Figure 3.9**, carboplatin-induced cleavage of PARP was more pronounced in A2780cp/dnRUNX3 cells than that in A2780cp/vector cells, suggesting that dnRUNX3 potentiates carboplatin-induced apoptosis in A2780cp cells.

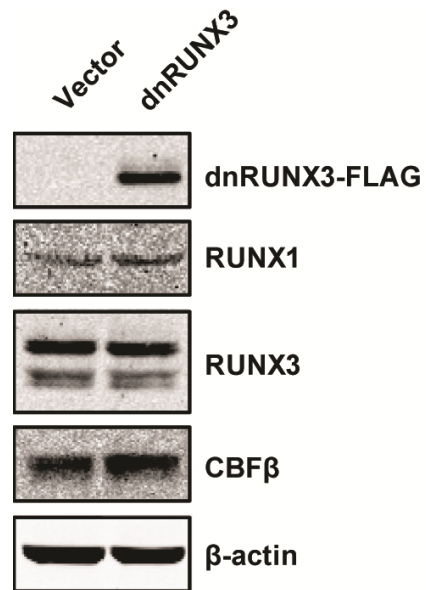


**Figure 3.7 Confirmation of dnRUNX3 overexpression in A2780cp cells by Western blotting.** dnRUNX3 overexpression in A2780cp cells was confirmed using anti-FLAG antibody. In addition, RUNX1, RUNX3 and CBF $\beta$  expression is in A2780cp/vector and A2780cp/dnRUNX3 cells is shown.  $\beta$ -actin was used as the loading control.

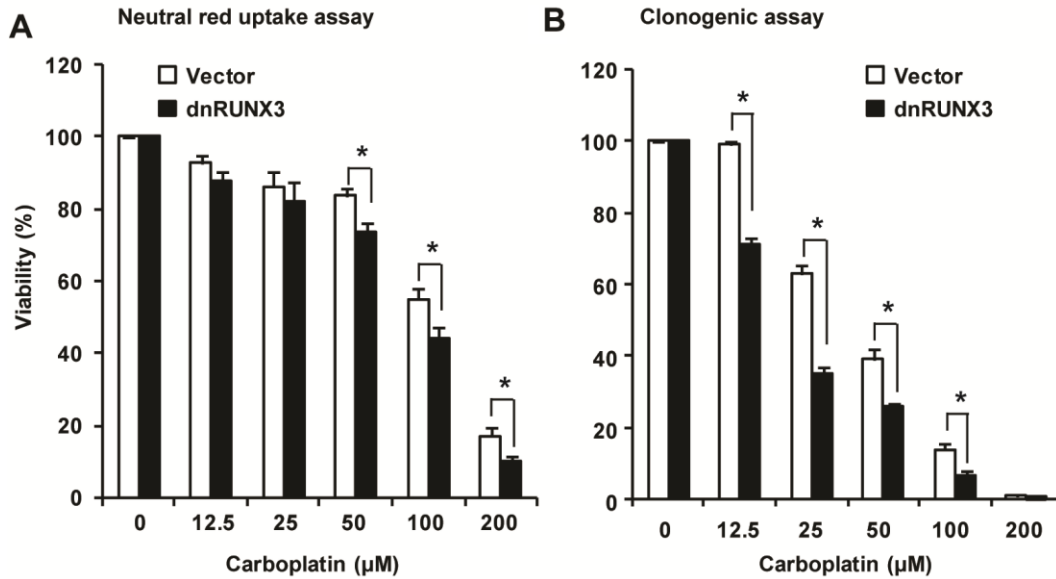


**Figure 3.8 dnRUNX3 increases the sensitivity of A2780cp cells to carboplatin.**

A2780s/Vector and A2780s/dnRUNX3 cells were treated with increasing concentrations of carboplatin. Cell viability was determined by the neutral red uptake assay (A) and the clonogenic assay (B) and expressed as a percentage relative to the respective untreated controls. Data are shown as mean  $\pm$  SEM of five independent experiments for the neutral red assay and three independent experiments for the clonogenic assay. \*Significantly different ( $P < 0.05$ ).

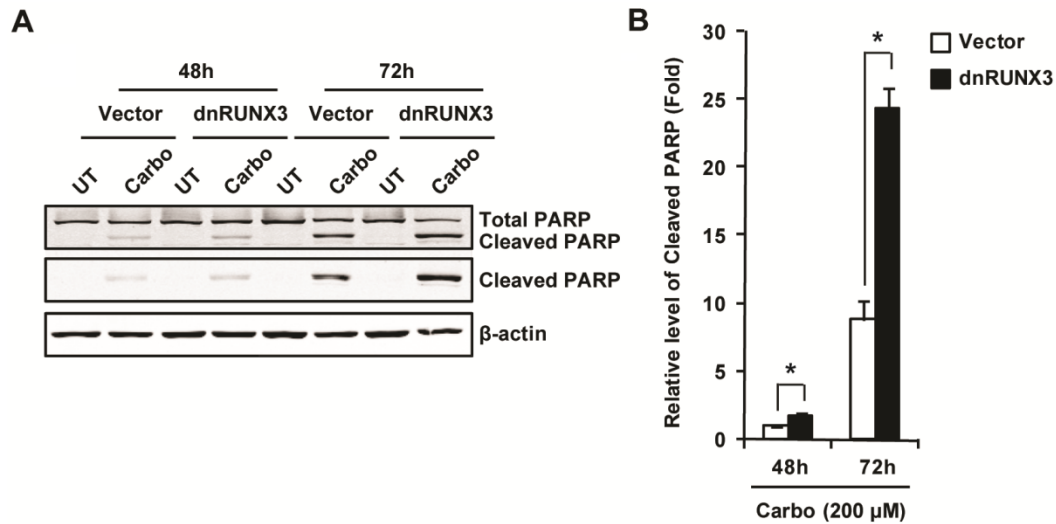


**Figure 3.9 dnRUNX3 potentiates carboplatin-induced apoptosis in A2780cp**

**cells.** (A) A2780cp/Vector and A2780cp/dnRUNX3 cells were left untreated or treated with 200 μM carboplatin for 48 or 72 h. Carboplatin-induced PARP cleavage was measured by Western blotting using antibodies against total PARP and against the cleaved PARP. β-actin was used as the loading control. (B) The Western blotting results of carboplatin-induced PARP cleavage were quantified using Odyssey imaging software. The density of the cleaved PARP bands was normalized to that of β-actin. The density of the bands in the carboplatin-treated vector cells at 48 h was designated as 1. The relative level (fold change) of cleaved PARP was shown as mean ± SEM of three independent experiments.

\*Significantly different ( $P < 0.05$ ).

### **3.1.6 dnRUNX3 decreases the expression of cellular inhibitor of apoptosis protein-2 (cIAP2) in A2780cp cells**

IAPs inhibit apoptosis by interfering with caspase activation<sup>291</sup>. Gene expression profiling of A2780s and A2780cp by a microarray analysis (Fu *et al*, *unpublished data*) showed that expression of the IAP family member cIAP2, but not that of other family members (cIAP1, XIAP and survivin), was elevated in A2780cp cells compared to A2780s cells.

qRT-PCR showed that cIAP2 mRNA level was 37.9 fold higher in A2780cp cells compared to A2780s cells (**Figure 3.10A**), which was confirmed at the protein level by Western blotting (**Figure 3.10B**). Overexpression of RUNX3 in A2780s cells increased the mRNA level of cIAP2 by 3.6 fold (**Figure 3.11A**). dnRUNX3 in A2780cp cells decreased the mRNA level of cIAP2 by 36% (**Figure 3.11B**), which was confirmed by Western blotting (**Figure 3.12A**).

Carboplatin treatment (200  $\mu$ M carboplatin for 48 h) significantly reduced the expression of cIAP2, which was potentiated by dnRUNX3 (**Figure 3.12B**). Quantification showed that overexpression of dnRUNX3 and carboplatin treatment decreased cIAP2 protein by 43% and 29%, respectively. However, combination of dnRUNX3 and carboplatin treatment decreased cIAP2 protein by 60% (**Figure 3.12C**). Taken together, these results suggest that RUNX3 regulates the expression of cIAP2 in A2780s and A2780cp cells, and potentiates carboplatin-induced decrease of cIAP2 in A2780cp cells. **Table 3.1** summarizes IC<sub>50</sub> values obtained in different experiments.

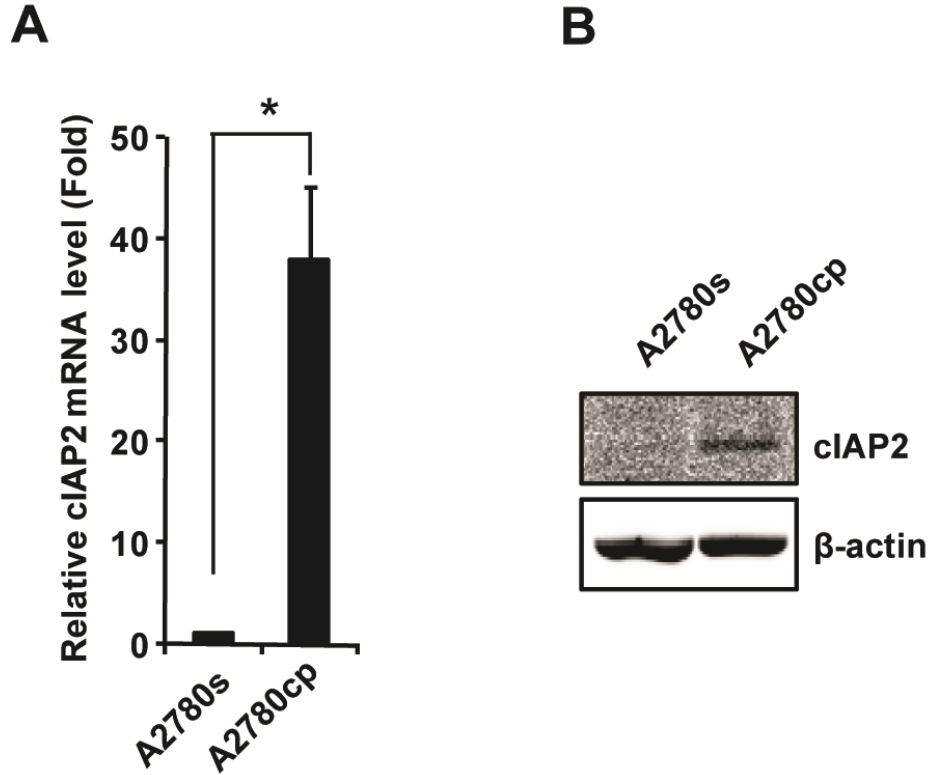


**Figure 3.10 Cellular inhibitor of apoptosis protein-2 (cIAP2) expression in A2780s and A2780cp cells.** (A) mRNA level of cIAP2 in A2780s and A2780cp was determined by qRT-PCR. Data are shown as mean  $\pm$  SEM of three independent experiments. (B) Protein level of cIAP2 in A2780s and A2780cp was determined by Western blotting.  $\beta$ -actin was used as the loading control. \*Significantly different ( $P < 0.05$ ).

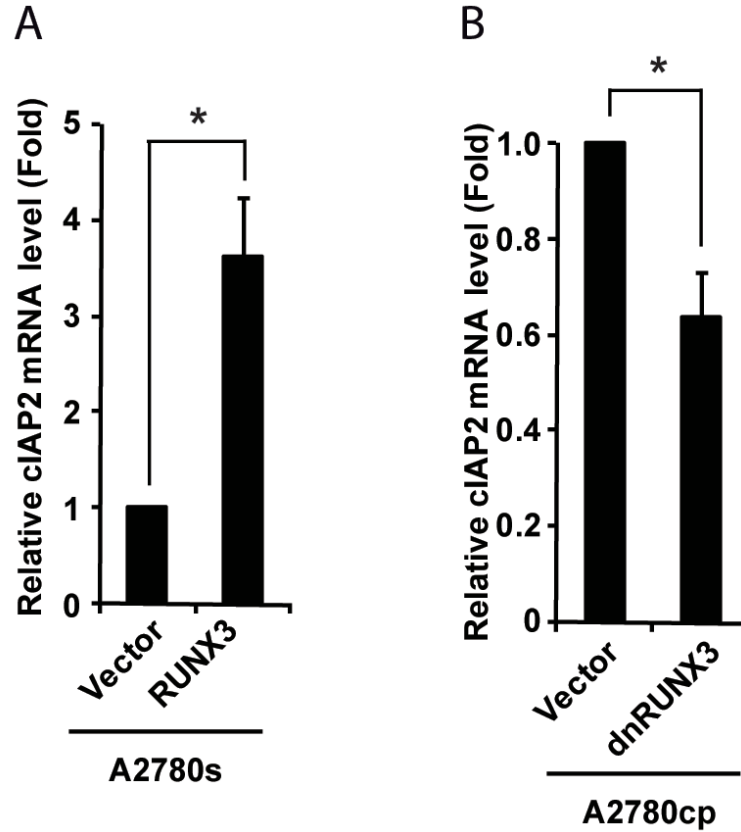


**Figure 3.11** Changes in *RUNX3* expression are associated with changes in *cIAP2* expression in A2780s and A2780cp cells. (A) Expression of cIAP2 was determined by qRT-PCR in A2780s/Vector and A2780s/RUNX3 cells (A) and A2780cp/Vector and A2780cp/dnRUNX3 cells (B). The relative level (fold change) of cIAP2 was shown as mean  $\pm$  SEM of three independent experiments. \*Significantly different ( $P < 0.05$ ).



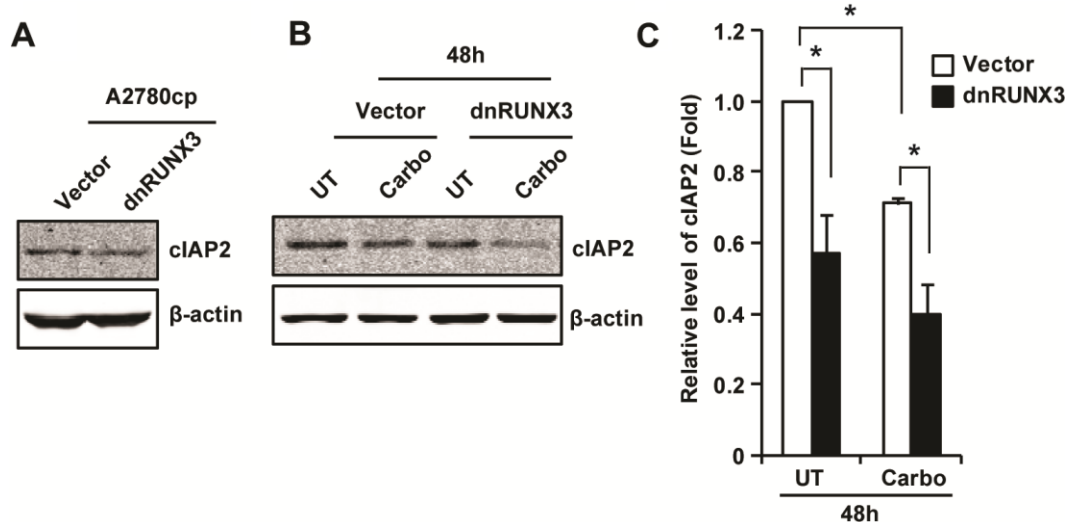


**Figure 3.12 dnRUNX3 overexpression is associated with decreased cIAP2 expression in A2780cp cells and potentiates carboplatin-induced cytotoxicity.**

(A) Expression of cIAP2 in A2780cp/Vector and A2780cp/dnRUNX3 was determined by Western blotting. β-actin was used as the loading control. (B) A2780cp/Vector and A2780cp/dnRUNX3 cells were left untreated or treated with 200 μM carboplatin for 48 h. cIAP2 protein level was measured by Western blotting. β-actin was used as the loading control. (C) The Western blotting results of cIAP2 were quantified using Odyssey imaging software. The density of cIAP2 bands was normalized to that of β-actin. The density of the bands in the untreated A2780cp/Vector cells was designated as 1. The relative level (fold change) of cIAP2 was shown as mean ± SEM of three independent experiments. \*Significantly different (P < 0.05).

**Table 3.1 Summary of IC<sub>50</sub> values measured for different experiments by two cytotoxicity assays**

<i>Cell lines / Experiment</i>	<i>Cell line</i>	<i>Assay</i>	<i>IC<sub>50</sub> (μM)</i>	<i>Fold-change (relative to control)</i>
<b>Paired EOC model</b>	A2780s	Clonogenic assay	3.7	-
	A2780cp		35.5	9.59
<b>RUNX3 overexpression</b>	A2780s/vector	Clonogenic assay	3.6	-
	A2780s/RUNX3		7.9	2.1
<b>RUNX3 knockdown</b>	A2780cp shRandom	Neutral red assay	123.4	-
	A2780cp shRUNX3-D		92.8	0.75
	A2780cp shRUNX3-E		103.9	0.84
<b>dnRUNX3 overexpression</b>	A2780cp/vector	Neutral red assay	110.0	-
	A2780cp/dnRUNX3		79.8	0.73
	A2780cp/vector	Clonogenic assay	36.9	-
	A2780cp/dnRUNX3		17.6	0.48

### **3.2 The role of Wnt/ $\beta$ -catenin signaling in EOC resistance to carboplatin**

The analysis of microarray data of the paired A2780s and A2780cp cell lines by IPA software demonstrated that several components of the Wnt/ $\beta$ -catenin signaling pathway are differentially expressed between these two cell lines. These data, together with subsequent validation by qRT-PCR, were previously reported in our laboratory<sup>274</sup>, and **Figure 3.13** shows an updated output of IPA software<sup>274</sup>. It was suggested that Wnt/ $\beta$ -catenin signaling is more active in A2780cp cells, and that further analysis is needed to confirm this higher activity and the potential of targeting this pathway to sensitize EOC cells to carboplatin<sup>274</sup>. Here, most of these future directions have been addressed.

#### **3.2.1 $\beta$ -catenin localization is nuclear in A2780cp and membranous in A2780s cells**

Upon the activation of Wnt/ $\beta$ -catenin signaling,  $\beta$ -catenin is translocated to the nucleus to bind LEF/TCF family members and modulate the transcription of Wnt/ $\beta$ -catenin signaling target genes. To confirm the higher activity of Wnt/ $\beta$ -catenin signaling in A2780cp cells, ICC was conducted using anti- $\beta$ -catenin antibody. As shown in **Figure 3.14**,  $\beta$ -catenin was found to be localized mainly in the nucleus of A2780cp, while it was localized in the membranes of A2780s cells. This represents another line of evidence that Wnt/ $\beta$ -catenin signaling is more active in A2780cp cells compared to A2780s cells, and might have a role in the development of platinum resistance.

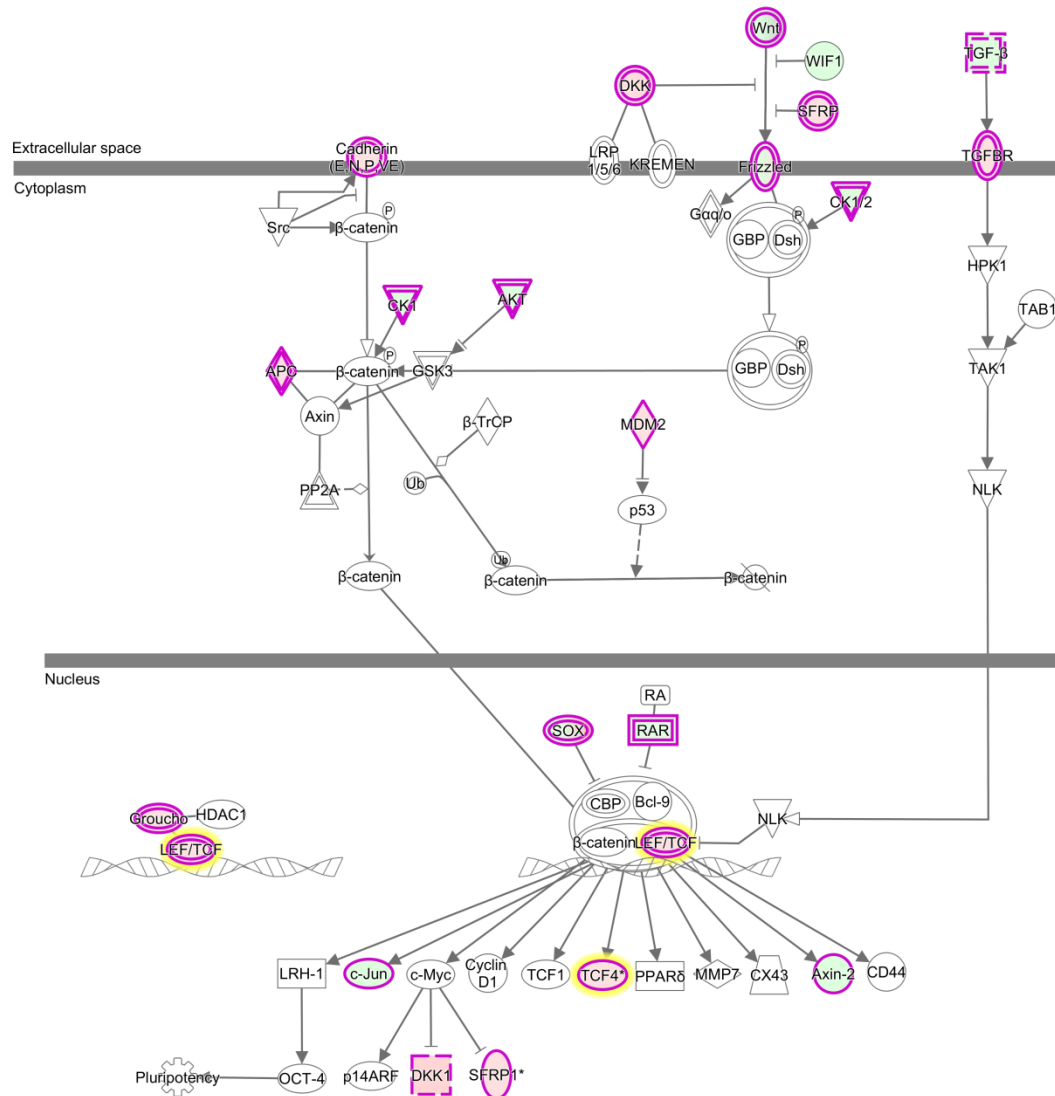


**Figure 3.13** IPA analysis of microarray data of A2780s-A2780cp paired cell line model suggests Wnt/β-catenin signaling is more active in A2780cp cells. Several components of Wnt/β-catenin signaling are differentially expressed between A2780s and A2780cp cells in a way that suggests Wnt/β-catenin signaling is upregulated in A2780cp cells and it might have a role in chemoresistance. Components upregulated are shaded in *green*, and those downregulated are shaded in *orange*.

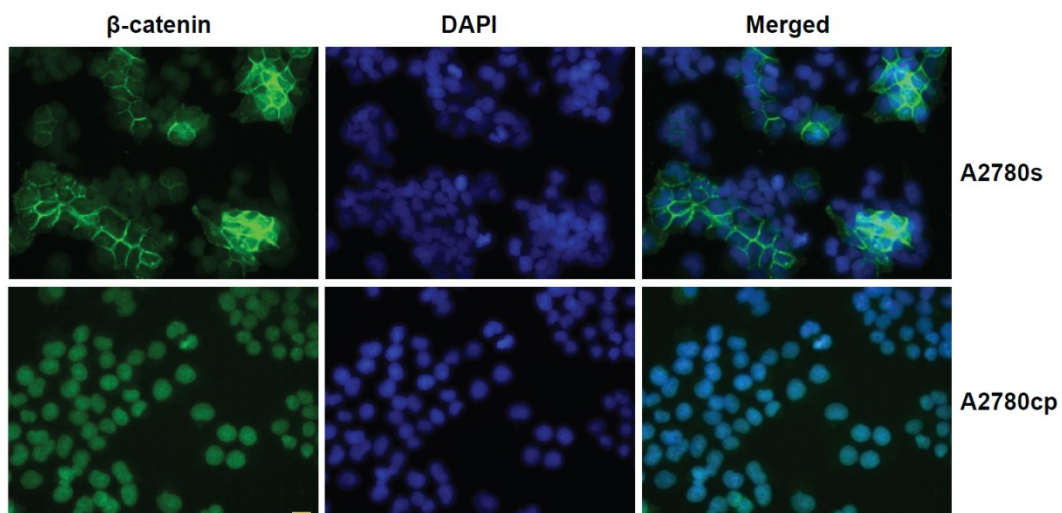


**Figure 3.14  $\beta$ -catenin intracellular localization in A2780s and A2780cp cells.**

Intracellular localization of  $\beta$ -catenin was examined by immunocytochemistry using anti- $\beta$ -catenin antibody. The nucleus was stained with DAPI. While  $\beta$ -catenin is mainly localized in the membranes of A2780s cells, it is localized in the nucleus of A2780cp cells. Scale bar = 20  $\mu$ M.

### **3.2.2 LEF/TCF-driven transcriptional activity of $\beta$ -catenin in A2780cp is higher than that in A2780s cells**

To further confirm the higher activity of Wnt/ $\beta$ -catenin signaling in A2780cp cells, a LEF/TCF-driven luciferase reporter assay was conducted. In this assay, A2780cp and A2780s cells were transfected with plasmids having LEF/TCF binding motifs associated with a gene encoding luciferase enzyme together with appropriate controls. As shown in **Figure 3.15**, relative LEF/TCF-driven transcriptional activity of  $\beta$ -catenin in A2780cp cells is approximately 4-fold that of its counterpart in A2780s cells. This again suggests that Wnt/ $\beta$ -catenin signaling is more active in the resistant A2780cp cells and might have a role in the development of carboplatin resistance.

### **3.2.3 Wnt extracellular modulators that negatively regulate Wnt/ $\beta$ -catenin signaling are downregulated in A2780cp cells**

Wnt/ $\beta$ -catenin signaling is regulated by three families of extracellular modulators, namely: DKKs, SFRPs and WIF-1. A number of these modulators were previously reported to be downregulated as assessed by microarray and qRT-PCR<sup>274</sup>. To further confirm these findings, DKK1 and SFRP1 were selected to test their expression by Western blotting. As shown in **Figure 3.16**, DKK1 and SFRP1 are downregulated in A2780cp cells compared to A2780s cells. Downregulation of DKK1 and SFRP1 might contribute to the higher Wnt/ $\beta$ -catenin signaling in A2780cp cells and therefore may have a role in the development of platinum resistance.

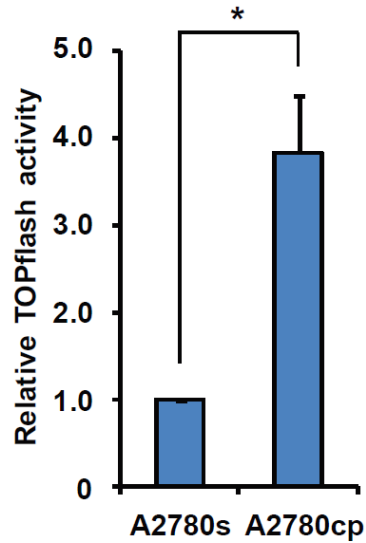


**Figure 3.15  $\beta$ -catenin transcriptional activity in A2780s and A2780cp cells.**  $\beta$ -catenin transcriptional activity was determined by TOPFlash luciferase assay. A2780s and A2780cp cells were transiently co-transfected with a TOPFlash (wild-type LEF/TCF binding sites) or a FOPFlash (mutated LEF/TCF binding sites) firefly luciferase construct with a Renilla luciferase construct. TOPFlash activity was normalized against FOPFlash activity and relative activity of A2780s cells was set as 1. Data are mean  $\pm$  SEM of three independent experiments. \*Significantly different ( $P < 0.05$ ).

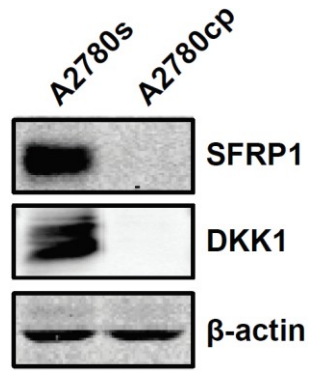


**Figure 3.16** Expression of selected Wnt signaling components in A2780s and A2780cp cells. Protein level of DKK1 and SFRP1 in A2780s and A2780cp cells was examined by Western blotting.  $\beta$ -Actin was the loading control.



### **3.2.4 Chemical inhibition of Wnt/ $\beta$ -catenin signaling sensitizes A2780cp cells to carboplatin in a synergistic manner**

To test the potential of targeting Wnt/ $\beta$ -catenin signaling in sensitizing the resistant A2780cp cells to carboplatin, the Wnt signaling small-molecule inhibitor CCT036477 was used. CCT036477 acts by blocking  $\beta$ -catenin- and TCF-induced transcription, without altering  $\beta$ -catenin levels<sup>206,292-294</sup>. Based on dose-response studies, carboplatin was used at concentrations of 12.5, 25, 50, 100 and 200  $\mu$ M and combined with CCT036477 at concentrations of 10, 15, 20 and 30  $\mu$ M. Response to single and combined treatments was measured after 72 h using neutral red uptake assay. The interaction between carboplatin and CCT036477 was then analyzed using the Chou-Talalay method (COMPUSYN<sup>TM</sup> software)<sup>282</sup> to find potential synergistic combinations. As shown in **Figure 3.17** and **Table 3.2**, synergistic combinations (CI <1) were observed at high doses of CCT036477 (20 and 30  $\mu$ M), and all the doses of carboplatin (12.5 through 200  $\mu$ M).

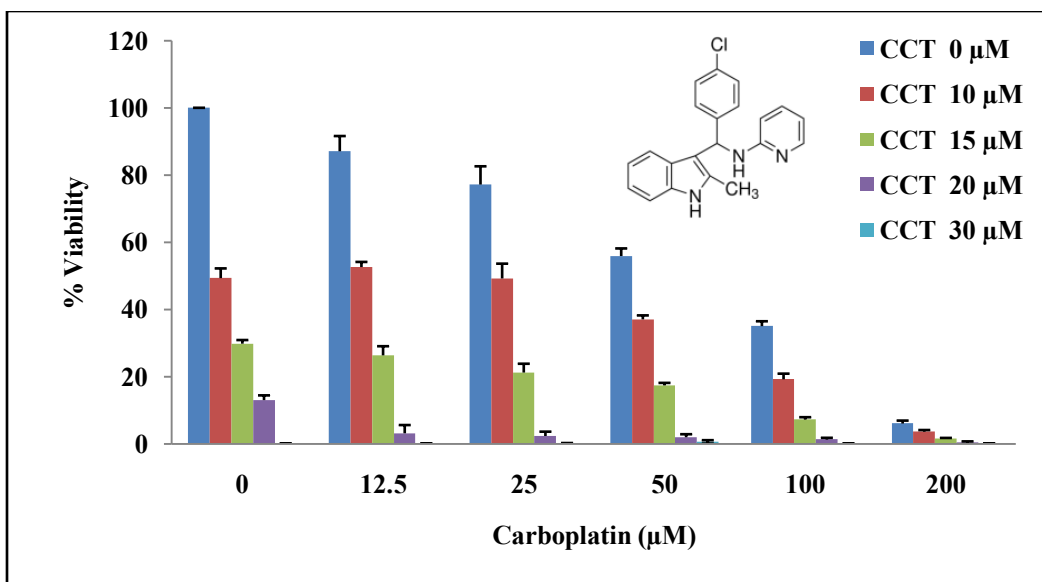


**Figure 3.17 Combination of carboplatin with the  $\beta$ -catenin inhibitor CCT036477 in A2780cp cells.** Carboplatin (at concentrations from 12.5 through 200  $\mu$ M) was combined with CCT036477 (at concentrations from 10 through 30  $\mu$ M) and viability of A2780cp cells was assessed by 72-hour neutral red uptake assay. The chemical structure of CCT036477 is shown.

**Table 3.2 Combination index (CI) values for different combinations of CCT036477 and carboplatin\***

Carbo ( $\mu$ M)	CCT036477 ( $\mu$ M)				
	0	10	15	20	30
0	NA	NA	NA	NA	NA
12.5	NA	1.72	1.56	0.8	0.22
25	NA	1.87	1.51	0.75	0.35
50	NA	1.86	1.56	0.74	0.66
100	NA	1.64	1.21	0.69	0.16
200	NA	0.94	0.75	0.5	0.25

\*  $CI < 1$  denotes synergism (shaded in green);  $CI = 1$  denotes additive interaction;  $CI > 1$  denotes antagonism

# **Chapter 4**

## **Discussion**

## 4. Discussion

Most EOCs respond well to the first-line chemotherapeutic agents. However, the majority of patients develop drug resistance over the course of treatment. A better understanding of the molecular mechanisms underlying the acquired drug resistance is therefore necessary to improve the management of this disease.

The paired cisplatin-sensitive A2780s and cisplatin-resistant A2780cp cell lines have been widely used to study the acquired chemoresistance of EOC<sup>295,296</sup>. In this study, A2780cp cells were also found to be resistant to carboplatin as assessed by the clonogenic assay; the IC<sub>50</sub> for A2780cp cells was approximately 10-fold that of A2780s cells (**Figure 3.3** and **Table 3.1**). In addition, cisplatin and carboplatin were reported to have a broad range of cross-resistance<sup>98,124</sup>. Accordingly, this chemoresistance model can be used to study carboplatin resistance. Genome expression profiling of this chemoresistance model by microarray followed by IPA analysis revealed thousands of differentially expressed genes between these two cell lines. From these differentially expressed genes, RUNX3 and the Wnt/ $\beta$ -catenin signaling pathway were selected for further analysis based on literature review.

### 4.1 The role of RUNX family members in EOC resistance to carboplatin

Two studies have demonstrated that RUNX3 plays an oncogenic role in EOC<sup>190,283</sup>. However, the role for RUNX3 in chemoresistance of EOC has not been reported. In our laboratory, RUNX3 was found to be expressed in primary EOC cells isolated from ascites of EOC patients, but not in normal OSE cells<sup>274</sup>. In addition, RUNX3 was found to be localized in the nucleus in primary EOC

cells<sup>274</sup>, which is consistent with the localization reported by Lee *et al.* and supports the functional role of RUNX3 as a transcription factor<sup>190</sup>. In this thesis, functional validation of the role of RUNX3 in chemoresistance to carboplatin was pursued. Previous results in our laboratory and results from the current study (**Figures 3.1 and 3.2**) have shown that RUNX3 expression is markedly elevated in A2780cp cells compared to A2780s cells. These data are supported by the data from the GEO database for the cisplatin-resistant A2780cp70 cells and chemoresistant EOC tissues compared to their respective controls<sup>284</sup>.

To validate the role of RUNX3 in chemoresistance, both gain- and loss-of-function studies were subsequently conducted. Overexpression of RUNX3 rendered A2780s cells more resistant to carboplatin (**Figure 3.4**). In addition, overexpression of dnRUNX3 and, to a lesser extent, knockdown of RUNX3 were able to partially sensitize A2780cp cells to carboplatin (**Figures 3.5 and 3.8**). Taken together, the expression and functional analysis suggest that RUNX3 contributes to carboplatin resistance of EOC cells.

Yano *et al* observed that dnRUNX3 is more potent in inhibiting TGF $\beta$ -induced apoptosis of gastric cancer SNU16 cells than the antisense DNA against *RUNX3* and suggested that dnRUNX3 may also inhibit the function of other RUNX proteins<sup>276</sup>. dnRUNX3 is a truncated protein that contains the Runt DNA binding domain, but lacks domains located at the carboxyl terminus, including the activation domain. dnRUNX3 has been shown to inhibit the activity of RUNX proteins likely via competing for the RUNX DNA binding sites<sup>177,290,297</sup>. The

three RUNX proteins (RUNX1-3) have been shown to have overlapping and distinct biological functions depending on cell context<sup>289</sup>.

Our results showed that RUNX1 is also expressed in A2780cp cells at a slightly higher level compared to A2780s cells (**Figures 3.1** and **3.2**). Thus, the less pronounced effect of RUNX3 knockdown on carboplatin resistance could be due to either the incomplete knockdown of RUNX3 or the compensation for decreased RUNX3 expression by RUNX1 or both. On the other hand, overexpression of dnRUNX3 likely inhibits both RUNX3 and RUNX1 functions, and thus renders A2780cp cells more sensitive to carboplatin. Therefore, a therapeutic strategy that inhibits the activity of all RUNX proteins could be a more effective approach to sensitize EOC cells to carboplatin.

IAPs that include cIAP1, cIAP2, XIAP and survivin inhibit apoptosis by interfering with caspase activation<sup>291</sup>. The microarray data have also shown that cIAP2 expression is elevated in A2780cp cells compared to A2780s cells<sup>274</sup>, which was confirmed by qRT-PCR and Western blotting (**Figure 3.10**). Upregulation of cIAP2 has been associated with cisplatin resistance in prostate cancer and lung cancer<sup>298,299</sup> and inhibition of IAPs including cIAP2 results in increased apoptosis in EOC cells<sup>300</sup>. Here, it has been shown that changes in *RUNX3* levels are associated with changes in *cIAP2* expression; overexpression of RUNX3 increases the expression of cIAP2 in A2780s cells and dnRUNX3 decreases the expression of cIAP2 in A2780cp cells (**Figure 3.11**). Interestingly, we also found that carboplatin treatment decreases the expression of cIAP2, suggesting that downregulation of cIAP2 can be one mechanism for carboplatin to

induce apoptosis in A2780cp cells (**Figure 3.12**). In addition, our finding that dnRUNX3 decreases the expression of cIAP2 and potentiates carboplatin-induced downregulation of cIAP2 in A2780cp cells suggests that dnRUNX3-induced sensitization of A2780cp cells to carboplatin could be at least partially attributed to the downregulation of cIAP2. Further studies are required to determine the role of cIAP2 in carboplatin resistance in A2780cp cells.

Cancer cells develop a variety of mechanisms to reduce platinum toxicity, including decreasing intracellular platinum accumulation and inhibiting platinum-induced apoptosis<sup>83,110,120</sup>. In this study, we report a role for RUNX3 in inhibiting carboplatin-induced apoptosis in A2780cp cells. However, the underlying mechanisms await further investigation. Additionally, it is important to confirm the role of RUNX3 in carboplatin resistance in other EOC cell lines. The interaction between cancer cells and the tumor microenvironment plays an important role in chemoresistance; therefore, it is also important that the role of RUNX proteins in carboplatin resistance be tested in pre-clinical *in vivo* models. In this regard, it is our future interest to test whether dnRUNX3 can sensitize A2780cp xenografts to carboplatin in mouse models.

Given the multifactorial nature of resistance to platinum-based compounds<sup>83,110,120</sup>, it becomes crucial to identify all potential mechanisms contributing to the resistance. Identifying the major mechanisms governing the resistant phenotype in a given patient will lead to the development of the best-suited combination therapy that achieves an optimal therapeutic outcome. This



cope with the emerging trend of precision oncology that aims at effectively managing cancer heterogeneity and drug resistance<sup>301</sup>.

#### **4.2 The role of Wnt/ $\beta$ -catenin signaling in EOC resistance to carboplatin**

Another pathway found to be differentially activated between the two cell lines used in this study is the Wnt/ $\beta$ -catenin signaling pathway. This pathway has been reported to play a role in the development of chemo-, radio- and immunoresistance in several malignancies<sup>302-307</sup>. Although many studies investigated Wnt/ $\beta$ -catenin signaling in the context of pathogenesis and progression of EOC (**Section 1.4.5**), its role in EOC resistance to chemotherapeutics is reported only in few studies. In this context, endothelin A receptor/ $\beta$ -arrestin signaling was found to induce EMT and chemoresistance to cisplatin via activation of Wnt/ $\beta$ -catenin signaling pathway in EOC cells and in a mouse xenograft model<sup>161,308</sup>. In another study, the PPAR $\gamma$  ligand rosiglitazone reversed the resistance of A2780 cells to taxol by downregulating FZD1 and thereby inhibiting the Wnt/ $\beta$ -catenin pathway<sup>309</sup>. In addition, activation of Wnt/ $\beta$ -catenin-ATP-binding cassette G2 signaling was reported to be one mechanism through which c-Kit induces chemoresistance and TIC of ovarian cancer cells<sup>310</sup>. Moreover, genetic silencing or chemical inhibition of DVL-1 was reported to sensitize paclitaxel-resistant A2780 cells through downregulation of AKT/GSK-3 $\beta$ / $\beta$ -catenin signaling<sup>311</sup>.

In our laboratory, IPA analysis of microarray data (**Figure 3.13**) and subsequent validation by qRT-PCR showed that several components of Wnt/ $\beta$ -catenin signaling are differentially expressed between A2780s and A2780cp cells

in a pattern that suggests higher activity of this pathway in the cisplatin-resistant cell line<sup>274</sup>. In this thesis, further confirmation of that higher activity was pursued using different strategies.

To gain further insight into Wnt/ $\beta$ -catenin signaling activity,  $\beta$ -catenin localization was assessed by ICC. The results showed that  $\beta$ -catenin is localized in the nuclei in A2780cp cells, whereas it was localized in the membranes in A2780s cells (**Figure 3.14**). This suggests an increased Wnt/ $\beta$ -catenin signaling activity in the chemoresistant cell line as compared to its sensitive counterpart. This finding is consistent with the previous studies by Lee *et al.* and Wang *et al.* which reported a positive correlation between  $\beta$ -catenin nuclear localization and poor prognosis in EOC<sup>312,313</sup>. Conversely, Bodnar *et al.* reported an association between membranous immunohistochemical staining of  $\beta$ -catenin and resistance to platinum chemotherapy in advanced EOC<sup>314</sup>. In addition, Usongo *et al.* reported that Wnt3a- or LiCl-mediated activation of canonical Wnt signaling enhanced OSE proliferation by promoting G1 to S phase cell cycle progression independently of  $\beta$ -catenin/TCF-driven transcriptional changes<sup>315</sup>.

To determine the involvement of  $\beta$ -catenin in this higher activity, we measured  $\beta$ -catenin transcriptional activity using a LEF/TCF-driven luciferase reporter assay. The transcriptional activity of  $\beta$ -catenin of A2780cp cells was found to be approximately 4-fold greater than that of A2780s cells (**Figure 3.15**). This confirms that nuclear localization of  $\beta$ -catenin in A2780cp cells is associated with increased transcriptional activity, and therefore  $\beta$ -catenin/TCF might mediate the higher activity of Wnt/ $\beta$ -catenin signaling. Taken together, these findings

suggest that Wnt/ $\beta$ -catenin signaling is more active in A2780cp cells and therefore might contribute to the development of resistance to platinum chemotherapeutics.

To test the potential utility of targeting Wnt/ $\beta$ -catenin signaling in reversing platinum resistance, the  $\beta$ -catenin inhibitor CCT036477 was combined with carboplatin at different concentrations of both drugs and CI was assessed using the Chou-Talalay method<sup>282</sup>. Synergism was observed at relatively high doses of CCT036477 (20 and 30  $\mu$ M). The extent of synergism, as assessed by CI value, was marked at all carboplatin combinations with 30  $\mu$ M CCT036477 except the 50  $\mu$ M carboplatin concentration (**Figure 3.17** and **Table 3.2**). Our results are supported by previous reports of EOC cells sensitization to chemotherapeutics by shRNA- and siRNA-mediated knockdown of  $\beta$ -catenin<sup>316,317</sup>. Since CCT036477 acts by suppressing  $\beta$ -catenin- and TCF-induced transcription, it is tempting to try other inhibitors that target different signaling nodes of Wnt/ $\beta$ -catenin signaling<sup>206</sup>. In this respect, the small-molecule anthelmintic drug niclosamide was reported to inhibit ovarian tumorsphere formation and sensitize primary EOC cells to carboplatin via inhibition of the Wnt/ $\beta$ -catenin signaling pathway<sup>318</sup>. Niclosamide acts on targets upstream to  $\beta$ -catenin; more specifically it acts by downregulating DVL2 expression<sup>319</sup> and degrading the coreceptors LRP 5/6<sup>320</sup>. Given the heterogeneity of EOC, it will be a more effective strategy to target more than one signaling pathway based on gene expression profiling and assessment of major determinants of EOC resistance on a personalized basis.

The Wnt extracellular modulators sFRPs, DKKs and WIF-1 negatively regulate the activity of Wnt signaling<sup>220</sup>. In the context of EOC, DKK2 was reported to be epigenetically silenced by hypermethylation in EOC and the extent of hypermethylation positively correlated with higher grades and stages of the disease. Moreover, the re-expression of DKK2 led to inhibiting the proliferative and invasive capacity of SKOV3 and ES-2 cell lines<sup>269</sup>. In another study, DKK1 was found to be overexpressed in ovarian serous papillary adenocarcinoma, and DKK1 expression was positively correlated with the FIGO stage<sup>271</sup>. In addition, SFRP4 and SFRP5 were found to be positively associated with chemosensitivity and favorable prognosis in independent reports<sup>160,273,321</sup>. In our laboratory, microarray data and subsequent validation by qRT-PCR have shown that SFRP1, SFRP3, DKK1 and DKK3 were downregulated in the chemoresistant A2780cp cells as compared to A2780s cells<sup>274</sup>. DKK1 and SFRP1 were selected for further analysis of their role in the chemoresistance of EOC cells because they have not been studied previously in this context. DKK1 and SFRP1 downregulation in A2780cp cells was confirmed by Western blotting (**Figure 3.16**). Gain- and loss-of-function experiments of DKK1 and SFRP1, alone and in combination, in A2780cp and A2780s cells, respectively are planned to assess their specific roles in chemoresistance.

#### **4.3 Potential crosstalk between RUNX transcription factors and Wnt/ $\beta$ -catenin signaling**

RUNX transcription factors were reported to exert a number of their effects via interaction with Wnt/ $\beta$ -catenin signaling<sup>169,176,180</sup>. In an attempt to explore the

potential crosstalk between RUNX3 and Wnt/ $\beta$ -catenin signaling in EOC cells, we compared the transcriptional activity of  $\beta$ -catenin between A2780s/Vector and A2780s/RUNX3 cells using LEF/TCF-driven luciferase reporter assay.  $\beta$ -catenin transcriptional activity was *not* significantly different between the two cell lines, which suggests that the chemoresistance induced by RUNX3 overexpression is independent of Wnt/ $\beta$ -catenin signaling (data not shown). As mentioned above, chemoresistant EOC is characterized by heterogeneity, and it is possible that different subpopulations of cells develop resistance via distinct molecular mechanisms.

#### **4.4 Conclusions and future directions**

In conclusion, EOC is a heterogeneous disease and carboplatin resistance of EOC is multifactorial. Here, two novel and independent molecular mechanisms are investigated, namely RUNX3 overexpression and activation of Wnt/ $\beta$ -catenin signaling. First, we confirmed that RUNX3 expression is higher in the carboplatin-resistant A2780cp cells compared to the carboplatin-sensitive A2780s cells. Carboplatin treatment induces RUNX3 expression in A2780s cells. Functionally, overexpression of RUNX3 renders A2780s cells more resistant to carboplatin and dnRUNX3 increases the sensitivity of A2780cp cells to carboplatin. Carboplatin sensitivity induced by dnRUNX3 overexpression was associated with cIAP2 downregulation, suggesting cIAP2 may have a role in carboplatin resistance. Because knockdown of RUNX3 alone is not sufficient to profoundly sensitize A2780cp cells to carboplatin, likely due to compensation by the expression of RUNX1, targeting all RUNX proteins could be an effective

strategy to tackle the chemoresistance. Second, Wnt/ $\beta$ -catenin signaling is more active in A2780cp cells compared to A2780s cells as assessed by localization and LEF/TCF-driven transcriptional activity of  $\beta$ -catenin. This higher activity is independent of RUNX3 overexpression and may be limited to subpopulations of EOC cells. Chemical inhibition of Wnt/ $\beta$ -catenin signaling by CCT036477 sensitizes A2780cp cells to carboplatin in a synergistic manner especially at high concentrations. The synergistic potential of other Wnt/ $\beta$ -catenin inhibitors needs to be assessed in the future. The Wnt negative regulators SFRP1 and DKK1 are downregulated in A2780cp cells, and their specific roles in EOC chemoresistance to carboplatin need to be determined through appropriate functional and mechanistic studies. Given the multifactorial nature of EOC resistance, the genetic profile of chemoresistant patients should be assessed to pinpoint the major determinant mechanisms of resistance and tailor the best-suited combination therapeutics on an individualized basis to achieve optimum therapeutic outcomes.

## References

1. Canadian Cancer Society's Advisory Committee on Cancer Statistics. Canadian Cancer Statistics 2014. Toronto, ON:2014.
2. Jayson GC, Kohn EC, Kitchener HC, Ledermann JA. Ovarian cancer. *Lancet*. Oct 11 2014;384(9951):1376-1388.
3. Siegel RL, Miller KD, Jemal A. Cancer statistics, 2015. *CA Cancer J Clin*. Jan-Feb 2015;65(1):5-29.
4. Torre LA, Bray F, Siegel RL, Ferlay J, Lortet-Tieulent J, Jemal A. Global cancer statistics, 2012. *CA Cancer J Clin*. Mar 2015;65(2):87-108.
5. Hennessy BT, Coleman RL, Markman M. Ovarian cancer. *Lancet*. Oct 17 2009;374(9698):1371-1382.
6. Sieh W, Salvador S, McGuire V, et al. Tubal ligation and risk of ovarian cancer subtypes: a pooled analysis of case-control studies. *Int J Epidemiol*. Apr 2013;42(2):579-589.
7. Hankinson SE, Hunter DJ, Colditz GA, et al. Tubal ligation, hysterectomy, and risk of ovarian cancer. A prospective study. *JAMA*. Dec 15 1993;270(23):2813-2818.
8. Jelovac D, Armstrong DK. Recent progress in the diagnosis and treatment of ovarian cancer. *CA Cancer J Clin*. May-Jun 2011;61(3):183-203.
9. Tsilidis KK, Allen NE, Key TJ, et al. Oral contraceptive use and reproductive factors and risk of ovarian cancer in the European Prospective Investigation into Cancer and Nutrition. *Br J Cancer*. Oct 25 2011;105(9):1436-1442.
10. Stewart LM, Holman CD, Finn JC, Preen DB, Hart R. In vitro fertilization is associated with an increased risk of borderline ovarian tumours. *Gynecol Oncol*. May 2013;129(2):372-376.
11. Cramer DW, Liberman RF, Titus-Ernstoff L, et al. Genital talc exposure and risk of ovarian cancer. *International journal of cancer. Journal international du cancer*. May 5 1999;81(3):351-356.
12. Muscat JE, Huncharek MS. Perineal talc use and ovarian cancer: a critical review. *Eur J Cancer Prev*. Apr 2008;17(2):139-146.
13. Vaughan S, Coward JI, Bast RC, Jr., et al. Rethinking ovarian cancer: recommendations for improving outcomes. *Nat Rev Cancer*. Oct 2011;11(10):719-725.
14. Chen VW, Ruiz B, Killeen JL, Cote TR, Wu XC, Correa CN. Pathology and classification of ovarian tumors. *Cancer*. May 15 2003;97(10 Suppl):2631-2642.
15. Scully R, Sobin L. *Histological typing of ovarian tumours*. Vol 9. New York: Springer Berlin; 1999.
16. Bast R, Romero I, Mills G. Molecular Pathogenesis of Ovarian Cancer. In: Mendelsohn J, Howley P, Israel M, eds. *The Molecular Basis of Cancer* 4th ed: Saunders; 2014:531-547.
17. Cho KR, Shih Ie M. Ovarian cancer. *Annu Rev Pathol*. 2009;4:287-313.
18. Bast RC, Jr., Hennessy B, Mills GB. The biology of ovarian cancer: new opportunities for translation. *Nat Rev Cancer*. Jun 2009;9(6):415-428.

19. Goff BA, Mandel L, Muntz HG, Melancon CH. Ovarian carcinoma diagnosis. *Cancer*. Nov 15 2000;89(10):2068-2075.
20. Prat J. Staging classification for cancer of the ovary, fallopian tube, and peritoneum. *International journal of gynaecology and obstetrics: the official organ of the International Federation of Gynaecology and Obstetrics*. Jan 2014;124(1):1-5.
21. Ricci F, Broggini M, Damia G. Revisiting ovarian cancer preclinical models: implications for a better management of the disease. *Cancer Treat Rev*. Oct 2013;39(6):561-568.
22. Nik NN, Vang R, Shih Ie M, Kurman RJ. Origin and pathogenesis of pelvic (ovarian, tubal, and primary peritoneal) serous carcinoma. *Annu Rev Pathol*. 2014;9:27-45.
23. Landen CN, Jr., Birrer MJ, Sood AK. Early events in the pathogenesis of epithelial ovarian cancer. *Journal of clinical oncology : official journal of the American Society of Clinical Oncology*. Feb 20 2008;26(6):995-1005.
24. Kurman RJ, Shih Ie M. Pathogenesis of ovarian cancer: lessons from morphology and molecular biology and their clinical implications. *International journal of gynecological pathology : official journal of the International Society of Gynecological Pathologists*. Apr 2008;27(2):151-160.
25. Cannistra SA. Cancer of the ovary. *The New England journal of medicine*. Dec 9 2004;351(24):2519-2529.
26. Rustin GJ. Use of CA-125 to assess response to new agents in ovarian cancer trials. *Journal of clinical oncology : official journal of the American Society of Clinical Oncology*. May 15 2003;21(10 Suppl):187s-193s.
27. Rustin GJ, Timmers P, Nelstrop A, et al. Comparison of CA-125 and standard definitions of progression of ovarian cancer in the intergroup trial of cisplatin and paclitaxel versus cisplatin and cyclophosphamide. *Journal of clinical oncology : official journal of the American Society of Clinical Oncology*. Jan 1 2006;24(1):45-51.
28. Fathalla MF. Incessant ovulation--a factor in ovarian neoplasia? *Lancet*. Jul 17 1971;2(7716):163.
29. Fleming JS, Beaugie CR, Haviv I, Chenevix-Trench G, Tan OL. Incessant ovulation, inflammation and epithelial ovarian carcinogenesis: revisiting old hypotheses. *Molecular and cellular endocrinology*. Mar 9 2006;247(1-2):4-21.
30. Kurman RJ. Origin and molecular pathogenesis of ovarian high-grade serous carcinoma. *Ann Oncol*. Dec 2013;24 Suppl 10:x16-21.
31. Lengyel E. Ovarian cancer development and metastasis. *Am J Pathol*. Sep 2010;177(3):1053-1064.
32. Lee KR, Young RH. The distinction between primary and metastatic mucinous carcinomas of the ovary: gross and histologic findings in 50 cases. *Am J Surg Pathol*. Mar 2003;27(3):281-292.
33. Zaino RJ, Brady MF, Lele SM, Michael H, Greer B, Bookman MA. Advanced stage mucinous adenocarcinoma of the ovary is both rare and



- highly lethal: a Gynecologic Oncology Group study. *Cancer*. Feb 1 2011;117(3):554-562.
34. Kelemen LE, Kobel M. Mucinous carcinomas of the ovary and colorectum: different organ, same dilemma. *Lancet Oncol*. Oct 2011;12(11):1071-1080.
  35. Berns EM, Bowtell DD. The changing view of high-grade serous ovarian cancer. *Cancer research*. Jun 1 2012;72(11):2701-2704.
  36. Flesken-Nikitin A, Hwang CI, Cheng CY, Michurina TV, Enikolopov G, Nikitin AY. Ovarian surface epithelium at the junction area contains a cancer-prone stem cell niche. *Nature*. Mar 14 2013;495(7440):241-245.
  37. Dubeau L, Drapkin R. Coming into focus: the nonovarian origins of ovarian cancer. *Ann Oncol*. Nov 2013;24 Suppl 8:viii28-viii35.
  38. Kurman RJ, Shih Ie M. Molecular pathogenesis and extraovarian origin of epithelial ovarian cancer--shifting the paradigm. *Hum Pathol*. Jul 2011;42(7):918-931.
  39. Kurman RJ, Shih Ie M. The origin and pathogenesis of epithelial ovarian cancer: a proposed unifying theory. *Am J Surg Pathol*. Mar 2010;34(3):433-443.
  40. Lim D, Oliva E. Precursors and pathogenesis of ovarian carcinoma. *Pathology*. Apr 2013;45(3):229-242.
  41. Kim J, Coffey DM, Creighton CJ, Yu Z, Hawkins SM, Matzuk MM. High-grade serous ovarian cancer arises from fallopian tube in a mouse model. *Proc Natl Acad Sci U S A*. Mar 6 2012;109(10):3921-3926.
  42. Hillier SG. Nonovarian origins of ovarian cancer. *Proc Natl Acad Sci U S A*. Mar 6 2012;109(10):3608-3609.
  43. Integrated genomic analyses of ovarian carcinoma. *Nature*. Jun 30 2011;474(7353):609-615.
  44. Feng W, Marquez RT, Lu Z, et al. Imprinted tumor suppressor genes ARHI and PEG3 are the most frequently down-regulated in human ovarian cancers by loss of heterozygosity and promoter methylation. *Cancer*. Apr 1 2008;112(7):1489-1502.
  45. Bowtell DD. The genesis and evolution of high-grade serous ovarian cancer. *Nat Rev Cancer*. Nov 2010;10(11):803-808.
  46. Ledermann JA, Raja FA, Fotopoulou C, et al. Newly diagnosed and relapsed epithelial ovarian carcinoma: ESMO Clinical Practice Guidelines for diagnosis, treatment and follow-up. *Ann Oncol*. Oct 2013;24 Suppl 6:vi24-32.
  47. King MC, Marks JH, Mandell JB, New York Breast Cancer Study G. Breast and ovarian cancer risks due to inherited mutations in BRCA1 and BRCA2. *Science*. Oct 24 2003;302(5645):643-646.
  48. Brayfield A. *Martindale: The Complete Drug Reference*. London: Pharmaceutical Press 2015.
  49. Bristow RE, Tomacruz RS, Armstrong DK, Trimble EL, Montz FJ. Survival effect of maximal cytoreductive surgery for advanced ovarian carcinoma during the platinum era: a meta-analysis. *Journal of clinical*

- oncology : official journal of the American Society of Clinical Oncology*. Mar 1 2002;20(5):1248-1259.
50. Naik R, Barton DP. Neoadjuvant chemotherapy or primary surgery in advanced ovarian cancer. *The New England journal of medicine*. Dec 9 2010;363(24):2370-2371; author reply 2372.
  51. Winter-Roach BA, Kitchener HC, Lawrie TA. Adjuvant (post-surgery) chemotherapy for early stage epithelial ovarian cancer. *Cochrane Database Syst Rev*. 2012;3:CD004706.
  52. Trimbos JB, Vergote I, Bolis G, et al. Impact of adjuvant chemotherapy and surgical staging in early-stage ovarian carcinoma: European Organisation for Research and Treatment of Cancer-Adjuvant ChemoTherapy in Ovarian Neoplasm trial. *J Natl Cancer Inst*. Jan 15 2003;95(2):113-125.
  53. Ozols RF, Bundy BN, Greer BE, et al. Phase III trial of carboplatin and paclitaxel compared with cisplatin and paclitaxel in patients with optimally resected stage III ovarian cancer: a Gynecologic Oncology Group study. *Journal of clinical oncology : official journal of the American Society of Clinical Oncology*. Sep 1 2003;21(17):3194-3200.
  54. Vasey PA, Jayson GC, Gordon A, et al. Phase III randomized trial of docetaxel-carboplatin versus paclitaxel-carboplatin as first-line chemotherapy for ovarian carcinoma. *J Natl Cancer Inst*. Nov 17 2004;96(22):1682-1691.
  55. Armstrong DK, Bundy B, Wenzel L, et al. Intraperitoneal cisplatin and paclitaxel in ovarian cancer. *The New England journal of medicine*. Jan 5 2006;354(1):34-43.
  56. Alberts DS, Liu PY, Hannigan EV, et al. Intraperitoneal cisplatin plus intravenous cyclophosphamide versus intravenous cisplatin plus intravenous cyclophosphamide for stage III ovarian cancer. *The New England journal of medicine*. Dec 26 1996;335(26):1950-1955.
  57. Markman M, Bundy BN, Alberts DS, et al. Phase III trial of standard-dose intravenous cisplatin plus paclitaxel versus moderately high-dose carboplatin followed by intravenous paclitaxel and intraperitoneal cisplatin in small-volume stage III ovarian carcinoma: an intergroup study of the Gynecologic Oncology Group, Southwestern Oncology Group, and Eastern Cooperative Oncology Group. *Journal of clinical oncology : official journal of the American Society of Clinical Oncology*. Feb 15 2001;19(4):1001-1007.
  58. Katsumata N, Yasuda M, Takahashi F, et al. Dose-dense paclitaxel once a week in combination with carboplatin every 3 weeks for advanced ovarian cancer: a phase 3, open-label, randomised controlled trial. *Lancet*. Oct 17 2009;374(9698):1331-1338.
  59. Katsumata N, Yasuda M, Isonishi S, et al. Long-term results of dose-dense paclitaxel and carboplatin versus conventional paclitaxel and carboplatin for treatment of advanced epithelial ovarian, fallopian tube, or primary peritoneal cancer (JGOG 3016): a randomised, controlled, open-label trial. *Lancet Oncol*. Sep 2013;14(10):1020-1026.

60. Burger RA, Brady MF, Bookman MA, et al. Incorporation of bevacizumab in the primary treatment of ovarian cancer. *The New England journal of medicine*. Dec 29 2011;365(26):2473-2483.
61. Perren TJ, Swart AM, Pfisterer J, et al. A phase 3 trial of bevacizumab in ovarian cancer. *The New England journal of medicine*. Dec 29 2011;365(26):2484-2496.
62. Markman M. Antineoplastic agents in the management of ovarian cancer: current status and emerging therapeutic strategies. *Trends Pharmacol Sci*. Oct 2008;29(10):515-519.
63. Thigpen JT, Blessing JA, Ball H, Hummel SJ, Barrett RJ. Phase II trial of paclitaxel in patients with progressive ovarian carcinoma after platinum-based chemotherapy: a Gynecologic Oncology Group study. *Journal of clinical oncology : official journal of the American Society of Clinical Oncology*. Sep 1994;12(9):1748-1753.
64. Modesitt SC, Jazaeri AA. Recurrent epithelial ovarian cancer: pharmacotherapy and novel therapeutics. *Expert Opin Pharmacother*. Oct 2007;8(14):2293-2305.
65. Friedlander M, Trimble E, Tinker A, et al. Clinical trials in recurrent ovarian cancer. *Int J Gynecol Cancer*. May 2011;21(4):771-775.
66. Colombo PE, Fabbro M, Theillet C, Bibeau F, Rouanet P, Ray-Coquard I. Sensitivity and resistance to treatment in the primary management of epithelial ovarian cancer. *Crit Rev Oncol Hematol*. Feb 2014;89(2):207-216.
67. Vasey PA. Resistance to chemotherapy in advanced ovarian cancer: mechanisms and current strategies. *Br J Cancer*. Dec 2003;89 Suppl 3:S23-28.
68. Agarwal R, Kaye SB. Ovarian cancer: strategies for overcoming resistance to chemotherapy. *Nat Rev Cancer*. Jul 2003;3(7):502-516.
69. Yap TA, Carden CP, Kaye SB. Beyond chemotherapy: targeted therapies in ovarian cancer. *Nat Rev Cancer*. Mar 2009;9(3):167-181.
70. Lee JM, Ledermann JA, Kohn EC. PARP Inhibitors for BRCA1/2 mutation-associated and BRCA-like malignancies. *Ann Oncol*. Jan 2014;25(1):32-40.
71. Fong PC, Boss DS, Yap TA, et al. Inhibition of poly(ADP-ribose) polymerase in tumors from BRCA mutation carriers. *The New England journal of medicine*. Jul 9 2009;361(2):123-134.
72. Lord CJ, Tutt AN, Ashworth A. Synthetic lethality and cancer therapy: lessons learned from the development of PARP inhibitors. *Annu Rev Med*. 2015;66:455-470.
73. McLornan DP, List A, Mufti GJ. Applying synthetic lethality for the selective targeting of cancer. *The New England journal of medicine*. Oct 30 2014;371(18):1725-1735.
74. Oza AM, Cibula D, Benzaquen AO, et al. Olaparib combined with chemotherapy for recurrent platinum-sensitive ovarian cancer: a randomised phase 2 trial. *Lancet Oncol*. Jan 2015;16(1):87-97.

75. Lynparza (Olaparib) monograph: Drugs@FDA. 2015; <http://www.accessdata.fda.gov/scripts/cder/drugsatfda/index.cfm?fuseaction=SearchDrugDetails>. Accessed 25 May 2015.
76. Kalachand R, Hennessy BT, Markman M. Molecular targeted therapy in ovarian cancer: what is on the horizon? *Drugs*. May 28 2011;71(8):947-967.
77. Lengyel E, Burdette JE, Kenny HA, et al. Epithelial ovarian cancer experimental models. *Oncogene*. Jul 10 2014;33(28):3619-3633.
78. Domcke S, Sinha R, Levine DA, Sander C, Schultz N. Evaluating cell lines as tumour models by comparison of genomic profiles. *Nat Commun*. 2013;4:2126.
79. McDermott M, Eustace AJ, Busschots S, et al. In vitro Development of Chemotherapy and Targeted Therapy Drug-Resistant Cancer Cell Lines: A Practical Guide with Case Studies. *Front Oncol*. 2014;4:40.
80. Peyrone M. On the influence of ammonia on platinum chloride. *Ann Chem Pharm*. 1844;51:1.
81. Kauffman G. Michele Peyrone (1813–1883), Discoverer of Cisplatin. *Platinum Metals Rev*. 2010;54(4):250-256.
82. Rosenberg B, Vancamp L, Krigas T. Inhibition of Cell Division in Escherichia Coli by Electrolysis Products from a Platinum Electrode. *Nature*. Feb 13 1965;205:698-699.
83. Kelland L. The resurgence of platinum-based cancer chemotherapy. *Nat Rev Cancer*. Aug 2007;7(8):573-584.
84. Rosenberg B, VanCamp L, Trosko JE, Mansour VH. Platinum compounds: a new class of potent antitumour agents. *Nature*. Apr 26 1969;222(5191):385-386.
85. Curt GA, Grygiel JJ, Corden BJ, et al. A phase I and pharmacokinetic study of diamminecyclobutane-dicarboxylatoplatinum (NSC 241240). *Cancer research*. Sep 1983;43(9):4470-4473.
86. Cisplatin Monograph: Drugs@FDA 2015. <http://www.accessdata.fda.gov/scripts/cder/drugsatfda/index.cfm?fuseaction=SearchDrugDetails>. Accessed 26 May 2015.
87. Rozencweig M, Nicaise C, Beer M, et al. Phase I study of carboplatin given on a five-day intravenous schedule. *Journal of clinical oncology : official journal of the American Society of Clinical Oncology*. Oct 1983;1(10):621-626.
88. Lee FH, Canetta R, Issell BF, Lenaz L. New platinum complexes in clinical trials. *Cancer Treat Rev*. Mar 1983;10(1):39-51.
89. Wiltshaw E, Evans BD, Jones AC, Baker JW, Calvert AH. JMS, successor to cisplatin in advanced ovarian carcinoma? *Lancet*. Mar 12 1983;1(8324):587.
90. Neijt JP, Nortier JW, Vendrik CP, Struyvenberg A. JM8 (cisplatin analogue) alone for previously untreated advanced ovarian carcinoma. *Lancet*. May 14 1983;1(8333):1109-1110.
91. Harrap KR. Preclinical studies identifying carboplatin as a viable cisplatin alternative. *Cancer Treat Rev*. Sep 1985;12 Suppl A:21-33.

92. Kelland L. Broadening the clinical use of platinum drug-based chemotherapy with new analogues. Satraplatin and picoplatin. *Expert opinion on investigational drugs*. Jul 2007;16(7):1009-1021.
93. Raymond E, Chaney SG, Taamma A, Cvitkovic E. Oxaliplatin: a review of preclinical and clinical studies. *Ann Oncol*. Oct 1998;9(10):1053-1071.
94. Yu Y, Lou LG, Liu WP, et al. Synthesis and anticancer activity of lipophilic platinum(II) complexes of 3,5-diisopropylsalicylate. *European journal of medicinal chemistry*. Jul 2008;43(7):1438-1443.
95. Sternberg CN, de Mulder P, Fossa S, et al. Lobaplatin in advanced urothelial tract tumors. The Genitourinary Group of the European Organization for Research and Treatment of Cancer (EORTC). *Ann Oncol*. Jul 1997;8(7):695-696.
96. Choy H, Park C, Yao M. Current status and future prospects for satraplatin, an oral platinum analogue. *Clin Cancer Res*. Mar 15 2008;14(6):1633-1638.
97. Chaney SG, Campbell SL, Bassett E, Wu Y. Recognition and processing of cisplatin- and oxaliplatin-DNA adducts. *Crit Rev Oncol Hematol*. Jan 2005;53(1):3-11.
98. Wang D, Lippard SJ. Cellular processing of platinum anticancer drugs. *Nature reviews. Drug discovery*. Apr 2005;4(4):307-320.
99. Sancho-Martinez SM, Prieto-Garcia L, Prieto M, Lopez-Novoa JM, Lopez-Hernandez FJ. Subcellular targets of cisplatin cytotoxicity: an integrated view. *Pharmacology & therapeutics*. Oct 2012;136(1):35-55.
100. Burger H, Loos WJ, Eechoute K, Verweij J, Mathijssen RH, Wiemer EA. Drug transporters of platinum-based anticancer agents and their clinical significance. *Drug resistance updates : reviews and commentaries in antimicrobial and anticancer chemotherapy*. Feb 2011;14(1):22-34.
101. Hall MD, Okabe M, Shen DW, Liang XJ, Gottesman MM. The role of cellular accumulation in determining sensitivity to platinum-based chemotherapy. *Annual review of pharmacology and toxicology*. 2008;48:495-535.
102. Knox RJ, Friedlos F, Lydall DA, Roberts JJ. Mechanism of cytotoxicity of anticancer platinum drugs: evidence that cis-diamminedichloroplatinum(II) and cis-diammine-(1,1-cyclobutanedicarboxylato)platinum(II) differ only in the kinetics of their interaction with DNA. *Cancer research*. Apr 1986;46(4 Pt 2):1972-1979.
103. Sundquist WI, Lippard SJ, Stollar BD. Monoclonal antibodies to DNA modified with cis- or trans-diamminedichloroplatinum(II). *Proc Natl Acad Sci U S A*. Dec 1987;84(23):8225-8229.
104. Micetich KC, Barnes D, Erickson LC. A comparative study of the cytotoxicity and DNA-damaging effects of cis-(diammino)(1,1-cyclobutanedicarboxylato)-platinum(II) and cis-diamminedichloroplatinum(II) on L1210 cells. *Cancer research*. Sep 1985;45(9):4043-4047.
105. Su WC, Chang SL, Chen TY, Chen JS, Tsao CJ. Comparison of in vitro growth-inhibitory activity of carboplatin and cisplatin on leukemic cells

- and hematopoietic progenitors: the myelosuppressive activity of carboplatin may be greater than its antileukemic effect. *Japanese journal of clinical oncology*. Dec 2000;30(12):562-567.
106. Fichtinger-Schepman AM, van der Veer JL, den Hartog JH, Lohman PH, Reedijk J. Adducts of the antitumor drug cis-diamminedichloroplatinum(II) with DNA: formation, identification, and quantitation. *Biochemistry*. Jan 29 1985;24(3):707-713.
  107. Takahara PM, Rosenzweig AC, Frederick CA, Lippard SJ. Crystal structure of double-stranded DNA containing the major adduct of the anticancer drug cisplatin. *Nature*. Oct 19 1995;377(6550):649-652.
  108. Huang H, Zhu L, Reid BR, Drobny GP, Hopkins PB. Solution structure of a cisplatin-induced DNA interstrand cross-link. *Science*. Dec 15 1995;270(5243):1842-1845.
  109. Teuben JM, Bauer C, Wang AH, Reedijk J. Solution structure of a DNA duplex containing a cis-diammineplatinum(II) 1,3-d(GTG) intrastrand cross-link, a major adduct in cells treated with the anticancer drug carboplatin. *Biochemistry*. Sep 21 1999;38(38):12305-12312.
  110. Siddik ZH. Cisplatin: mode of cytotoxic action and molecular basis of resistance. *Oncogene*. Oct 20 2003;22(47):7265-7279.
  111. Kartalou M, Essigmann JM. Recognition of cisplatin adducts by cellular proteins. *Mutation research*. Jul 1 2001;478(1-2):1-21.
  112. Koberle B, Masters JR, Hartley JA, Wood RD. Defective repair of cisplatin-induced DNA damage caused by reduced XPA protein in testicular germ cell tumours. *Current biology : CB*. Mar 11 1999;9(5):273-276.
  113. Lage H, Dietel M. Involvement of the DNA mismatch repair system in antineoplastic drug resistance. *Journal of cancer research and clinical oncology*. 1999;125(3-4):156-165.
  114. Stratheer G, MacKean MJ, Illand M, Brown R. A role for methylation of the hMLH1 promoter in loss of hMLH1 expression and drug resistance in ovarian cancer. *Oncogene*. Apr 8 1999;18(14):2335-2341.
  115. Drummond JT, Anthoney A, Brown R, Modrich P. Cisplatin and adriamycin resistance are associated with MutLalpha and mismatch repair deficiency in an ovarian tumor cell line. *The Journal of biological chemistry*. Aug 16 1996;271(33):19645-19648.
  116. LaCasse EC, Mahoney DJ, Cheung HH, Plenchette S, Baird S, Korneluk RG. IAP-targeted therapies for cancer. *Oncogene*. Oct 20 2008;27(48):6252-6275.
  117. Delbridge AR, Strasser A. The BCL-2 protein family, BH3-mimetics and cancer therapy. *Cell death and differentiation*. Jul 2015;22(7):1071-1080.
  118. Yu F, Megyesi J, Price PM. Cytoplasmic initiation of cisplatin cytotoxicity. *American journal of physiology. Renal physiology*. Jul 2008;295(1):F44-52.
  119. Sheikh-Hamad D. Cisplatin-induced cytotoxicity: is the nucleus relevant? *American journal of physiology. Renal physiology*. Jul 2008;295(1):F42-43.

120. Galluzzi L, Senovilla L, Vitale I, et al. Molecular mechanisms of cisplatin resistance. *Oncogene*. Apr 12 2012;31(15):1869-1883.
121. van Rensburg CE, Joone GK, O'Sullivan JF. Clofazimine and B4121 sensitize an intrinsically resistant human colon cancer cell line to P-glycoprotein substrates. *Oncol Rep*. Jan-Feb 2000;7(1):193-195.
122. Martin LP, Hamilton TC, Schilder RJ. Platinum resistance: the role of DNA repair pathways. *Clin Cancer Res*. Mar 1 2008;14(5):1291-1295.
123. Stewart DJ. Mechanisms of resistance to cisplatin and carboplatin. *Crit Rev Oncol Hematol*. Jul 2007;63(1):12-31.
124. Rixe O, Ortuzar W, Alvarez M, et al. Oxaliplatin, tetraplatin, cisplatin, and carboplatin: spectrum of activity in drug-resistant cell lines and in the cell lines of the National Cancer Institute's Anticancer Drug Screen panel. *Biochem Pharmacol*. Dec 24 1996;52(12):1855-1865.
125. Eckstein N. Platinum resistance in breast and ovarian cancer cell lines. *J Exp Clin Cancer Res*. 2011;30:91.
126. Shen DW, Pouliot LM, Hall MD, Gottesman MM. Cisplatin resistance: a cellular self-defense mechanism resulting from multiple epigenetic and genetic changes. *Pharmacol Rev*. Jul 2012;64(3):706-721.
127. Ali AY, Farrand L, Kim JY, et al. Molecular determinants of ovarian cancer chemoresistance: new insights into an old conundrum. *Ann N Y Acad Sci*. Oct 2012;1271:58-67.
128. Rabik CA, Dolan ME. Molecular mechanisms of resistance and toxicity associated with platinating agents. *Cancer Treat Rev*. Feb 2007;33(1):9-23.
129. Chien J, Kuang R, Landen C, Shridhar V. Platinum-sensitive recurrence in ovarian cancer: the role of tumor microenvironment. *Front Oncol*. 2013;3:251.
130. Fu S, Naing A, Fu C, Kuo MT, Kurzrock R. Overcoming platinum resistance through the use of a copper-lowering agent. *Mol Cancer Ther*. Jun 2012;11(6):1221-1225.
131. Nakayama K, Kanzaki A, Ogawa K, Miyazaki K, Neamati N, Takebayashi Y. Copper-transporting P-type adenosine triphosphatase (ATP7B) as a cisplatin based chemoresistance marker in ovarian carcinoma: comparative analysis with expression of MDR1, MRP1, MRP2, LRP and BCRP. *International journal of cancer. Journal international du cancer*. Oct 10 2002;101(5):488-495.
132. Samimi G, Safaei R, Katano K, et al. Increased expression of the copper efflux transporter ATP7A mediates resistance to cisplatin, carboplatin, and oxaliplatin in ovarian cancer cells. *Clin Cancer Res*. Jul 15 2004;10(14):4661-4669.
133. Verschoor ML, Singh G. Ets-1 regulates intracellular glutathione levels: key target for resistant ovarian cancer. *Mol Cancer*. 2013;12(1):138.
134. Okuno S, Sato H, Kuriyama-Matsumura K, et al. Role of cystine transport in intracellular glutathione level and cisplatin resistance in human ovarian cancer cell lines. *Br J Cancer*. Mar 24 2003;88(6):951-956.

135. Ferry KV, Hamilton TC, Johnson SW. Increased nucleotide excision repair in cisplatin-resistant ovarian cancer cells: role of ERCC1-XPF. *Biochem Pharmacol.* Nov 1 2000;60(9):1305-1313.
136. Gifford G, Paul J, Vasey PA, Kaye SB, Brown R. The acquisition of hMLH1 methylation in plasma DNA after chemotherapy predicts poor survival for ovarian cancer patients. *Clin Cancer Res.* Jul 1 2004;10(13):4420-4426.
137. Stefanou DT, Bamias A, Episkopou H, et al. Aberrant DNA damage response pathways may predict the outcome of platinum chemotherapy in ovarian cancer. *PLoS One.* 2015;10(2):e0117654.
138. Liu JR, Opipari AW, Tan L, et al. Dysfunctional apoptosome activation in ovarian cancer: implications for chemoresistance. *Cancer research.* Feb 1 2002;62(3):924-931.
139. Woo MG, Xue K, Liu J, McBride H, Tsang BK. Calpain-mediated processing of p53-associated parkin-like cytoplasmic protein (PARC) affects chemosensitivity of human ovarian cancer cells by promoting p53 subcellular trafficking. *The Journal of biological chemistry.* Feb 3 2012;287(6):3963-3975.
140. Castino R, Peracchio C, Salini A, et al. Chemotherapy drug response in ovarian cancer cells strictly depends on a cathepsin D-Bax activation loop. *J Cell Mol Med.* Jun 2009;13(6):1096-1109.
141. Smith G, Ng MT, Shepherd L, et al. Individuality in FGF1 expression significantly influences platinum resistance and progression-free survival in ovarian cancer. *Br J Cancer.* Oct 9 2012;107(8):1327-1336.
142. Ryner L, Guan Y, Firestein R, et al. Upregulation of Periostin and Reactive Stroma Is Associated with Primary Chemoresistance and Predicts Clinical Outcomes in Epithelial Ovarian Cancer. *Clin Cancer Res.* Apr 2 2015.
143. Engels K, Knauer SK, Loibl S, et al. NO signaling confers cytoprotectivity through the survivin network in ovarian carcinomas. *Cancer research.* Jul 1 2008;68(13):5159-5166.
144. Ratner ES, Keane FK, Lindner R, et al. A KRAS variant is a biomarker of poor outcome, platinum chemotherapy resistance and a potential target for therapy in ovarian cancer. *Oncogene.* Oct 18 2012;31(42):4559-4566.
145. Zhang P, Zhang P, Zhou M, et al. Exon 4 deletion variant of epidermal growth factor receptor enhances invasiveness and cisplatin resistance in epithelial ovarian cancer. *Carcinogenesis.* Nov 2013;34(11):2639-2646.
146. Sorrentino A, Liu CG, Addario A, Peschle C, Scambia G, Ferlini C. Role of microRNAs in drug-resistant ovarian cancer cells. *Gynecol Oncol.* Dec 2008;111(3):478-486.
147. Vecchione A, Belletti B, Lovat F, et al. A microRNA signature defines chemoresistance in ovarian cancer through modulation of angiogenesis. *Proc Natl Acad Sci U S A.* Jun 11 2013;110(24):9845-9850.
148. Zhu X, Shen H, Yin X, et al. miR-186 regulation of Twist1 and ovarian cancer sensitivity to cisplatin. *Oncogene.* Apr 13 2015.



149. Vang S, Wu HT, Fischer A, et al. Identification of ovarian cancer metastatic miRNAs. *PLoS One*. 2013;8(3):e58226.
150. Xiang Y, Ma N, Wang D, et al. MiR-152 and miR-185 co-contribute to ovarian cancer cells cisplatin sensitivity by targeting DNMT1 directly: a novel epigenetic therapy independent of decitabine. *Oncogene*. Jan 16 2014;33(3):378-386.
151. van Jaarsveld MT, Helleman J, Boersma AW, et al. miR-141 regulates KEAP1 and modulates cisplatin sensitivity in ovarian cancer cells. *Oncogene*. Sep 5 2013;32(36):4284-4293.
152. Bagnoli M, De Cecco L, Granata A, et al. Identification of a chrXq27.3 microRNA cluster associated with early relapse in advanced stage ovarian cancer patients. *Oncotarget*. Dec 2011;2(12):1265-1278.
153. Yang N, Kaur S, Volinia S, et al. MicroRNA microarray identifies Let-7i as a novel biomarker and therapeutic target in human epithelial ovarian cancer. *Cancer research*. Dec 15 2008;68(24):10307-10314.
154. Yang H, Kong W, He L, et al. MicroRNA expression profiling in human ovarian cancer: miR-214 induces cell survival and cisplatin resistance by targeting PTEN. *Cancer research*. Jan 15 2008;68(2):425-433.
155. Konstantinopoulos PA, Spentzos D, Fountzilas E, et al. Keap1 mutations and Nrf2 pathway activation in epithelial ovarian cancer. *Cancer research*. Aug 1 2011;71(15):5081-5089.
156. Palmieri C, Gojis O, Rudraraju B, et al. Expression of steroid receptor coactivator 3 in ovarian epithelial cancer is a poor prognostic factor and a marker for platinum resistance. *Br J Cancer*. May 28 2013;108(10):2039-2044.
157. Chiu WT, Huang YF, Tsai HY, et al. FOXM1 confers to epithelial-mesenchymal transition, stemness and chemoresistance in epithelial ovarian carcinoma cells. *Oncotarget*. Feb 10 2015;6(4):2349-2365.
158. Zhang X, George J, Deb S, et al. The Hippo pathway transcriptional co-activator, YAP, is an ovarian cancer oncogene. *Oncogene*. Jun 23 2011;30(25):2810-2822.
159. Cao L, Petrusca DN, Satpathy M, Nakshatri H, Petrache I, Matei D. Tissue transglutaminase protects epithelial ovarian cancer cells from cisplatin-induced apoptosis by promoting cell survival signaling. *Carcinogenesis*. Oct 2008;29(10):1893-1900.
160. Su HY, Lai HC, Lin YW, et al. Epigenetic silencing of SFRP5 is related to malignant phenotype and chemoresistance of ovarian cancer through Wnt signaling pathway. *International journal of cancer. Journal international du cancer*. Aug 1 2010;127(3):555-567.
161. Rosano L, Cianfrocca R, Tocci P, et al. Endothelin A receptor/beta-arrestin signaling to the Wnt pathway renders ovarian cancer cells resistant to chemotherapy. *Cancer research*. Dec 15 2014;74(24):7453-7464.
162. Miow QH, Tan TZ, Ye J, et al. Epithelial-mesenchymal status renders differential responses to cisplatin in ovarian cancer. *Oncogene*. Apr 9 2015;34(15):1899-1907.

163. Arts HJ, Hollema H, Lemstra W, et al. Heat-shock-protein-27 (hsp27) expression in ovarian carcinoma: relation in response to chemotherapy and prognosis. *International journal of cancer. Journal international du cancer*. Jun 21 1999;84(3):234-238.
164. Ziebarth AJ, Nowsheen S, Steg AD, et al. Endoglin (CD105) contributes to platinum resistance and is a target for tumor-specific therapy in epithelial ovarian cancer. *Clin Cancer Res*. Jan 1 2013;19(1):170-182.
165. Bradley A, Zheng H, Ziebarth A, et al. EDD enhances cell survival and cisplatin resistance and is a therapeutic target for epithelial ovarian cancer. *Carcinogenesis*. May 2014;35(5):1100-1109.
166. Bhattacharyya S, Saha S, Giri K, et al. Cystathionine beta-synthase (CBS) contributes to advanced ovarian cancer progression and drug resistance. *PLoS One*. 2013;8(11):e79167.
167. Lei Y, Henderson BR, Emmanuel C, Harnett PR, deFazio A. Inhibition of ANKRD1 sensitizes human ovarian cancer cells to endoplasmic reticulum stress-induced apoptosis. *Oncogene*. Jan 22 2015;34(4):485-495.
168. Blyth K, Cameron ER, Neil JC. The RUNX genes: gain or loss of function in cancer. *Nat Rev Cancer*. May 2005;5(5):376-387.
169. Ito Y, Bae SC, Chuang LS. The RUNX family: developmental regulators in cancer. *Nat Rev Cancer*. Feb 2015;15(2):81-95.
170. Lund AH, van Lohuizen M. RUNX: a trilogy of cancer genes. *Cancer Cell*. Apr 2002;1(3):213-215.
171. Coffman JA. Runx transcription factors and the developmental balance between cell proliferation and differentiation. *Cell biology international*. 2003;27(4):315-324.
172. Ogawa E, Inuzuka M, Maruyama M, et al. Molecular cloning and characterization of PEBP2 beta, the heterodimeric partner of a novel Drosophila runt-related DNA binding protein PEBP2 alpha. *Virology*. May 1993;194(1):314-331.
173. Huang G, Shigesada K, Ito K, Wee HJ, Yokomizo T, Ito Y. Dimerization with PEBP2beta protects RUNX1/AML1 from ubiquitin-proteasome-mediated degradation. *EMBO J*. Feb 15 2001;20(4):723-733.
174. Huang X, Peng JW, Speck NA, Bushweller JH. Solution structure of core binding factor beta and map of the CBF alpha binding site. *Nat Struct Biol*. Jul 1999;6(7):624-627.
175. Tahirov TH, Inoue-Bungo T, Morii H, et al. Structural analyses of DNA recognition by the AML1/Runx-1 Runt domain and its allosteric control by CBFbeta. *Cell*. Mar 9 2001;104(5):755-767.
176. Chuang LS, Ito K, Ito Y. RUNX family: Regulation and diversification of roles through interacting proteins. *International journal of cancer. Journal international du cancer*. Mar 15 2013;132(6):1260-1271.
177. Durst KL, Hiebert SW. Role of RUNX family members in transcriptional repression and gene silencing. *Oncogene*. May 24 2004;23(24):4220-4224.
178. Bae SC, Lee YH. Phosphorylation, acetylation and ubiquitination: the molecular basis of RUNX regulation. *Gene*. Jan 17 2006;366(1):58-66.

179. Ito Y, Miyazono K. RUNX transcription factors as key targets of TGF-beta superfamily signaling. *Curr Opin Genet Dev*. Feb 2003;13(1):43-47.
180. Ito K, Lim AC, Salto-Tellez M, et al. RUNX3 attenuates beta-catenin/T cell factors in intestinal tumorigenesis. *Cancer Cell*. Sep 9 2008;14(3):226-237.
181. Pratap J, Wixted JJ, Gaur T, et al. Runx2 transcriptional activation of Indian Hedgehog and a downstream bone metastatic pathway in breast cancer cells. *Cancer research*. Oct 1 2008;68(19):7795-7802.
182. Hilton MJ, Tu X, Wu X, et al. Notch signaling maintains bone marrow mesenchymal progenitors by suppressing osteoblast differentiation. *Nat Med*. Mar 2008;14(3):306-314.
183. Della Gatta G, Palomero T, Perez-Garcia A, et al. Reverse engineering of TLX oncogenic transcriptional networks identifies RUNX1 as tumor suppressor in T-ALL. *Nat Med*. Mar 2012;18(3):436-440.
184. Osato M. Point mutations in the RUNX1/AML1 gene: another actor in RUNX leukemia. *Oncogene*. May 24 2004;23(24):4284-4296.
185. Pratap J, Lian JB, Javed A, et al. Regulatory roles of Runx2 in metastatic tumor and cancer cell interactions with bone. *Cancer Metastasis Rev*. Dec 2006;25(4):589-600.
186. Li QL, Ito K, Sakakura C, et al. Causal relationship between the loss of RUNX3 expression and gastric cancer. *Cell*. Apr 5 2002;109(1):113-124.
187. Ito K, Liu Q, Salto-Tellez M, et al. RUNX3, a novel tumor suppressor, is frequently inactivated in gastric cancer by protein mislocalization. *Cancer research*. Sep 1 2005;65(17):7743-7750.
188. Kim WJ, Kim EJ, Jeong P, et al. RUNX3 inactivation by point mutations and aberrant DNA methylation in bladder tumors. *Cancer research*. Oct 15 2005;65(20):9347-9354.
189. Yu F, Gao W, Yokochi T, et al. RUNX3 interacts with MYCN and facilitates protein degradation in neuroblastoma. *Oncogene*. May 15 2014;33(20):2601-2609.
190. Lee CW, Chuang LS, Kimura S, et al. RUNX3 functions as an oncogene in ovarian cancer. *Gynecol Oncol*. Aug 2011;122(2):410-417.
191. Lee KS, Lee YS, Lee JM, et al. Runx3 is required for the differentiation of lung epithelial cells and suppression of lung cancer. *Oncogene*. Jun 10 2010;29(23):3349-3361.
192. Ito Y. Oncogenic potential of the RUNX gene family: 'overview'. *Oncogene*. May 24 2004;23(24):4198-4208.
193. Bae SC, Choi JK. Tumor suppressor activity of RUNX3. *Oncogene*. May 24 2004;23(24):4336-4340.
194. Wang ZQ, Keita M, Bachvarova M, et al. Inhibition of RUNX2 transcriptional activity blocks the proliferation, migration and invasion of epithelial ovarian carcinoma cells. *PLoS One*. 2013;8(10):e74384.
195. Keita M, Bachvarova M, Morin C, et al. The RUNX1 transcription factor is expressed in serous epithelial ovarian carcinoma and contributes to cell proliferation, migration and invasion. *Cell Cycle*. Mar 15 2013;12(6):972-986.

196. Keita M, Wang ZQ, Pelletier JF, et al. Global methylation profiling in serous ovarian cancer is indicative for distinct aberrant DNA methylation signatures associated with tumor aggressiveness and disease progression. *Gynecol Oncol.* Feb 2013;128(2):356-363.
197. Li W, Xu S, Lin S, Zhao W. Overexpression of runt-related transcription factor-2 is associated with advanced tumor progression and poor prognosis in epithelial ovarian cancer. *J Biomed Biotechnol.* 2012;2012:456534.
198. Yoshizaki T, Enomoto T, Fujita M, et al. Frequent inactivation of RUNX3 in endometrial carcinoma. *Gynecol Oncol.* Sep 2008;110(3):439-444.
199. Davis JN, Rogers D, Adams L, et al. Association of core-binding factor beta with the malignant phenotype of prostate and ovarian cancer cells. *J Cell Physiol.* Nov 2010;225(3):875-887.
200. Nusslein-Volhard C, Wieschaus E. Mutations affecting segment number and polarity in *Drosophila*. *Nature.* Oct 30 1980;287(5785):795-801.
201. Nusse R, Varmus HE. Many tumors induced by the mouse mammary tumor virus contain a provirus integrated in the same region of the host genome. *Cell.* Nov 1982;31(1):99-109.
202. Rijsewijk F, Schuermann M, Wagenaar E, Parren P, Weigel D, Nusse R. The *Drosophila* homolog of the mouse mammary oncogene int-1 is identical to the segment polarity gene wingless. *Cell.* Aug 14 1987;50(4):649-657.
203. Clevers H, Nusse R. Wnt/beta-catenin signaling and disease. *Cell.* Jun 8 2012;149(6):1192-1205.
204. Logan CY, Nusse R. The Wnt signaling pathway in development and disease. *Annu Rev Cell Dev Biol.* 2004;20:781-810.
205. Clevers H. Wnt/beta-catenin signaling in development and disease. *Cell.* Nov 3 2006;127(3):469-480.
206. Anastas JN, Moon RT. WNT signalling pathways as therapeutic targets in cancer. *Nat Rev Cancer.* Jan 2013;13(1):11-26.
207. Stamos JL, Weis WI. The beta-catenin destruction complex. *Cold Spring Harb Perspect Biol.* Jan 2013;5(1):a007898.
208. MacDonald BT, He X. Frizzled and LRP5/6 receptors for Wnt/beta-catenin signaling. *Cold Spring Harb Perspect Biol.* Dec 2012;4(12).
209. Cadigan KM, Waterman ML. TCF/LEFs and Wnt signaling in the nucleus. *Cold Spring Harb Perspect Biol.* Nov 2012;4(11).
210. Willert K, Nusse R. Wnt proteins. *Cold Spring Harb Perspect Biol.* Sep 2012;4(9):a007864.
211. Cruciat CM, Niehrs C. Secreted and transmembrane wnt inhibitors and activators. *Cold Spring Harb Perspect Biol.* Mar 2013;5(3):a015081.
212. Nusse R. Wnt signaling. *Cold Spring Harb Perspect Biol.* May 2012;4(5).
213. Angers S, Moon RT. Proximal events in Wnt signal transduction. *Nat Rev Mol Cell Biol.* Jul 2009;10(7):468-477.
214. Rosenbluh J, Wang X, Hahn WC. Genomic insights into WNT/beta-catenin signaling. *Trends Pharmacol Sci.* Feb 2014;35(2):103-109.
215. Herr P, Hausmann G, Basler K. WNT secretion and signalling in human disease. *Trends Mol Med.* Aug 2012;18(8):483-493.

216. Valenta T, Hausmann G, Basler K. The many faces and functions of beta-catenin. *EMBO J*. Jun 13 2012;31(12):2714-2736.
217. Niehrs C. The complex world of WNT receptor signalling. *Nat Rev Mol Cell Biol*. Dec 2012;13(12):767-779.
218. Schulte G. International Union of Basic and Clinical Pharmacology. LXXX. The class Frizzled receptors. *Pharmacol Rev*. Dec 2010;62(4):632-667.
219. Port F, Basler K. Wnt trafficking: new insights into Wnt maturation, secretion and spreading. *Traffic*. Oct 2010;11(10):1265-1271.
220. Baarsma HA, Konigshoff M, Gosens R. The WNT signaling pathway from ligand secretion to gene transcription: molecular mechanisms and pharmacological targets. *Pharmacology & therapeutics*. Apr 2013;138(1):66-83.
221. Staal FJ, Clevers HC. WNT signalling and haematopoiesis: a WNT-WNT situation. *Nat Rev Immunol*. Jan 2005;5(1):21-30.
222. Reya T, Duncan AW, Ailles L, et al. A role for Wnt signalling in self-renewal of haematopoietic stem cells. *Nature*. May 22 2003;423(6938):409-414.
223. MacDonald BT, Tamai K, He X. Wnt/beta-catenin signaling: components, mechanisms, and diseases. *Developmental cell*. Jul 2009;17(1):9-26.
224. Clevers H, Loh KM, Nusse R. Stem cell signaling. An integral program for tissue renewal and regeneration: Wnt signaling and stem cell control. *Science*. Oct 3 2014;346(6205):1248012.
225. Kahn M. Can we safely target the WNT pathway? *Nature reviews. Drug discovery*. Jul 2014;13(7):513-532.
226. Moon RT, Kohn AD, De Ferrari GV, Kaykas A. WNT and beta-catenin signalling: diseases and therapies. *Nature reviews. Genetics*. Sep 2004;5(9):691-701.
227. Klaus A, Birchmeier W. Wnt signalling and its impact on development and cancer. *Nat Rev Cancer*. May 2008;8(5):387-398.
228. Ashton-Rickardt PG, Dunlop MG, Nakamura Y, et al. High frequency of APC loss in sporadic colorectal carcinoma due to breaks clustered in 5q21-22. *Oncogene*. Oct 1989;4(10):1169-1174.
229. Groden J, Thliveris A, Samowitz W, et al. Identification and characterization of the familial adenomatous polyposis coli gene. *Cell*. Aug 9 1991;66(3):589-600.
230. Nishisho I, Nakamura Y, Miyoshi Y, et al. Mutations of chromosome 5q21 genes in FAP and colorectal cancer patients. *Science*. Aug 9 1991;253(5020):665-669.
231. Segditsas S, Tomlinson I. Colorectal cancer and genetic alterations in the Wnt pathway. *Oncogene*. Dec 4 2006;25(57):7531-7537.
232. Korinek V, Barker N, Morin PJ, et al. Constitutive transcriptional activation by a beta-catenin-Tcf complex in APC<sup>-/-</sup> colon carcinoma. *Science*. Mar 21 1997;275(5307):1784-1787.

233. Morin PJ, Sparks AB, Korinek V, et al. Activation of beta-catenin-Tcf signaling in colon cancer by mutations in beta-catenin or APC. *Science*. Mar 21 1997;275(5307):1787-1790.
234. Rubinfeld B, Robbins P, El-Gamil M, Albert I, Porfiri E, Polakis P. Stabilization of beta-catenin by genetic defects in melanoma cell lines. *Science*. Mar 21 1997;275(5307):1790-1792.
235. Liu W, Dong X, Mai M, et al. Mutations in AXIN2 cause colorectal cancer with defective mismatch repair by activating beta-catenin/TCF signalling. *Nat Genet*. Oct 2000;26(2):146-147.
236. Satoh S, Daigo Y, Furukawa Y, et al. AXIN1 mutations in hepatocellular carcinomas, and growth suppression in cancer cells by virus-mediated transfer of AXIN1. *Nat Genet*. Mar 2000;24(3):245-250.
237. Suzuki H, Watkins DN, Jair KW, et al. Epigenetic inactivation of SFRP genes allows constitutive WNT signaling in colorectal cancer. *Nat Genet*. Apr 2004;36(4):417-422.
238. Ugolini F, Charafe-Jauffret E, Bardou VJ, et al. WNT pathway and mammary carcinogenesis: loss of expression of candidate tumor suppressor gene SFRP1 in most invasive carcinomas except of the medullary type. *Oncogene*. Sep 13 2001;20(41):5810-5817.
239. Uematsu K, He B, You L, Xu Z, McCormick F, Jablons DM. Activation of the Wnt pathway in non small cell lung cancer: evidence of dishevelled overexpression. *Oncogene*. Oct 16 2003;22(46):7218-7221.
240. Uematsu K, Kanazawa S, You L, et al. Wnt pathway activation in mesothelioma: evidence of Dishevelled overexpression and transcriptional activity of beta-catenin. *Cancer research*. Aug 1 2003;63(15):4547-4551.
241. Wissmann C, Wild PJ, Kaiser S, et al. WIF1, a component of the Wnt pathway, is down-regulated in prostate, breast, lung, and bladder cancer. *The Journal of pathology*. Oct 2003;201(2):204-212.
242. Bjorklund P, Akerstrom G, Westin G. An LRP5 receptor with internal deletion in hyperparathyroid tumors with implications for deregulated WNT/beta-catenin signaling. *PLoS medicine*. Nov 27 2007;4(11):e328.
243. Takeda H, Lyle S, Lazar AJ, Zouboulis CC, Smyth I, Watt FM. Human sebaceous tumors harbor inactivating mutations in LEF1. *Nat Med*. Apr 2006;12(4):395-397.
244. Majid S, Saini S, Dahiya R. Wnt signaling pathways in urological cancers: past decades and still growing. *Mol Cancer*. 2012;11:7.
245. Gong A, Huang S. FoxM1 and Wnt/beta-catenin signaling in glioma stem cells. *Cancer research*. Nov 15 2012;72(22):5658-5662.
246. Takebe N, Miele L, Harris PJ, et al. Targeting Notch, Hedgehog, and Wnt pathways in cancer stem cells: clinical update. *Nature reviews. Clinical oncology*. Apr 7 2015.
247. Zimmerman ZF, Moon RT, Chien AJ. Targeting Wnt pathways in disease. *Cold Spring Harb Perspect Biol*. Nov 2012;4(11).
248. Polakis P. Drugging Wnt signalling in cancer. *EMBO J*. Jun 13 2012;31(12):2737-2746.

249. Barker N, Clevers H. Mining the Wnt pathway for cancer therapeutics. *Nature reviews. Drug discovery*. Dec 2006;5(12):997-1014.
250. Dodge ME, Lum L. Drugging the cancer stem cell compartment: lessons learned from the hedgehog and Wnt signal transduction pathways. *Annual review of pharmacology and toxicology*. 2011;51:289-310.
251. Madan B, Virshup DM. Targeting Wnts at the Source-New Mechanisms, New Biomarkers, New Drugs. *Mol Cancer Ther*. May 2015;14(5):1087-1094.
252. McCubrey JA, Steelman LS, Bertrand FE, et al. GSK-3 as potential target for therapeutic intervention in cancer. *Oncotarget*. May 30 2014;5(10):2881-2911.
253. Takahashi-Yanaga F, Kahn M. Targeting Wnt signaling: can we safely eradicate cancer stem cells? *Clin Cancer Res*. Jun 15 2010;16(12):3153-3162.
254. Catalogue of Somatic Mutations in Cancer (COSMIC) database. [http://cancer.sanger.ac.uk/cosmic/browse/tissue#sn=ovary&ss=all&hn=carcinoma&sh=&in=t&src=tissue&all\\_data=n](http://cancer.sanger.ac.uk/cosmic/browse/tissue#sn=ovary&ss=all&hn=carcinoma&sh=&in=t&src=tissue&all_data=n).
255. Sagae S, Kobayashi K, Nishioka Y, et al. Mutational analysis of beta-catenin gene in Japanese ovarian carcinomas: frequent mutations in endometrioid carcinomas. *Japanese journal of cancer research : Gann*. May 1999;90(5):510-515.
256. Palacios J, Gamallo C. Mutations in the beta-catenin gene (CTNNB1) in endometrioid ovarian carcinomas. *Cancer research*. Apr 1 1998;58(7):1344-1347.
257. Gamallo C, Palacios J, Moreno G, Calvo de Mora J, Suarez A, Armas A. beta-catenin expression pattern in stage I and II ovarian carcinomas : relationship with beta-catenin gene mutations, clinicopathological features, and clinical outcome. *Am J Pathol*. Aug 1999;155(2):527-536.
258. Wright K, Wilson P, Morland S, et al. beta-catenin mutation and expression analysis in ovarian cancer: exon 3 mutations and nuclear translocation in 16% of endometrioid tumours. *International journal of cancer. Journal international du cancer*. Aug 27 1999;82(5):625-629.
259. Moreno-Bueno G, Gamallo C, Perez-Gallego L, de Mora JC, Suarez A, Palacios J. beta-Catenin expression pattern, beta-catenin gene mutations, and microsatellite instability in endometrioid ovarian carcinomas and synchronous endometrial carcinomas. *Diagnostic molecular pathology : the American journal of surgical pathology, part B*. Jun 2001;10(2):116-122.
260. Arend RC, Londono-Joshi AI, Straughn JM, Jr., Buchsbaum DJ. The Wnt/beta-catenin pathway in ovarian cancer: a review. *Gynecol Oncol*. Dec 2013;131(3):772-779.
261. Huang X, McGann JC, Liu BY, et al. Phosphorylation of Dishevelled by protein kinase RIPK4 regulates Wnt signaling. *Science*. Mar 22 2013;339(6126):1441-1445.

262. Yoshioka S, King ML, Ran S, et al. WNT7A regulates tumor growth and progression in ovarian cancer through the WNT/beta-catenin pathway. *Mol Cancer Res.* Mar 2012;10(3):469-482.
263. Ford CE, Punnia-Moorthy G, Henry CE, et al. The non-canonical Wnt ligand, Wnt5a, is upregulated and associated with epithelial to mesenchymal transition in epithelial ovarian cancer. *Gynecol Oncol.* Aug 2014;134(2):338-345.
264. Bitler BG, Nicodemus JP, Li H, et al. Wnt5a suppresses epithelial ovarian cancer by promoting cellular senescence. *Cancer research.* Oct 1 2011;71(19):6184-6194.
265. Qi H, Sun B, Zhao X, et al. Wnt5a promotes vasculogenic mimicry and epithelial-mesenchymal transition via protein kinase Calpha in epithelial ovarian cancer. *Oncol Rep.* Aug 2014;32(2):771-779.
266. Jannesari-Ladani F, Hossein G, Monhasery N, Shahoei SH, Izadi Mood N. Wnt5a influences viability, migration, adhesion, colony formation, E- and N-cadherin expression of human ovarian cancer cell line SKOV-3. *Folia Biol (Praha).* 2014;60(2):57-67.
267. Chen S, Wang J, Gou WF, et al. The involvement of RhoA and Wnt-5a in the tumorigenesis and progression of ovarian epithelial carcinoma. *Int J Mol Sci.* 2013;14(12):24187-24199.
268. Peng C, Zhang X, Yu H, Wu D, Zheng J. Wnt5a as a predictor in poor clinical outcome of patients and a mediator in chemoresistance of ovarian cancer. *Int J Gynecol Cancer.* Feb 2011;21(2):280-288.
269. Zhu J, Zhang S, Gu L, Di W. Epigenetic silencing of DKK2 and Wnt signal pathway components in human ovarian carcinoma. *Carcinogenesis.* Dec 2012;33(12):2334-2343.
270. Barbolina MV, Liu Y, Gurler H, et al. Matrix rigidity activates Wnt signaling through down-regulation of Dickkopf-1 protein. *The Journal of biological chemistry.* Jan 4 2013;288(1):141-151.
271. Wang S, Zhang S. Dickkopf-1 is frequently overexpressed in ovarian serous carcinoma and involved in tumor invasion. *Clin Exp Metastasis.* Aug 2011;28(6):581-591.
272. Ford CE, Jary E, Ma SS, Nixdorf S, Heinzelmann-Schwarz VA, Ward RL. The Wnt gatekeeper SFRP4 modulates EMT, cell migration and downstream Wnt signalling in serous ovarian cancer cells. *PLoS One.* 2013;8(1):e54362.
273. Saran U, Arfuso F, Zeps N, Dharmarajan A. Secreted frizzled-related protein 4 expression is positively associated with responsiveness to cisplatin of ovarian cancer cell lines in vitro and with lower tumour grade in mucinous ovarian cancers. *BMC Cell Biol.* 2012;13:25.
274. Zepeda N. *MSc thesis, The Role of RUNX3 in Chemoresistance in Epithelial Ovarian Cancer.* Department of Oncology, University of Alberta; 2014.
275. Behrens BC, Hamilton TC, Masuda H, et al. Characterization of a cis-diamminedichloroplatinum(II)-resistant human ovarian cancer cell line



- and its use in evaluation of platinum analogues. *Cancer research*. Jan 15 1987;47(2):414-418.
276. Yano T, Ito K, Fukamachi H, et al. The RUNX3 tumor suppressor upregulates Bim in gastric epithelial cells undergoing transforming growth factor beta-induced apoptosis. *Molecular and cellular biology*. Jun 2006;26(12):4474-4488.
  277. Repetto G, del Peso A, Zurita JL. Neutral red uptake assay for the estimation of cell viability/cytotoxicity. *Nat Protoc*. 2008;3(7):1125-1131.
  278. Franken NA, Rodermond HM, Stap J, Haveman J, van Bree C. Clonogenic assay of cells in vitro. *Nat Protoc*. 2006;1(5):2315-2319.
  279. Munshi A, Hobbs M, Meyn RE. Clonogenic cell survival assay. *Methods in molecular medicine*. 2005;110:21-28.
  280. Fu Y, Sies H, Lei XG. Opposite roles of selenium-dependent glutathione peroxidase-1 in superoxide generator diquat- and peroxynitrite-induced apoptosis and signaling. *The Journal of biological chemistry*. Nov 16 2001;276(46):43004-43009.
  281. Livak KJ, Schmittgen TD. Analysis of relative gene expression data using real-time quantitative PCR and the 2(-Delta Delta C(T)) Method. *Methods*. Dec 2001;25(4):402-408.
  282. Chou TC. Drug combination studies and their synergy quantification using the Chou-Talalay method. *Cancer research*. Jan 15 2010;70(2):440-446.
  283. Nevadunsky NS, Barbieri JS, Kwong J, et al. RUNX3 protein is overexpressed in human epithelial ovarian cancer. *Gynecol Oncol*. Feb 2009;112(2):325-330.
  284. Barghout SH, Zepeda N, Vincent K, et al. RUNX3 contributes to carboplatin resistance in epithelial ovarian cancer cells. *Gynecologic Oncology*. 15 July 2015;In press.
  285. Salto-Tellez M, Peh BK, Ito K, et al. RUNX3 protein is overexpressed in human basal cell carcinomas. *Oncogene*. Dec 7 2006;25(58):7646-7649.
  286. Fu Y, Chang AC, Fournier M, Chang L, Niessen K, Karsan A. RUNX3 maintains the mesenchymal phenotype after termination of the Notch signal. *The Journal of biological chemistry*. Apr 1 2011;286(13):11803-11813.
  287. du Bois A, Luck HJ, Meier W, et al. A randomized clinical trial of cisplatin/paclitaxel versus carboplatin/paclitaxel as first-line treatment of ovarian cancer. *Journal of the National Cancer Institute*. Sep 3 2003;95(17):1320-1329.
  288. Neijt JP, Engelholm SA, Tuxen MK, et al. Exploratory phase III study of paclitaxel and cisplatin versus paclitaxel and carboplatin in advanced ovarian cancer. *J Clin Oncol*. Sep 2000;18(17):3084-3092.
  289. Chuang LS, Ito Y. RUNX3 is multifunctional in carcinogenesis of multiple solid tumors. *Oncogene*. May 6 2010;29(18):2605-2615.
  290. Bruno L, Mazzearella L, Hoogenkamp M, et al. Runx proteins regulate Foxp3 expression. *J Exp Med*. Oct 26 2009;206(11):2329-2337.

291. Schimmer AD. Inhibitor of apoptosis proteins: translating basic knowledge into clinical practice. *Cancer research*. Oct 15 2004;64(20):7183-7190.
292. Ewan K, Pajak B, Stubbs M, et al. A useful approach to identify novel small-molecule inhibitors of Wnt-dependent transcription. *Cancer research*. Jul 15 2010;70(14):5963-5973.
293. Jarde T, Evans RJ, McQuillan KL, et al. In vivo and in vitro models for the therapeutic targeting of Wnt signaling using a Tet-ODeltaN89beta-catenin system. *Oncogene*. Feb 14 2013;32(7):883-893.
294. Mathur R, Sehgal L, Braun FK, et al. Targeting Wnt pathway in mantle cell lymphoma-initiating cells. *J Hematol Oncol*. 2015;8(1):63.
295. Farrand L, Byun S, Kim JY, et al. Piceatannol enhances cisplatin sensitivity in ovarian cancer via modulation of p53, X-linked inhibitor of apoptosis protein (XIAP), and mitochondrial fission. *The Journal of biological chemistry*. Aug 16 2013;288(33):23740-23750.
296. Farrand L, Kim JY, Byun S, et al. The Diarylheptanoid Hirsutenone Sensitizes Chemoresistant Ovarian Cancer Cells to Cisplatin via Modulation of Apoptosis-inducing Factor and X-linked Inhibitor of Apoptosis. *The Journal of biological chemistry*. Jan 17 2014;289(3):1723-1731.
297. Telfer JC, Hedblom EE, Anderson MK, Laurent MN, Rothenberg EV. Localization of the domains in Runx transcription factors required for the repression of CD4 in thymocytes. *J Immunol*. Apr 1 2004;172(7):4359-4370.
298. Nomura T, Yamasaki M, Nomura Y, Mimata H. Expression of the inhibitors of apoptosis proteins in cisplatin-resistant prostate cancer cells. *Oncology reports*. Oct 2005;14(4):993-997.
299. Wu HH, Wu JY, Cheng YW, et al. cIAP2 upregulated by E6 oncoprotein via epidermal growth factor receptor/phosphatidylinositol 3-kinase/AKT pathway confers resistance to cisplatin in human papillomavirus 16/18-infected lung cancer. *Clin Cancer Res*. Nov 1 2010;16(21):5200-5210.
300. Zeng C, Vangveravong S, McDunn JE, Hawkins WG, Mach RH. Sigma-2 receptor ligand as a novel method for delivering a SMAC mimetic drug for treating ovarian cancer. *British journal of cancer*. Oct 29 2013;109(9):2368-2377.
301. Collins FS, Varmus H. A new initiative on precision medicine. *The New England journal of medicine*. Feb 26 2015;372(9):793-795.
302. Understanding Resistance to Cancer Immunotherapy. *Cancer Discov*. Jun 8 2015.
303. Woodward WA, Chen MS, Behbod F, Alfaro MP, Buchholz TA, Rosen JM. WNT/beta-catenin mediates radiation resistance of mouse mammary progenitor cells. *Proc Natl Acad Sci U S A*. Jan 9 2007;104(2):618-623.
304. Ayadi M, Bouygues A, Ouaret D, et al. Chronic chemotherapeutic stress promotes evolution of stemness and WNT/beta-catenin signaling in colorectal cancer cells: implications for clinical use of WNT-signaling inhibitors. *Oncotarget*. May 11 2015.

305. Spranger S, Bao R, Gajewski TF. Melanoma-intrinsic beta-catenin signalling prevents anti-tumour immunity. *Nature*. May 11 2015.
306. Tzeng HE, Yang L, Chen K, et al. The pan-PI3K inhibitor GDC-0941 activates canonical WNT signaling to confer resistance in TNBC cells: resistance reversal with WNT inhibitor. *Oncotarget*. May 10 2015;6(13):11061-11073.
307. Jang GB, Hong IS, Kim RJ, et al. Wnt/beta-Catenin Small-Molecule Inhibitor CWP232228 Preferentially Inhibits the Growth of Breast Cancer Stem-like Cells. *Cancer research*. Apr 15 2015;75(8):1691-1702.
308. Rosano L, Cianfrocca R, Spinella F, et al. Acquisition of chemoresistance and EMT phenotype is linked with activation of the endothelin A receptor pathway in ovarian carcinoma cells. *Clin Cancer Res*. Apr 15 2011;17(8):2350-2360.
309. Zhang H, Jing X, Wu X, et al. Suppression of multidrug resistance by rosiglitazone treatment in human ovarian cancer cells through downregulation of FZD1 and MDR1 genes. *Anticancer Drugs*. Aug 2015;26(7):706-715.
310. Chau WK, Ip CK, Mak AS, Lai HC, Wong AS. c-Kit mediates chemoresistance and tumor-initiating capacity of ovarian cancer cells through activation of Wnt/beta-catenin-ATP-binding cassette G2 signaling. *Oncogene*. May 30 2013;32(22):2767-2781.
311. Zhang K, Song H, Yang P, et al. Silencing dishevelled-1 sensitizes paclitaxel-resistant human ovarian cancer cells via AKT/GSK-3beta/beta-catenin signalling. *Cell proliferation*. Apr 2015;48(2):249-258.
312. Lee CM, Shvartsman H, Deavers MT, et al. beta-catenin nuclear localization is associated with grade in ovarian serous carcinoma. *Gynecol Oncol*. Mar 2003;88(3):363-368.
313. Wang H, Makki MS, Wen J, et al. Overexpression of beta-catenin and cyclinD1 predicts a poor prognosis in ovarian serous carcinomas. *Int J Clin Exp Pathol*. 2013;7(1):264-271.
314. Bodnar L, Stanczak A, Cierniak S, et al. Wnt/beta-catenin pathway as a potential prognostic and predictive marker in patients with advanced ovarian cancer. *Journal of ovarian research*. 2014;7:16.
315. Usongo M, Li X, Farookhi R. Activation of the canonical WNT signaling pathway promotes ovarian surface epithelial proliferation without inducing beta-catenin/Tcf-mediated reporter expression. *Developmental dynamics : an official publication of the American Association of Anatomists*. Mar 2013;242(3):291-300.
316. Wang J, Zhou D, He X, et al. Effect of downregulated beta-catenin on cell proliferative activity, the sensitivity to chemotherapy drug and tumorigenicity of ovarian cancer cells. *Cell Mol Biol (Noisy-le-grand)*. 2011;57 Suppl:OL1606-1613.
317. Zhao H, Wei W, Sun Y, Gao J, Wang Q, Zheng J. Interference with the expression of beta-catenin reverses cisplatin resistance in A2780/DDP cells and inhibits the progression of ovarian cancer in mouse model. *DNA and cell biology*. Jan 2015;34(1):55-62.

- 318.** Arend RC, Londono-Joshi AI, Samant RS, et al. Inhibition of Wnt/beta-catenin pathway by niclosamide: a therapeutic target for ovarian cancer. *Gynecol Oncol.* Jul 2014;134(1):112-120.
- 319.** Osada T, Chen M, Yang XY, et al. Antihelminth compound niclosamide downregulates Wnt signaling and elicits antitumor responses in tumors with activating APC mutations. *Cancer research.* Jun 15 2011;71(12):4172-4182.
- 320.** Lu W, Lin C, Roberts MJ, Waud WR, Piazza GA, Li Y. Niclosamide suppresses cancer cell growth by inducing Wnt co-receptor LRP6 degradation and inhibiting the Wnt/beta-catenin pathway. *PLoS One.* 2011;6(12):e29290.
- 321.** Drake J, Shearwood AM, White J, et al. Expression of secreted frizzled-related protein 4 (SFRP4) in primary serous ovarian tumours. *European journal of gynaecological oncology.* 2009;30(2):133-141.